Analyses of differential effects of alpha1 AMPK and alpha2 AMPK on survival and metabolism in cardiac cells

Inauguraldissertation
zur Erlangung des Grades eines Doktors der Humanbiologie
des Fachbereichs Medizin
der Justus-Liebig-Universität Gießen

vorgelegt von Ruping Pan
geboren am 09.11.1982
in Shanghai, China

Gießen (2013)

Aus dem Physiologischen Institut
Der Justus-Liebig-Universität Gießen
(Direktor: Prof. Dr. med. Rainer Schulz)

Gutachter:

Gutachter:

Tag der Disputation:

Table of contents

1. Introduction

Metabolic diseases such as diabetes or obesity are commonly associated with cardiovascular disorders. Adiponectin which is an adipose-derived protein is downregulated in subjects with obesity-related disorders (Diez and Iglesias 2003). Therefore, low levels of adiponectin result in obesity-related cardiovascular diseases, including ischemic heart diseases and peripheral artery diseases (Ouchi, Kihara et al. 1999; Kumada, Kihara et al. 2003; Nakamura, Shimada et al. 2004). Previous studies have shown that adiponectin has beneficial effects on cardiovascular systems. The cardioprotective effects of adiponectin include inhibition of pro-inflammatory and hypertrophic responses, antioxidation effect (Shibata, Ouchi et al. 2004; Antonopoulos, Lee et al. 2011), angiogenic effect and antiatherosclerotic effect (Wong, Wang et al. 2004). These effects are mainly mediated by AMP-activated protein kinase (AMPK), an energy sensor, which is a very important enzyme in maintaining the energy balance within the cells. Thus, adiponectin and AMPK could be potential therapeutic targets for cardiovascular diseases.

1.1 Adiponectin and its receptors

Adiponectin, which is also called adipocyte complement-related protein of 30 kDa (acrp30), is an adipocyte-derived protein which is abundantly present in human plasma ranging from 3 to 30 μg/ml (Arita, Kihara et al. 1999). Adiponectin is composed of four distinct domains: a C-terminal globular domain, 22 collagen repeats, a variable region and an amino-terminal signal peptide (Scherer, Williams et al. 1995). It structurally belongs to the complement 1q family and exists in the serum as low molecular weight (LMW), middle molecular weight (MMW) and high molecular weight (HMW) proteins (Waki, Yamauchi et al. 2003). The LMW form is the basic unit consisting of a homotrimer (90kDa). Several homotrimers can be assembled into multimeric isoforms through disulfide in cysteine. The LMW form is formed by cysteine in the globular domain, while the MMW and HMW form is formed by the cysteine in the collagen-like

domain (Scherer, Williams et al. 1995; Waki, Yamauchi et al. 2003). In plasma, adiponectin exists mainly as a full-length protein. Only a small amount of adiponectin may circulate as globular fragment which is most likely generated by proteolytic cleavage in the blood (Fruebis, Tsao et al. 2001; Waki, Yamauchi et al. 2005). The adiponectin globular domain is detected only as a monomer (Waki, Yamauchi et al. 2003). It protects myocardium from ischemia/reperfusion injury by inhibiting the oxidative/nitrate stress in mice (Tao, Gao et al. 2007). The HMW adiponectin levels are selectively suppressed in obese patients with ischemic heart disease, which indicates that the HMW form is the most active form regarding protection against insulin resistance (Yamauchi, Kamon et al. 2002; Aso, Yamamoto et al. 2006; Lara-Castro, Luo et al. 2006; Inoue, Kotooka et al. 2007). A lower ratio of HMW to LMW adiponectin has been shown to reflect hypoadiponectinaemia (Catalano, Hoegh et al. 2006; Plaisance, Grandjean et al. 2008). Recent studies show that adiponectin is also expressed in cardiomyocytes which acts as a cardioprotective molecule protecting against myocardial ischemia/reperfusion injury (Wang, Lau et al. 2010). Adiponectin knockout mice show diet-induced insulin resistance (Maeda, Shimomura et al. 2002), increased intimal hyperplasia after acute vascular injury (Kubota, Terauchi et al. 2002), and impaired angiogenic responses to ischemia (Shibata, Ouchi et al. 2004).

AdipoR1, adipoR2 (Kadowaki and Yamauchi 2005), T-cadherin (Hug, Wang et al. 2004) are three adiponectin receptors which have been identified so far. AdipoR1 and adipoR2 are integral membrane proteins, in which the N-terminus is internally localized while the C-terminus is externally localized. AdipoR1 is originally reported as a receptor for globular adiponectin, whereas adipoR2 is reported as a receptor for full-length adiponectin (Kadowaki and Yamauchi 2005). However, they also bind with the high molecular weight adiponectin (Yamauchi, Kamon et al. 2003; Yamauchi, Nio et al. 2007). Supression of adipoR1 and of adipoR2 reduces adiponectin-induced fatty acid oxidation (Yamauchi, Kamon et al. 2002). Disruption of adipoR1 results in an abrogation of adiponectin-induced AMPK activation, whereas that of adipoR2 results in decreased activity of peroxisome proliferator-activated receptor alpha (PPAR-α) (Yamauchi, Nio et al. 2007). T-cadherin is identified as an adiponectin receptor by its ability to specially

bind the high molecular weight adiponectin in vitro (Hug, Wang et al. 2004). It also binds with the hexameric adiponectin (Hug, Wang et al. 2004). Recently, it is shown that T-cadherin directly binds with high molecular weight adiponectin and is critical for AMPK phosphorylation and adiponectin-mediated cardioprotection in mice (Denzel, Scimia et al. 2010).

APPL1 (adaptor protein containing pleckstrin homology domain, phosphotyrosine binding domain and leucine zipper motif) binds to the N-terminus of the adiponectin receptors and mediates adiponectin signaling via activation of AMPK and mitogen-activated protein kinase (MAPK). Interestingly, it is found that APPL2, an isoform of APPL1, binds to the adipoR1 under basal conditions and blocks the interaction between adipoR1 and APPL1. Once adiponectin interacts with the adipoRs, APPL2 is seperated from adipoR1 and APPL1 can then bind (Wang, Xin et al. 2009). Activated AMPK, together with activated p38 MAPK, stimulate the glucose uptake and fatty acid oxidation in the heart and skeletal muscle, while activated AMPK and PPAR-α stimulate fatty acid oxidation in the muscle and liver (Yamauchi, Kamon et al. 2001). The adiponectin-induced activation of PPAR-α differs in muscle and liver, while PPAR-α in muscle is activated by AMPK and MAPK via adipoR1 (Yamauchi, Kamon et al. 2003; Yamauchi, Kamon et al. 2003), and PPAR-α in liver is activated by MAPK via adipoR2 (Yamauchi, Nio et al. 2007).

1.2 AMPK and its regulation

AMPK is a heterotrimeric complex (Figure 1), which consists of the catalytic α subunit and the two regulatory subunits β and γ (Hardie and Hawley 2001). There are two α isoforms (α1, α2), two β isoforms (β1, β2), and three γ isoforms (γ1, γ2 and γ3) (Thornton, Snowden et al. 1998; Cheung, Salt et al. 2000). At the α subunit, there is a phosphorylation site at Threonine 172, which is the activation site of AMPK (Hawley, Davison et al. 1996). At the β subunit, there is a glycogen binding site which targets the AMPK complex to intracellular glycogen (McBride, Ghilagaber et al. 2009). At the γ subunit, there is an AMP binding site, which is responsible for the AMP binding and

AMP-dependent AMPK activation by AMPK kinases (Cheung, Salt et al. 2000). In the absence of AMP, association of the autoinhibitory domain with the kinase domain blocks the active site cleft between the small and large lobes of the kinase domain, and prevents access of AMPK kinases to activating Thr172 site.

Different compositions of AMPK complex may fulfill their different functions depending on the distribution of the isoforms. The α1 isoform is widely expressed in many tissues, while the α2 isoform is highly expressed in cardiac and skeletal muscle and partially exists in liver (Arad, Seidman et al. 2007). The complex α2β2γ2 mainly exists in the heart (Arad, Seidman et al. 2007). Subcellular localization of AMPK is also an important determinant of cell signaling. The α1 isoform is mainly localized in the cytoplasm (2-fold more than in the nucleus), while the α2 isoform shows an equal distribution in the cytoplasm and the nucleus in the INS-1 cells (Salt, Celler et al. 1998). A starvation which activates AMPK has no effect on the cytoplasmic/nuclear ratio for either α1 or α2 AMPK (Salt, Celler et al. 1998). In Hela or HEK293 cells, AMPK is present in the cytoplasm and nucleus and accumulates in the nuclei under various stressful conditions (heat shock or oxidant exposure) (Kodiha, Rassi et al. 2007).

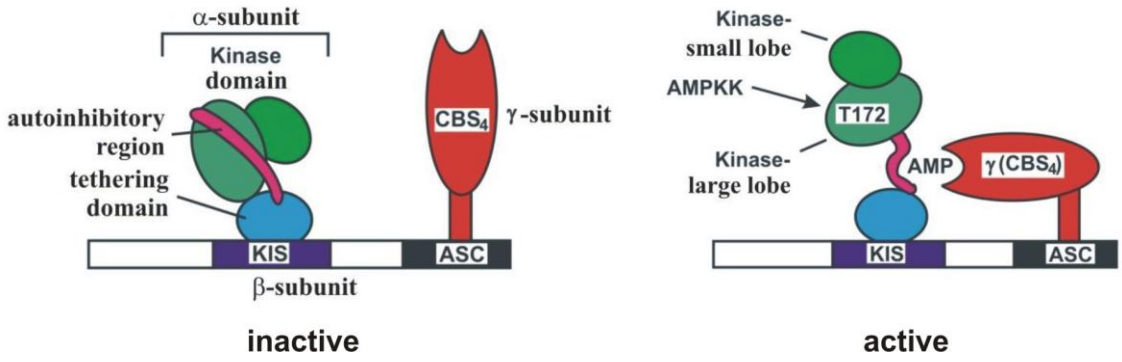

Figure 1: Structure of AMPK (inactive form and active form) Modified from: Cheung et el., Biochemical Journal (2000) Volume 346, 659-669.

So far, there are three known AMPK upstream kinases: LKB1 (Serine/threonine-protein kinase STK11, encoded by the Peutz-Jegher syndrome tumor suppressor gene), Ca^{2+}-calmodulin-dependent kinase kinase β (CaMKKβ) and possibly transforming growth factor-β-activated kinase (TAK1). LKB1 is a complex enzyme consisting of two

additional non-catalytic subunits STRAD and MO25. It has been widely accepted as one of the major upstream kinases phosphorylating AMPK at T172 (Hawley, Boudeau et al. 2003; Woods, Johnstone et al. 2003; Shaw, Kosmatka et al. 2004), and has been reported to be responsible for AICAR and metformin mediated AMPK activation (Woods, Johnstone et al. 2003; Shaw, Kosmatka et al. 2004). LKB1 has been shown to be the major upstream kinase of the α2 catalytic subunit of AMPK in mammalian cells (Imai, Inukai et al. 2006). It acts as an AMP-dependent AMPK activator (Sakamoto, McCarthy et al. 2005; Sanders, Grondin et al. 2007). In hearts lacking LKB1, the basal activity of α2 AMPK is vastly reduced and not increased by ischemia or anoxia, while a significant basal activity of α1 AMPK is observed in these hearts and markedly induced by ischemia or anoxia (Sakamoto, Zarrinpashneh et al. 2006). The LKB1 deficient hearts, which are lacking α2 AMPK activation, display increased mTOR signaling, decreased energy efficiency and impaired cardiac function (Ikeda, Sato et al. 2009; Jessen, Koh et al. 2010). CaMKKβ is reported as an alternative upstream kinase of AMPK which acts as an AMP-independent activator of AMPK in LKB1-deficient cells. It phosphorylates and activates AMPK in response to increased calcium, which has been observed in immune cells and endothelial cells (Hawley, Pan et al. 2005; Stahmann, Woods et al. 2006). TAK1 is found to phosphorylate and activate AMPK via LKB1 (Momcilovic, Hong et al. 2006; Xie, Zhang et al. 2006).

AMPK senses any circumstance that causes energy deficit including hypoxia, ischemia, glucose deprivation, metabolic poisons, oxidative and hyperosmotic stress and starvation. A very small rise in AMP levels can induce a dramatic increase in the activity of AMPK (Hardie and Hawley 2001). Whenever the ratio AMP/ATP increases, AMPK is activated and ATP-generating pathways including fatty acid oxidation and glycolysis are switched on. On the other hand, in response to a rise in ATP levels, AMPK switches on ATP-consuming pathways including fatty acid synthesis and cholesterol synthesis (Carling and Hardie 1989; Corton, Gillespie et al. 1994). AMPK can also be negatively regulated by glycogen whenever bound to the glycogen binding site in the β subunit. In muscle, high glycogen content represses AMPK activity (Derave, Ai et al. 2000; Wojtaszewski, Jorgensen et al. 2002).

1.3 Physiological and pharmacological AMPK activators

As mentioned before, AMPK activation requires phosphorylation at Threonine 172 of the α subunit. AMPK can be both pharmacologically and physiologically activated. There are many AMPK activators, in which AICAR, metformin are the most common ones. Metformin (Fryer, Parbu-Patel et al. 2002) is a widely used drug for type 2 diabetes, which belongs to the biguanides. Some studies have demonstrated that metformin might activate AMPK by decreasing cellular energy charge because it can act as an inhibitor of complex I of the respiratory chain (El-Mir, Nogueira et al. 2000). Compared to other anti-diabetic drugs, metformin improves cardiovascular functions and reduces cardiovascular risks in diabetes (Gundewar, Calvert et al. 2009). However, its use to activate AMPK is not recommended, because of its inhibitory effects on complex I and glucose phosphorylation (Guigas, Bertrand et al. 2006).

AICAR is an adenosine analog which can be phosphorylated to form 5 aminoimidazole-4-carboxamide-1-β-D-ribofuranosyl-5'-monophosphate (ZMP). ZMP mimics the multiple effects of AMP on AMPK, not only causing allosteric activation but also promoting phosphorylation and activation of the upstream kinases. It is reported that AICAR stimulates AMPK activity and glucose transport in skeletal muscle (Wojtaszewski, Jorgensen et al. 2002). AICAR also induces late pre-conditioning and protects against myocardial ischemia/reperfusion injury (Kristiansen, Solskov et al. 2009). However, its use to activate AMPK in cardiomyocytes is also not recommended, because of its poor metabolism in these cells (Javaux, Vincent et al. 1995) and inhibition of AMPK-independent mitochondrial oxidative phosphorylation (Guigas, Taleux et al. 2007) and glucose phosphorylation (Guigas, Bertrand et al. 2006).

A-769662, a direct activator of AMPK, activates native rat AMPK by mimicking effects of AMP and inhibition of dephosphorylation, and in addition causes a phosphorylation of ACC (Cool, Zinker et al. 2006). It binds in part on S108 which is located in the carbohydrate binding domain of the β subunit and causes an allosterical activation of AMPK. The autophosphorylation at S108 caused by A-769662 binding protects the activating phosphorylation at T172 from upstream kinases (Sanders, Ali et al. 2007). It is

also reported recently that the activation of AMPK by A-769662 requires β1 isoform of AMPK (Treebak, Birk et al. 2009). Similar to other AMPK activators, A-769662 has been shown to possess cardioprotective potential. Mice hearts pre-treated with A-769662 demonstrate smaller infarct sizes after ischemia/reperfusion injury (Kim, Miller et al. 2011).

Under physiological conditions, AMPK can also be activated by adipose tissue derived hormones. The adipocytokine leptin can activate α2 AMPK, resulting in fatty acid oxidation in skeletal muscle (Minokoshi, Kim et al. 2002). The adipocytokine adiponectin can phosphorylate and activate AMPK both in vivo and in vitro, followed by a stimulation of glucose utilization and fatty acid oxidation (Yamauchi, Kamon et al. 2002). Many groups have demonstrated that adiponectin has cardioprotective effects which are mainly mediated by AMPK (Chen, Montagnani et al. 2003; Yamauchi, Kamon et al. 2003; Ouchi, Kobayashi et al. 2004; Shibata, Ouchi et al. 2004; Shibata, Sato et al. 2005; Cheng, Lam et al. 2007). Adiponectin stimulates nitric oxide production in endothelial cells through AMPK-dependent phosphorylation of eNOS (Chen, Montagnani et al. 2003; Cheng, Lam et al. 2007). Adiponectin protects against myocardial ischemia/reperfusion injury through AMPK and cyclooxygenase (COX)-2-dependent mechanisms (Shibata, Sato et al. 2005). Its interaction with adipoR1 and adipoR2 leads to enhanced glucose uptake and fatty acid oxidation which is mediated by AMPK and MAPK in the heart (Yamauchi, Kamon et al. 2003). Furthermore, adiponectin activates AMPK and inhibits both extracellular signal regulated kinase (ERK) activation and the hypertrophic response to α-adrenergic receptor stimulation in rat neonatal cardiomyocytes (Shibata, Ouchi et al. 2004).

Other potential activators of AMPK include norepinephrine, phenylephrine, isoproterenol, vasopressin, migration inhibitory factor (MIF), resveratrol and ROS. (Xu, Zhao et al. 2007; Horman, Morel et al. 2008; Saeedi, Saran et al. 2009; Jaswal, Lund et al. 2010).

1.4 AMPK and its cellular effects

AMPK is known as an energy sensor maintaining energy balance within the cells. As shown in Figure 2, it is activated in response to low ATP levels, AMPK upstream kinases or adipokines such as adiponectin, and results in angiogenesis, glycolysis, fatty acid oxidation, mitochondrial biogenesis, muscle contraction and inhibition of protein synthesis. Mammalian target of rapamycin (mTOR) has been shown to be inhibited by AMPK through TSC2 phosphorylation (Inoki, Zhu et al. 2003), which leads to the inhibition of p70 ribosomal protein S6 kinase (p70S6 kinase), thus inhibition of protein synthesis. AMPK also phosphorylates eukaryotic elongation factor-2 (eEF2) kinase, resulting in phosphorylation and inhibition of eEF2 (Chan, Soltys et al. 2004). Besides various roles in cellular and whole body metabolism as described in paragraph 1.4.1-1.4.5, AMPK was also described to activate angiogenesis via phosphorylation of VEGF (Zwetsloot, Westerkamp et al. 2008) and influence MLCK in smooth muscles (Horman, Morel et al. 2008).

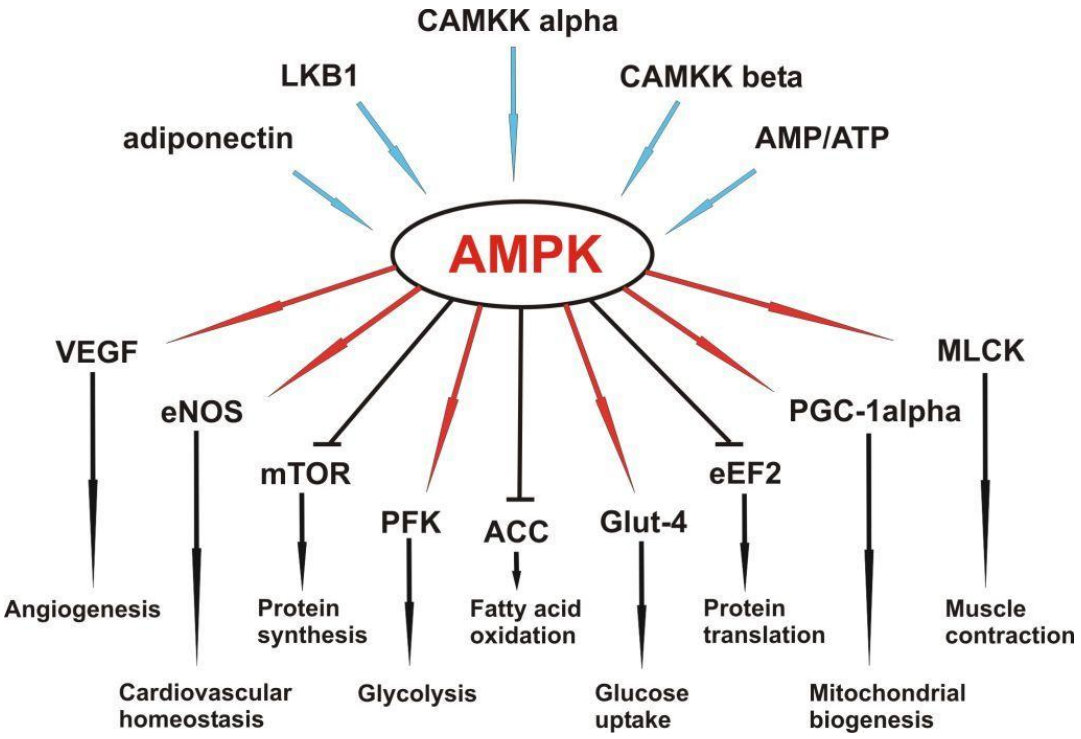

Figure 2: AMPK signaling pathways (AMPK upstreams and downstream targets).

1.4.1 Role of AMPK in mitochondrial biogenesis

Mitochondrial biogenesis is the process by which new mitochondria are formed in the cells. It is thought that higher mitochondrial copy number is protective for the cells, since mitochondria are key regulators of the metabolic activity of the cells (McBride, Neuspiel et al. 2006). Mitochondrial biogenesis results in the synthesis and assembly of mitochondrial components controlling mitochondrial number and determining the cellular energy production.

PGC-1α is the key mitochondrial transcriptional coactivator in the cells. Deletion of PGC-1α leads to a general reduction of mitochondrial gene expression (Handschin, Chin et al. 2007). PGC-1α orchestrates a constellation of transcription factors, such as estrogen-related receptor alpha (ERRα), nuclear respiratory factor 1/2 (NRF1/2), peroxisome proliferator-activated receptors (PPARs) and retinoid X receptor (RXR), to induce mitochondrial gene expression (Canto and Auwerx 2010) (Figure 3). NRF1 and NRF2 activate the mitochondrial transcription factor A (Tfam) which initiates the transcription of the mitochondrial DNA and leads to the production of mitochondrial proteins (Scarpulla 1997; Reznick and Shulman 2006). ERRα regulates the expression of genes involved in oxidative phosphorylation and mitochondrial biogenesis (Schreiber, Emter et al. 2004). PGC-1α, interacting with the nuclear hormone receptors PPARγ and thyroid hormone receptor, activates the transcription of mitochondrial uncoupling protein-1 and therefore regulates the mitochondrial uncoupled respiration and thermogenesis (Puigserver, Wu et al. 1998). The heterodimer, from the binding of PGC-1α to PPARα and RXR, is involved in the regulation of enzymes, transporters and proteins of fatty acid oxidation (Lehman, Barger et al. 2000).

PGC-1α is the key downstream mediator of the effects of AMPK on mitochondrial biogenesis. AMPK phosphorylates PGC-1α at Thr177 and Ser538, which is required for the induction of PGC-1α target genes and thus also the mitochondrial biogenic response (Jager, Handschin et al. 2007). The deacetylase SIRT1 (silent mating type information regulator 2 homolog 1) deacetylates PGC-1α, which enhances the activity of PGC-1α and its transcriptional activation that is important for skeletal muscle function and exercise-induced mitochondrial biogenesis (Gurd 2011; Li, Muhlfeld et al. 2011; Li,

Pan et al. 2011).

Physiological and pharmacological activation of AMPK by adiponectin, AICAR and metformin promotes mitochondrial biogenesis via upregulation of PGC-1α (Civitarese, Ukropcova et al. 2006). On the contrary, muscle-specific deletions of either AMPK or PGC-1α lead to a generalized reduction in mitochondrial gene expression and exercise intolerance (Jorgensen, Wojtaszewski et al. 2005; Handschin, Chin et al. 2007). Dominant negative α1 AMPK (T172A) reduces the effect of metformin and AICAR on NRF1 and Tfam expression and mitochondrial proliferation in HUVEC (Kukidome, Nishikawa et al. 2006), whereas α2 AMPK deletion leads to a reduction of pyruvate-dependent mitochondrial respiration in heart, which may due to a decrease in cardiolipin content that is required for the electron transfer in complex I and III (Fry and Green 1981; Athea, Viollet et al. 2007).

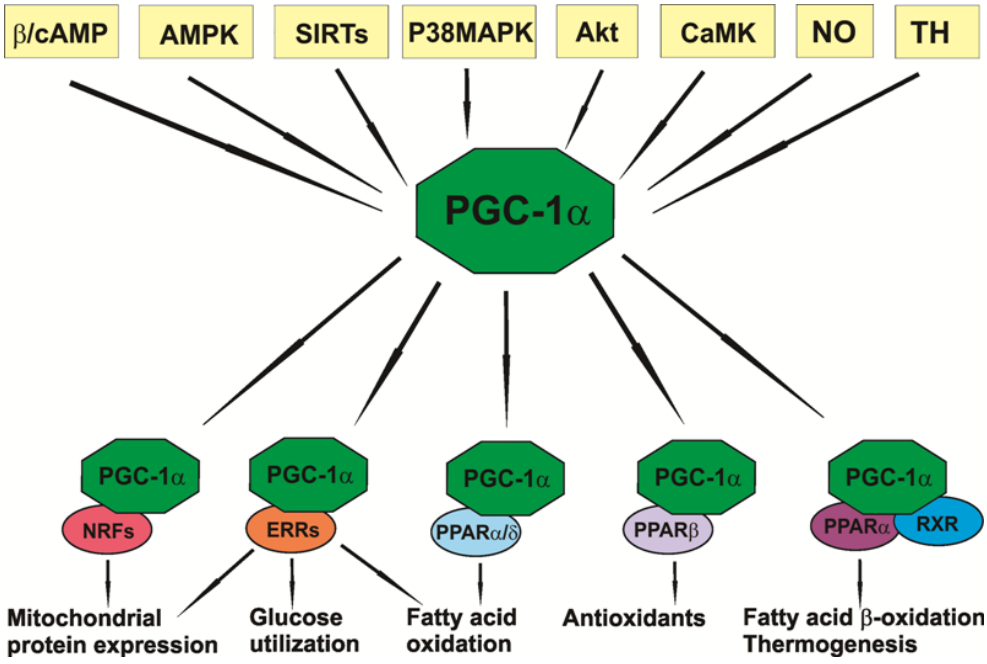

Figure 3: AMPK-mediated mitochondrial biogenesis

1.4.2 Role of AMPK in lipid transport and utilization

AMPK regulates lipid metabolism including fatty acid oxidation, triglyceride hydrolysis, long-chain fatty acid uptake and cholesterol synthesis. Acetyl CoA carboxylase (ACC) is one of the direct downstream targets of AMPK, which can be phosphorylated and inactivated by AMPK. It controls the conversion of acetyl-CoA to malonyl-CoA, an inhibitor of Carnitine Palmitoyl Transferase 1 (CPT1). CPT1 is responsible for the entry of long-chain fatty acyl-CoA into mitochondria. Decreased ACC activity results in lower malonyl-CoA levels, thus causing an increase in fatty acid oxidation (Kahn, Alquier et al. 2005). In addition, AMPK phosphorylates and activates malonyl-CoA decarboxylase (MCD), which promotes degradation of malonyl-CoA, thus causing an increase in fatty acid oxidation in heart as well (Goodwin and Taegtmeyer 1999).

The lipoprotein lipase (LPL) catalyzes the hydrolytic cleavage of fatty acids from triglycerides in chylomicrons, very-low-density lipoproteins, and low-density lipoproteins. Its activity in coronary lumen is reported to be increased by activated AMPK (An, Pulinilkunnil et al. 2005). During metabolic stress, AMPK-mediated recruitment of LPL to the coronary lumen could represent an immediate compensatory response by the heart to guarantee the fatty acid supply.

In addition to the inhibition of triglyceride synthesis in liver and muscle (Muoio, Seefeld et al. 1999), AMPK increases the phosphorylation of hormone-sensitive lipase (HSL) at Ser565 in adipocytes. HSL is responsible for the hydrolysis of triglycerides, and phosphorylation at Ser565 precludes its isoproterenol-induced translocation to the lipid droplet, a major requirement for lipolysis activation (Daval, Diot-Dupuy et al. 2005).

AMPK signaling also regulates cellular long-chain fatty acids (LCFA) uptake through translocation of CD36 (fatty acid translocase), one enzyme which acts as acceptor for fatty acids and enhances fatty acid diffusion, from intracellular storage membranes to the sarcolemma in cardiomyocytes (Habets, Coumans et al. 2007). AMPK also phosphorylates and inactivates 3-hydroxy-3-methylglutaryl-CoA reductase (HMGR), leading to an inhibition of cholesterol synthesis (Henin, Vincent et al. 1995).

1.4.3 Role of AMPK in glucose transport and utilization

AMPK regulates glucose metabolism by inducing glucose uptake and glycolysis and by inhibition of glycogen synthesis. Contraction and AICAR-induced AMPK activity plays an important role in the glucose uptake, which is mediated by an increased translocation of glucose transporter 4 (Glut4) to the cell membrane (Kurth-Kraczek, Hirshman et al. 1999; Russell, Bergeron et al. 1999). AMPK also directly phosphorylates the Glut4 enhancer factor (GEF) which is essential for the regulation of Glut4 expression at the transcriptional level (Merrill, Kurth et al. 1997). AS160 (Akt substrate of 160 kDa) inhibits the fusion of GLUT4-vesicles with the plasma membrane and keeps the GLUT4-vesicles in the cytosol (Koumanov, Richardson et al. 2011). Insulin and AMPK activation in skeletal muscle induces the phosphorylation of AS160, which leads to an inhibition of AS160 activity and Glut4 translocation (Eguez, Lee et al. 2005; Treebak, Glund et al. 2006). AMPK induces glycolysis by phosphorylating and activating phosphofructokinase-2 (PFK-2) which increases the production of fructose-2,6-bisphosphate (F-2,6-P2) (Marsin, Bertrand et al. 2000). Glycogen synthase (GS), which is the key enzyme in the regulation of glycogen synthesis in skeletal muscle, has been shown to be phosphorylated and inhibited by AMPK in vitro (Carling and Hardie 1989). Pharmacological activation of AMPK by AICAR also leads to glycogen synthase deactivation in vivo (Wojtaszewski, Jorgensen et al. 2002).

1.4.4 Role of AMPK in cell proliferation

Many published studies indicate that AMPK activation strongly suppresses cell proliferation in non-malignant cells as well as in tumor cells (Rattan, Giri et al. 2005; Du, Guan et al. 2008; Zhou, Huang et al. 2009). This effect may be mediated through multiple mechanisms including the regulation of cell cycle (Williamson, Bolster et al. 2006) and inhibition of protein synthesis (Bolster, Crozier et al. 2002). AICAR-induced AMPK activation inhibits growth and proliferation of cardiac fibroblasts, which involves inhibitory interactions between ERK and AMPK (Du, Guan et al. 2008).

Although most studies have shown that AMPK activation suppresses cell proliferation, there are also reports showing that AMPK activation by AICAR enhances angiotensin

II-induced cardiac fibroblasts proliferation (Hattori, Akimoto et al. 2006). Furthermore, in vivo administration of AICAR exacerbates myocardial hypertrophy. Another group has shown that AMPK activity is required for proliferation and migration in response to VEGF in human aortic endothelial cells (Reihill, Ewart et al. 2011). Additionally, two independent groups have demonstrated that AMPKα null mutations result in abnormal cellular architecture and cell polarity (Lee, Koh et al. 2007; Mirouse, Swick et al. 2007). The cells appear somewhat spherical in shape, lose their epithelial organization and form apparent multi-layered structures.

1.4.5 Role of AMPK in cell death

Adiponectin-AMPK signaling has been found to have an anti-apoptotic effect on cardiomyocytes (Konishi, Haraguchi et al. 2011; Park, Youn et al. 2011). It is shown that the anti-apoptotic effect of adiponectin on doxorubicin-induced cardiomyopathy is mediated by AMPK, since the suppression of AMPK results in increased apoptosis of cardiomyocytes (Konishi, Haraguchi et al. 2011). Metformin and A-769662-mediated AMPK activation is also reported to result in anti-apoptotic effects (Gundewar, Calvert et al. 2009; Sasaki, Asanuma et al. 2009; Kim, Miller et al. 2011). In endothelial cells, it has been shown that α1 but not α2 AMPK activation promotes cell survival by increasing NF-κB-mediated expression of the anti-apoptotic proteins Bcl-2 and Survivin (Liu, Liang et al. 2010). Furthermore, α2 AMPK dominant negative in mice shows enhanced myocardial injury following ischemia/reperfusion (Wang, Gao et al. 2009).

However, AMPK activation also displays pro-apoptotic effects. Others have reported that AMPK activation contributes to doxorubicin-induced cell death and apoptosis in H9C2 cells, which is mediated by JNK, p53 and mTORC1 (Chen, Wu et al. 2011). Another group shows that AMPK mediates apoptosis in response to bioenergetic stress through activation of the pro-apoptotic gene Bcl-2 modifying factor (Bmf) (Kilbride, Farrelly et al. 2010).

Activation of AMPK results in increased expression of the antioxidant enzyme MnSOD and reduced hyperglycemia-induced mitochondrial ROS production (Kukidome, Nishikawa et al. 2006). Besides, AMPK-mediated reduction in ROS production is

probably also mediated via induction of the redox protein thioredoxin (Trx) (Li, Song et al. 2009).

1.5 Cardiac effects of AMPK

AMPK monitors cellular energy status in the heart in order to meet the enormous energy demand for continuous contraction of the heart. It controls multiple catabolic and anabolic biochemical pathways and regulates the cardiac function in both physiological and pathophysiological conditions. During ischemia, intrinsic AMPK activation protects the heart against injury through mechanisms of glucose uptake induction and anti-apoptosis (Russell, Li et al. 2004). AMPK activators both activate AMPK before ischemia and enhance the degree of ischemic AMPK activation (Kim, Miller et al. 2011). AMPK activation also appears to modulate the myocardial response to pressure overload via modulation of pathways involved in cardiac hypertrophy. This effect is mediated by activation of Akt (Chan, Dolinsky et al. 2008), inhibition of protein synthesis (mTOR signaling) (Zhang, Hu et al. 2008), inhibition of nuclear factor-κB (NF-κB) and blunting the increase in cardiac angiotensin II and endothelin (Li, Yin et al. 2007; Chan, Dolinsky et al. 2008). The role of AMPK activation in heart failure is displayed with diminishing of contractile dysfunction, apoptosis and fibrosis (Sasaki, Asanuma et al. 2009). Furthermore, AMPK phosphorylates endothelial nitric oxide synthase (eNOS) at Ser633, which plays a central role in maintaining cardiovascular homeostasis by controlling NO bioavailability (Chen, Peng et al. 2009). AMPK-induced PGC-1α expression and NO activation are also involved in the metformin-related improvement in survival and cardiac function in mice (Gundewar, Calvert et al. 2009). Furthermore, AMPK mediates the stimulation of adiponectin on angiogenesis by promoting cross-talk between AMPK and Akt signaling in endothelial cells (Ouchi, Kobayashi et al. 2004). Adiponectin, as a physiological AMPK activator, prevents progressive cardiac remodelling in pressure-overloaded condition, which is mediated by AMPK activation and glucose metabolism (Liao, Takashima et al. 2005). It also protects the heart from ischemia/reperfusion injury through mechanisms of AMPK activation and COX-2-dependent TNF-α inhibition (Shibata, Sato et al. 2005).

1.6 Purpose of the study

The purpose of this study is to dissect the cellular role of α1 and α2 AMPK in H9C2 cardiomyoblasts.

In the present study, the following areas are investigated:

- Is there any difference between α1 and α2 AMPK in their mediation of adiponectin-induced changes in mitochondrial biogenesis and mitochondrial function in cardiac tissues and H9C2 cardiomyoblasts?
- Is there any difference between α1 and α2 AMPK in their regulation of cell proliferation in H9C2 cardiomyoblasts?
- Is there any difference between α1 and α2 AMPK in their effect on cell death?
- Are there differences in cellular responses between physiological (adiponectin) and pharmacological (A-769662) AMPK activation in H9C2 cardiomyoblasts?
- Which adiponectin receptor is mediating the adiponectin-induced cellular effects in H9C2 cardiomyoblasts?
- Which AMPK kinase is mediating the adiponectin-induced AMPK activation in H9C2 cardiomyoblasts?

2. Materials

2.1. Reagents

Acetic acid	Roth
Acetyl-Coenzyme A	Sigma-Aldrich Chemie GmbH
Acrylamide	Serva Electrophoresis GmbH
Ampliqon Taq®-Polymerase and related buffer	Biomol GmbH
Annexin V	Roche
APS	Merck
Agarose	Sigma-Aldrich Chemie GmbH
Ammonium acetate	Amersham Pharmacia Biotech Inc.
Antimycin A	Sigma-Aldrich Chemie GmbH
A-769662	Abbott Laboratories
AraA (adenine 9-β-D-arabinofuranoside)	Sigma-Aldrich Chemie GmbH
BCIP	AppliChem
Boric acid	Roth
Bovine serum albumin	Sigma-Aldrich Chemie GmbH
Bromphenol blue	Merck, Darmstadt
Calcium chloride	Roth
Chloroform, minimum 99%	Sigma-Aldrich Chemie GmbH
Compound C	Merck
Coenzyme Q	Sigma-Aldrich Chemie GmbH
Coomassie Brillant Blue G250	Serva Electrophoresis GmbH
p-Coumaric acid	Sigma-Aldrich Chemie GmbH
Cytochrome c	Sigma-Aldrich Chemie GmbH
DAPI	AppliChem
5,5'-Dithiobis-(2-nitrobenzoic acid) (DTNB)	Sigma-Aldrich Chemie GmbH
2,6-Dichlorophenolindophenol (DCPIP)	Sigma-Aldrich Chemie GmbH
Decylubichinol	Sigma-Aldrich Chemie GmbH
Dithiothreitol	Sigma-Aldrich Chemie GmbH
DMF	Merck
dNTP-Mix	Fermentas
DTT	Roth
Ethanol	Riedel-deHaën

Ethylendiamintetraacetate (EDTA)	Roth
Fructose-6-Phosphate	Sigma-Aldrich Chemie GmbH
Glucose	Serva Electrophoresis GmbH
Glycerol	Roth
Glycin	Roth
GoTaq® DNA Polymerase	Promega
G-6-PDH	Sigma-Aldrich Chemie GmbH
GelRed™	Biotium
Hydrochloric acid	Riedel-deHaën
Hydrogen peroxide	AppliChem
HEPES	Roth
Isopropanol	Fluka Chemie AG
Luminol	Sigma-Aldrich Chemie GmbH
Lysozyme	Serva Electrophoresis GmbH
Methanol	Merck
$MgCl_2 \cdot 6H_2O$	Sigma-Aldrich Chemie GmbH
M- MLV Reverse Transcriptase and 5x buffer	Promega
Nicotinamidadenindinucleotide (NADH)	Sigma-Aldrich Chemie GmbH
Nicotinamidadenin-dinucleotidphosphate (NADPH)	Sigma-Aldrich Chemie GmbH
2-(N-morpholino)-ethanesulphonic acid (MES)	Sigma-Aldrich Chemie GmbH
Oxalacetate	Sigma-Aldrich Chemie GmbH
Ponceau S	Merck
Phenazine methosulfate (PMS)	Sigma-Aldrich Chemie GmbH
Primer (diverse)	Invitrogen
Pyruvate	Sigma-Aldrich Chemie GmbH
Potassium acetate	Roth
Potassium chloride	Roth
Potassium cyanide (KCN)	Sigma-Aldrich Chemie GmbH
Restriction enzymes (diverse)	Fermentas GmbH
RNase A	Roth
RNase Out	Invitrogen
Rotenone	Sigma-Aldrich Chemie GmbH
Sodium azide	Sigma-Aldrich Chemie GmbH

Sodium chloride	Roth
Sodium hydroxide (NaOH)	Sigma-Aldrich Chemie GmbH
SDS ultrapure	Roth
Succinate	Sigma-Aldrich Chemie GmbH
Skim milk	Milbona
Tri-Reagent	Sigma-Aldrich Chemie GmbH
Tween 20	Sigma-Aldrich Chemie GmbH
TEMED	Fluka Chemie AG
Tris-(Hydroxymethyl)-aminomethan	Roth
Tetracycline Hydrochloride	Calbiochem
Triton X-100	Sigma-Aldrich Chemie GmbH
T4 DNA Ligase	Invitrogen

2.2. Cell culture

CellTiter-Blue®	Promega
DMSO	AppliChem
DMEM	PAA Laboratories GmbH
FBS	Biochrom AG
Formaldehyde	Roth
Glutardialdehyde	Merck
G418 Sulphate	PAA Laboratories GmbH
Glutamate	PAA Laboratories GmbH
Lipofectamine™ RNAiMax	Invitrogen
Lipofectamine™ 2000	Invitrogen
Na-Pyruvate	PAA Laboratories GmbH
Opti-MEM®I	GIBCO™ Invitrogen Corporation
Penicillin, Streptomycin	PAA Laboratories GmbH
PBS Tablets	GIBCO™ Invitrogen Corporation
Trypsin / EDTA	PAA Laboratories GmbH
Trypan-Blue	Sigma-Aldrich Chemie GmbH
Zeocin	Invitrogen

3. Methods

3.1 Animals

Male C57BL/6J mice were obtained from Charles River Germany (Sandhofer Weg 7, 97633 Sulzfeld). α1 and α2AMPK knockout mice were originally from Dr. Benoit Viollet's group in France. Wistar rats were obtained from Janvier SAS France (CS 4105, LE GENEST ST ISLE, F-53941 St Berthevin Cedex). All the animals were 8 to 12 weeks old and housed in an air-conditioned room with a 12:12 h dark-light cycle and given standard diet with free access to tap water.

3.2 Cell culture

3.2.1 Isolation and culture of rat adult cardiomyocytes

After the rat was sacrificed, the aorta was cannulated and the heart was fixed on a trestle, followed by perfusing with perfusion medium (110 mM NaCl, 2.5 mM KCl, 1.2 mM KH_2PO_4, 1.2 mM $MgSO_4 \cdot 7H_2O$, 25 mM HEPES, 11 mM glucose-monohydrate, pH 7.4) which contains 0.4% collagenase and 250 µM $CaCl_2$ with a speed of 1 drop/second for 25 min. Afterwards, the whole heart was cut once horizontally and once vertically with the Mclwain tissue chopper (the Mickle Laboratory Engineering co. LTD., England), and again several times with a scalpel. Cells were then collected in a tube with 25 ml perfusion medium which contains collagenase, and digested for 5 min at 37°C. Afterwards, cells were centrifugated at 400rpm for 1min and resuspended in perfusion medium in which the concentration of $CaCl_2$ raises from 125 µM, 250 mM, 500 µM to 1 mM. Cells were finally resuspended in 20 ml CCT medium containing 1% penicillin/streptomycin and plated on the dishes which were precoated with 1% FBS overnight. The cells were incubated with 0% CO_2 and 100% humidity at 37°C for 2 h, and then the medium was gently changed to fresh CCT medium containing 1% penicillin-streptomycin, followed by different treatments.

3.2.2 Culture of H9C2 cardiomyoblasts and cell treatment

H9C2 cardiomyoblasts were cultured in Dulbecco's Modified Eagle Medium (DMEM) containing 4.5 g/l glucose and 3.7 g/l Na_2CO_3 and supplemented with 100 U/ml penicillin/streptomycin, 10% fetal bovine serum (FBS), 1 mM Na-pyruvate and 4 mM glutamate (Biochrom AG, Berlin, Germany).

The cells were cultured in a humidified incubator with 5% CO_2 at 37°C and subcultured when they were 60% - 80% confluent. After aspiration of the culture medium, the cells were washed once with warm PBS, and incubated with 0.05% trypsin/0.02% EDTA solution for 5 min in the incubator. When detached from the bottom, cells were collected into a tube together with double amount of normal medium, followed by centrifugation at 1500 rpm for 5 min. Afterwards the cells were resuspended in 1 ml fresh medium, counted under microscope with the help of trypan-blue solution and a cell counting chamber, and seeded on new dishes with an appropriate number.

Cells were treated with adiponectin with a concentration of 4 µg/ml, AraA with a concentration of 500 µM, compound C 10 µM, A-769662 10 µM, H_2O_2 75 µM for different time periods.

3.2.3 Isolation of recombinant human adiponectin

Stable HEK293 cells with an overexpression of HA-tagged human adiponectin were provided by H. Staiger from University of Tübingen, Germany. Cells were cultured in complete DMEM medium containing additionally 1 mg/ml G418 (Geneticin). When the cells were 90-100% confluent, medium was changed to serum-free medium. And those serum-free medium was collected every 2-3 days for 2-3 times. HA-tagged adiponectin was purified from the medium by means of the µMACS Epitope Tag Protein Isolation Kit (Miltenyi Biotec) according to the manufacturer's manual. Finally, purified recombinant adiponectin was quantified by the BCA Protein Assay Kit (Pierce, Rockfort, USA). The quality of the recombinant protein was controlled by Western blot.

3.2.4 Transfection in H9C2 cardiomyoblasts

For transfection in H9C2 cardiomyoblasts, transfection conditions including cell density, amount of transfection reagent, DNA/siRNA concentration, incubation time for forming liposome-DNA/siRNA complexes, and the incubation time of complexes with cells were always first optimized. The transfection time varied from 24 to 72 h. For DNA plasmid transfection into H9C2 cardiomyoblasts, Lipofectamine 2000 Reagent was used. And for RNAi oligonucleotide transfection, Lipofectamine RNAiMax was used according to the instructions of the manufacturer (Invitrogen).

3.2.5 Generation of the inducible stable H9C2 cell lines

H9C2 cardiomyoblasts were co-transfected with pcDNA 6/TR for an overexpression of the Tet-repressor and one of the inducible shRNA plasmids (pENTR H1/TO, pENTR H1/TO α1 AMPK shRNA or pENTR H1/TO α2 AMPK shRNA) with a Tet-on/Tet-off system. Plasmids were designed and produced according to the manual of BLOCK-iT™-Inducible H1 RNAi Entry Vector Kits (Invitrogen). This transfection followed the same protocol as for transient transfection. On the next day, cells were trypsinized, counted, and put into the first row of a 96 well plate with an appropriate number. These cells were further diluted 1:2 serially in the same 96 well plate until one single cell was obtained in a single well. In the mean time, medium containing 1 mg/ml G418 and 250 µg/ml zeocin was used for further culture. Finally, a series of single cells became a series of stable cell lines. Knock down of AMPK in those stable H9C2 cell lines was achieved by incubating with 10 µg/ml tetracycline for 96 h, and the knock-down efficiency of each stable cell line was inspected by Western blot. The most efficient ones were used for further studies.

3.2.6 BrdU-labling

H9C2 cardiomyoblasts were seeded on 10 mm glass cover slips within 35 mm dishes the day before, and transfected with siRNAs for 48 h. Afterwards, cells were incubated with 10 µM bromodeoxyuridine (BrdU) in medium for 2 h and fixed with 4%

paraformaldehyde for 10 min at RT, followed by permeablization with 0.1% triton in PBS for 10min at RT and denaturation with 1 N HCl in 0.1%triton/PBS for 30min at 37°C. After that, cells were blocked with 5% FBS in 0.1% triton/PBS for 30 min at RT, and incubated with anti-BrdU antibody (1:100; Roche) overnight. After three times washing with PBS for 15 min, cells were incubated with Cy3-conjugated anti-mouse antibody (1:1000; Sigma) for 1 h, followed by three times washing with PBS for 15 min. Cells were counterstained with DAPI (1:25000 in PBS) for 1 h. Finally, cells were embedded in Vectashield® fluorescent mounting medium (Vector Laboratories, Inc.) and analyzed under the fluorescence microscope (Olympus IX70).

3.2.7 Annexin V staining

H9C2 cardiomyoblasts were seeded on 10 mm glass cover slips within 35 mm dishes the day before. Cells were preincubated with 4 µg/ml adiponectin or 10 µM A-769662 for 24h, and then treated with 75 µM H_2O_2 for another 24 h. Cells were washed once with warm PBS, followed by staining with Annexin V (1:50, Roche) and 1 µg/ml propidium iodide (PI) which were diluted in the incubation buffer (10 µM HEPES/NAOH, pH 7.4; 140 mM NaCl; 5 mM $CaCl_2$) by putting the cover slip on slide for 10 min. Data were analyzed under the fluorescence microscope (Olympus IX70).

3.2.8 CellTiter-Blue® Cell Viability Assay

CellTiter-Blue® Cell Viability Assay (Promega) is a method to detect a fluorescent signal which is produced by viable cells, since the viable cells can convert a redox dye resazurin into the fluorescent product resorufin. The fluorescent signal is proportional to the number of living cells. To perform this cell viability assay, H9C2 cardiomyoblasts were seeded on a white sterile fluorometric 96well-plate containing 100 µl medium. After being transfected with different siRNAs for 48 h, cells were incubated with 20 µl CellTiter-Blue® cell viability assay reagent at 37°C for 2 h. The fluorescence was read on $530_{Ex}/590_{Em}$ nm with the help of the program Magellan™ (Tecan) and the infinite® 200 PRO series Microplate Reader (Tecan).

3.2.9 Caspase-Glo® 3/7 Assay

Caspase-Glo® 3/7 Assay (Promega) is a luminescent assay that measures caspase-3 and -7 activities. Caspase-3/7 cleavage of the luminogenic substrate containing the DEVD sequence leads to a release of a substrate for luciferase (aminoluciferin), which results in the luciferase reaction and the production of light. The luminescent signal is proportional to the activity of caspase-3 and -7. To perform this assay, cells were seeded on a black sterile fluorometric 96well-plate containing 50 µl medium. After being transfected with different siRNAs for 48 h, cells were incubated with 50 µl caspase-Glo reagent at room temperature for 2 h. The luminescence were read with the help of the program Magellan™ (Tecan) and the infinite® 200 PRO series Microplate Reader (Tecan).

3.3 RNA / DNA analysis

3.3.1 RNA isolation from cells

The cells were scraped with the help of cell-scraper in 1ml (for 35 mm dishes) TRI-Reagent® (Sigma, Taufkirchen, Germany). After incubation at room temperature for 10 min, the lysate was incubated with 200 µl chloroform, vortexed for 15 seconds and incubated at room temperature for 10 min. Then the lysate was centrifugated at 14000 rpm at 4°C for 15 min. The upper phase was transfered into a new tube and incubated with 500 µl isopropanol, vortexed again and incubated at room temperature for another 10 min. Afterwards, the RNA was precipitated by centrifugation at 14000 rpm at 4°C for 30 min, and pellet was washed twice with 75% ethanol. At last, the RNA pellet was dried at room temperature for 5 min, and dissolved in appropriate amount of sterile DEPC-water. The concentration of the RNA was double measured with the help of NanoDrop (Peqlab, Erlangen, Germany) with their absorbance at 260 nm and 280 nm. The quality of the RNA was checked with 1% (w/v) agarose gel electrophoresis. After isolation and measurement, the RNA was frozen at -80°C for long-term storage.

3.3.2 Reverse transcription (RT)

For the reverse transcription, 500 ng RNA was diluted in 10 µl DEPC-H_2O. After being denatured at 72°C for 3 min, RNA was added 15 µl of a master mix (Promega, Madison, WI, U.S.A) with the contents shown in table 1 into each sample and incubated for 30 min at 42°C. Then the temperature was raised to 95°C for 1 min to inactivate the enzymes, followed by cooling to 4°C. Finally, the product was added an equal volume of sterile water and further used for PCR or stored at -20°C.

Table 1: RT master mix content

Substance	Volume in µl
30 µg/ml random primers	3.0
M-MLV RT 5x buffer	5.0
12.5 mM dNTP	1.0
40 U/µl RNase out (ribonuclease inhibitor)	0.25
200 U/µl reverse transcriptase	0.25
DEPC-dH_2O	5.5

3.3.3 Polymerase chain reaction (PCR)

The complementary DNA (cDNA), which was synthesized by reverse transcription, was further used in semi-quantitative PCR for detecting the expression of different isoforms of AMPK, genes related to mitochondrial biogenesis, adiponectin receptors, AMPK kinases and some house keeping genes.

All PCRs were performed in 500 µl PCR tubes containing 25 µl of a mixture as shown in table 2. The primers that were used are shown in table 3. The PCR procedure is shown in table 4.

Table 2: Regular PCR master mix

Substance	Volume in µl
5x Green Goltaq flexi buffer	5.0
25 mM $MgCl_2$	1.5
100 µM dNTP mix	3.0
10 pmol/µl sense primer	0.5
10 pmol/µl anti sense primer	0.5
Gotaq polymerase	0.125
cDNA	2.0
dH_2O	12.375

Substance	Volume in µl
10x Pfu buffer	2.5
100 µM dNTP mix	3.0
10 pmol/µl sense primer	0.5
10 pmol/µl anti sense primer	0.5
Ampliqon Taq DNA polymerase	0.25
cDNA	2.0
dH_2O	16.25

Table 3: Primer sequences used in regular PCR

Name of the Primers	Specificity of the Primers	Sequence of sense primer Sequence of antisense primer	Length of fragments (bp)
α1 AMPK	rat	5´-CCCCTATTATTTGCGTGTGC-3´ 3´-ACTTCTGAGGGCTTTCCTTGA-5´	239
α2 AMPK	rat	5´-AGCATCGATGATGAGGTGGT-3´ 3´-CAACGGGCTAAAGCAGTGAT-5´	247
β1 AMPK	rat	5´-ACCGTATTTCGATGGACAGG-3´ 3´-CCCGTGTCCTTGTTCAAGAT-5´	421
β2 AMPK	rat	5´-ATGGGAAACACCACCAGTGA-3´ 3´-TGGGTGGGCTTCACAGAA-5´	218
γ1 AMPK	rat	5´-CAGCTCCGGAGAATGAACA-3´ 3´-CAAGCTGGCATTTGGAGAA-5´	382
γ2 AMPK	rat	5´-TTCCAGGAGGAAGAAGACTCAG-3´ 3´-ATTCACCAAAGGCTTGAAGGT-5´	341
γ3 AMPK	rat	5´-AAAGCTTCCAGATGGACGAG-3´ 3´-AGCTCACAGTCCCAGACCTC-5´	283
PGC-1α	rat	5´-CCGAGAATTCATGGAGCAAT-3´ 3´-GTGTGAGGAGGGTCATCGTT-5´	114
NRF1	rat	5´-TGTGCGTTCATTTGGCTAAG-3´ 3´-GTTAAGGGCCATGGTGACAG-5´	230
Tfam	rat	5´-CGCCTGTCAGCCTTATCTGT-3´ 3´-CCCATCAGCTGACTTGGAGT-5´	288
ND1	rat	5´-ATTTATTATCGCCCCAACCC-3´ 3´-CAGGCGGGGATTAATAGTCA-5´	354

ND5	rat	5´-ACCCATGCATTCTTCAAAGC-3´ 3´-AATGCTAGGCGTTTGATTGG-5´	386
NDUFB8	rat	5´-TGCGTGTGGAAGACTACAG-3´ 3´-CAGGAAACCGGTGTAGGAGA-5´	208
COX I	rat	5´-ACAGTAGGGGGCCTAACAGG-3´ 3´-CACTTCTCGTTTTGATGCGA-5´	402
COX III	rat	5´-GAACATACCAAGGCCACCAC-3´ 3´-GAGCCGTAAATTCCGTCTGA-5´	391
COX IV	rat	5´-TTGGCAAGAGAGCCATTTCT-3´ 3´-ACTCATTGGTGCCCTTGTTC-5´	270
adipoR1	rat	5´-CTATCGCTGAGGGCTTTGTC-3´ 3´-TGTCTGTGAAGGACCAGCAG-5´	497
adipoR2	rat	5´-TGGGAAGTTTTGTTCCTTGG-3´ 3´-AGAGGGCAGCTCCTGTGATA-5´	300
LKB1	rat	5´-GAGGTTCTCCATCCGACAGA-3´ 3´-CTGACCCACTTCCTCTTCCA-5´	259
CAMKKβ	rat	5´-CCATCCCTGTCCTACTCACC-3´ 3´-CCTGTCGGATCAGCTTCTTT-5´	244
18 S	rat	5´-GTTGGTGGAGCGATTTGTCTGG-3´ 3´-AGGGCAGGGACTTAATCAACGC-5´	351
GAPDH	rat	5´-CATCACCATCTTCCAGGAGCG-3´ 3´-TGACCTTGCCCACAGCCTTG-5´	442

Table 4: Regular PCR procedure

1. First denaturation	95°C	2 min.
2. Denaturation	95°C	30 sec.
3. Annealing	gene-related	30 sec.
4. Extension	72°C	30 sec.
5. Final extension	72°C	2 min.
6. Pause	4°C	

3.3.4 Gelelectrophoresis

After amplification, 25 µl of each PCR product, along with a ladder with known molecular weight (50 bp-1 kb DNA ladder (Invitrogen, Germany)), were loaded on a 1% agarose gel (1% (w/v) agarose boiled in 1x TBE buffer [89 mM Tris–HCl, pH 8.0; 89 mM boric acid; 2.5 mM EDTA, pH 8.8]) containing GelRed™ (1:50000, Biotium). An electrophoresis was performed in 1x TBE buffer at 80-160 volt. Before loading on the gel, the PCR products were mixed with sample buffer (50% (v/v) 1x Tris-EDTA (TE)

buffer [10 mM Tris-HCl, pH 8.8; 1 mM EDTA, pH 8.0]; 50% (v/v) glycerol; 0.25% (w/v) bromophenol blue). The resulting bands were photographed and analyzed with Quantity One system.

3.3.5 Real time PCR

Real-time PCR and subsequent data analysis were performed using the Mx3000P Multiplex Quantitative PCR System (Stratagene). PCR strip tubes, optical caps, and Brilliant SYBRgreen Quantitative PCR-Mastermix and primer pairs were purchased from Invitrogen. The Plexor® qPCR System (Promega) was purchased from Promega. DNA amplification was performed with the thermal cycling profile shown in table 8 and 9. Primer sequences used are listed in table 5 and 3, and the reaction mixtures are shown in table 6 and 7.

Table 5: Primer sequences used in Plexor real-time PCR

Name of the Primers	**Sequence of sense primer** **Sequence of antisense primer**	**Length of fragments (bp)**
GAPDH	5'-CGGGAAGCTTGTCATCAATGGAAA-3' 5'-Texas Red-iso-dC-TGGACTCCACGACGTACTCAG-3'	84
ND1	5'-CCCTACTTCTAACCTCCCTGTTCTTATG-3' 5'-HEX-iso-dC-AGTGGTAGGAAGTTTTTTCATAGGAGG-3'	100
NDUFB8	5'-CGGTTTCCTGGCTTTCATGATATTC-3' 5'-FAM-iso-dC-CGTTCCAGGTACAGATTATTGTAAGGA-3'	108
PGC-1□	5'-AAGGTCCTTTTCTCGACACAGG-3' 5'-Cy5-iso-dC-TGCCTGGAGACCTTGATCTTGAC-3'	71

Table 6: Real-time PCR master mix of Plexor system

Substance	Volume in µl
Platinum qPCR supermix-UDG	12.5
10 µM each sense primer	0.5
10 µM each anti-sense primer	0.5
2.5 µM GAPDH sense primer	0.5
2.5 µM GAPDH anti-sense primer	0.5
cDNA	4.0
dH_2O	4.5

Table 7: Real-time master mix of SYBRgreen qPCR system

Substance	Volume in µl
SYBRgreen supermix	12.5
Sense	0.25
Anti-sense	0.25
ROX reference dye	0.05
cDNA	2.0
dH_2O	9.95

Table 8: Real-time PCR procedure of Plexor system

1. Denaturation	95°C	2 min.
2. Denaturation	95°C	5 sec.
3. Annealing and extension	60°C	35 sec.
4. Dissociation	60-95°C	

Table 9: Real-time PCR procedure of SYBRgreen qPCR system

1. Denaturation	95°C	10 min.
2. Denaturation	95°C	30 sec.
3. Annealing	60°C	30 sec.
4. Extension	72°C	30 sec.
5. Dissociation	60-95°C	

3.3.6 RNA interference

RNA interference method was used for different gene knockdown in H9C2 cardiomyoblasts. siRNA oligos (ds RNA) as well as inducible shRNA plasmids were transfected into the cells. Former were ordered from Qiagen which are listed in table 10.

Table 10: siRNA oligos (Qiagen) for gene knock down

Name of the Oligo	Specificity of the oligo	Sequence of sense strand Sequence of antisense strand
α1 AMPK	rat	5'-GGCACCCUCAUAUAAUCAATT-3' 5'-UUGAUUAUAUGAGGGUGCCTG-3'
α2 AMPK	rat	5'-GGCCAUAAAGUGGCAGUUATT-3' 5'-UAACUGCCACUUUAUGGCCTG-3'
adipoR1	rat	5'-GGCUCUAUUACUCCUUCUATT-3' 5'-UAGAAGGAGUAAUAGAGCCAG-3'
adipoR2	rat	5'-AAAUUGGAUUACUCUGGUATT-3' 5'-UACCAGAGUAAUCCAAUUUAG-3'
T-cadherin	rat	5'-CCACCAUUGUGAUCGAUGATT-3' 5'-UCAUCGAUCACAAUGGUGGCT-3'
LKB1	rat	5'-GGGCGGUCAAGAUCCUCAATT-3' 5'-UUGAGAUCUUGACCGCCCTG-3'
CaMKKβ	rat	5'-GGCCCGGUUCUACUUCCAATT-3' 5'-UUGGAAGUAGAACCGGGCCTG-3'

The plasmids which can express shRNA were prepared with the help of BLOCK-iT™-Inducible H1 RNAi Entry Vector Kits (Invitrogen). The sequences of oligonuleotides of shRNA are shown in table 11. These single-stranded DNAs were later annealed and ligated in pENTR/H1/TO vector according to the manual of this kit. The annealing reaction and ligation reaction are shown in table 12. At last, it was transformed into chemical competent One Shot® TOP10 *E. coli* and cloned. Whenever this plasmid is co-transfected with pcDNA 6/TR into H9C2 cardiomyoblasts, Tet-repressor can bind on H1/TO RNAi cassette, and the expression of shRNA can be induced by tetracycline.

Table 11: Oligonucleotides for making the inducible siRNA plasmids

Specific for α1AMPK rat	top-strand: CACCGCTGTGGCTCGCCCAATTATGCGAACATAATTGGGCGAGCCACAGC bottom strand: AAAAGCTGTGGCTCGCCCAATTATGTTCGCATAATTGGGCGAGCCACAGC
Specific for α2AMPK rat	top strand: CACCGCTGACTTCGGACTCTCTAATCGAAATTAGAGAGTCGGAAGTCAGC bottom strand: AAAAGCTGACTTCGGACTCTCTAATTTCGATTAGAGAGTCCGAAGTCAGC

Table 12: Annealing and ligation reaction for making the inducible siRNA plasmids

Annealing Reaction	200 µM top strand oligo	10 µl
	200 µM bottom strand oligo	10 µl
	10 x Oligo annealing buffer	4 µl
	DNase/RNase-free water	16 µl
Ligation Reaction	5 x ligation buffer	2 µl
	pENTR/H1/TO (0.75 ng/µl)	1 µl
	ds Oligo (5 nM; 1:10.000 dilution)	2.5 µl
	DNase/RNase-free water	4 µl
	T4 DNA Ligase (1 U/µl)	0.5 µl

3.4 Protein analysis

3.4.1 Extraction of total proteins from cells and tissues

For the extraction of total proteins, the cells were scraped in 80-150 µl SDS lysis buffer (1 M Tris-HCl, pH 7.5; 1% (v/v) Sodiumdodecylsulfate (SDS), 4 M NaCl and freshly added 1:200 phosphatase/protease-inhibitor-mix). Tissues were 1:20 lysed in SDS lysis buffer and broken with Precellys tissue homogenizer (Peqlab). Then they were sonicated for 10 seconds and incubated on ice for 15 min followed by centrifugation for 20 min at 14000 rpm at 4°C. The supernatant was transferred into a new tube and the protein concentration was measured by the infinite® 200 PRO series Microplate Reader

(Tecan) with a wave length of 570 nm, using the BCA™ Protein assay kit, and bovine serum albumin (BSA) was used as standard (Pierce, Rockfort, USA) according to the manufacturer's manual.

3.4.2 SDS polyacrylamide gel electrophoresis (SDS-PAGE)

For running a SDS-PAGE, 40-100 µg protein aliquots were prepared in 1x SDS loading buffer (6 x SDS: 0.66 g DTT; 0.4 g SDS; 6 ml glycerol; 2 ml 1.25 M Tris-HCl, pH 6.8; 0.2 mg bromphenolblue; and 10 ml dH_2O), followed by denaturation for 5 min at 95°C. The SDS polyacrylamide gel, whose components are shown in table 13, was prepared with the help of the mini-protean II cell system (Bio-Rad, Munich, Germany). The samples were run on the gel together with a marker (PageRuler™ Prestained Protein Ladder Plus SM 1811; Fermentas) at 80 volt and as soon as the bromophenol blue colour enters the running gel, the voltage was increased to 140 volt.

Table 13: SDS polyacrylamide gels

	Running gel		**Stacking gel**
Concentration	**5%**	**10%**	
Sterile water	5.80 ml	4.30 ml	2.95 ml
40% acrylamid	1.50 ml	3.00 ml	0.50 ml
Buffer (1.5 M Tris-HCl, pH 8.8)	4.50 ml	4.50 ml	-
Buffer (1 M Tris-HCl, pH 6.8)	-	-	0.50 ml
10% SDS	120 µl	120 µl	40 µl
10x APS	100 µl	100 µl	25 µl
TEMED	10 µl	10 µl	5 µl

3.4.3 Western blot

Western blot is an immunological method to detect a specific protein by antibodies. Following the SDS-PAGE, an electroblotting was performed in a transfer buffer (table 14) with the help of the mini blot transfer cell-system (Bio-Rad, Munich, Germany) for 1 h at

120 Volt at 4°C, and the proteins were transfered from the gel to a nitrocellulose membrane (0.45 µM, Protran Schleicher and Schuell Bio Science GmbH Whatman group, Dassel, Germany). The membrane was stained with Ponceau S solution (table 14) afterwards and the gel can be stained with coomassie staining solution (table 14) to confirm the protein amount after blotting. Afterwards, the membrane was blocked with 5% skimmed milk which was dissolved in TBS-T buffer (table 14) for 1 h. Then the membrane was incubated with a primary antibody (table 15) which was diluted in 2.5% milk containing 0.02% NaN_3 overnight at 4°C. The next day, the membrane was washed for three times (10 min) with TBS-T buffer, and incubated with horseradish peroxidase-conjugated secondary antibody (table 16) which was diluted in 2.5% milk for 1 h at room temperature. After 3 times' washing with TBS-T buffer, the membrane was covered with an enhanced chemoluminescence (ECL) solution (100 mM Tris-HCl, pH 8.5; 0.225 mM coumaric acid; 1.25 mM luminol; 0.009% (v/v) H_2O_2) for 1 min. Finally, signals were developed by means of the machine Fusion FX7 (Peqlab, Erlangen Germany) and analyzed by FUSION-CAPT™ Software (Peqlab, Erlangen Germany) or Quantity One Software (BioRad, München Germany).

Table 14: Solutions used for Western blot

10 x running buffer	250 mM Tris 2 M glycine 35 mM SDS dest. H_2O
Transfer buffer	25 mM Tris 192 mM glycine 20% (v/v) methanol dest. H_2O
Ponceau S solution	0.5 g Ponceau S 1% (v/v) acetic acid dest. H_2O
TBS-T	100 mM NaCl 10 mM Tris 0.2% (v/v) Tween 20 dest. H_2O

Table 15: Primary antibodies used for western blot

Antibodies	Company	Species	Dilution
AMPKα	Cell Signalig Technology, Inc	Rabbit	1:1000
phospho-AMPKα (Thr 172)	Cell Signalig Technology, Inc	Rabbit	1:1000
AMPKα1	Abcam	Rabbit	1:1000
AMPKα2	Abcam	Rabbit	1:1000
phospho-ACC (Ser 79)	Cell Signalig Technology, Inc	Rabbit	1:500
GAPDH	Cell Signalig Technology, Inc	Rabbit	1:2000
adipoR1	IBL, Japan	Rabbit	1:250
LKB1	Cell Signalig Technology, Inc	Rabbit	1:1000
Complex I (mito.)	Invitrogen	Mouse	1:1000
Complex I (nucl.)	Invitrogen	Mouse	1:1000
Complex IV (mito.)	Invitrogen	Mouse	1:1000
Complex IV (nucl.)	Cell Signalig Technology, Inc	Rabbit	1:1000
Anti-BrdU	Roche	Mouse	1:100

Table 16: Secondary antibodies used for western blot

Antibodies	Company	Dilution
Anti-rabbit IgG HRP-linked	Santa-Cruz biotechnology inc.	1:5000
Anti-mouse IgG HRP-linked	Santa-Cruz biotechnology inc.	1:5000
Anti-mouse Cy3-conjugated	Sigma	1:1000

3.5 Enzyme activity measurement

The cells were trypsinized, washed with PBS and resuspended in an appropriate volume of Chappel-Perry-Medium (100 mM KCl, 5 mM $MgCl_2$, 1 mM EDTA, 50 mM Tris pH 7.5) with a concentration of $20x10^6$ cells/ml. Then they were homogenized by ultrasound with a frequency of 40 sec/ml. Small aliquots were made afterwards and stored in liquid nitrogen for further measurement.

All the enzyme activities were double measured by the photometer (Cary 50 Scan UV-Visible Spectrophotometer, Varian). The volume of all the reactions was at the end 1 ml. Before starting the reaction, all the reaction samples were incubated at 30°C for 10 min.

The enzyme activities can be calculated according to the formulas bellow:

$$U/ml = \frac{\Delta E/min \bullet Vm \bullet Fd}{\varepsilon \bullet Vs \bullet d} \qquad U/mg = \frac{U/ml}{c}$$

ΔE/min = Extinction variation / minute
Vm. = Measurement volume [µl]
Fd. = Dilution factor
ε = Extinction coefficient
Vs. = Sample volume [µl]
d = Diameter of the cuvette
c = Protein concentration in mg/ml

3.5.1 Mitochondrial complex I (NADH:Ubiquinone-Oxidoreductase)

The principle of the mitochondrial enzyme activity measurement is shown in Figure 4 below. NADH can be oxidized by NADH:Ubiquinone-Oxidoreductase. After the inhibition of Complex III and Complex IV, the activity of Complex I can be obtained.

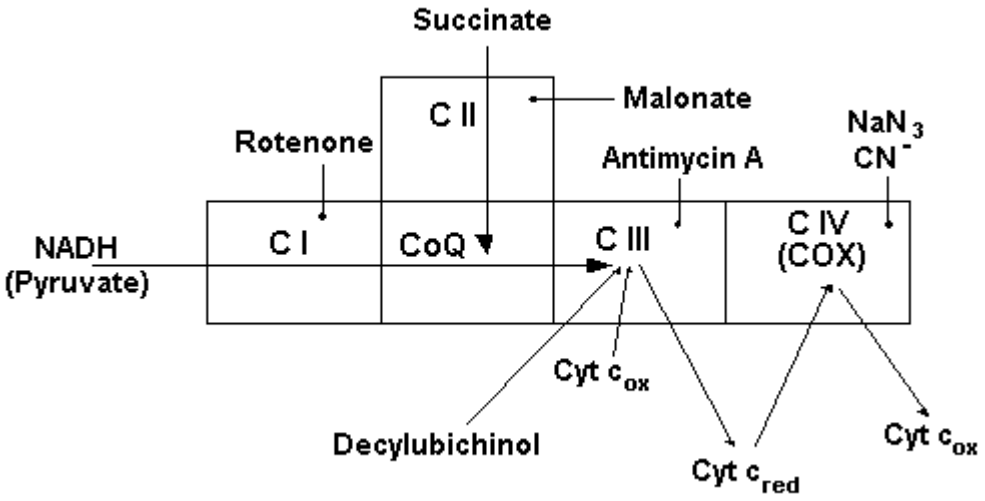

Figure 4: Roles of enzymes and molecules in respiratory chain *(C I: complex I; C II: complex II; C III, complex III; C IV, complex IV; CoQ: coenzyme Q, COX: cytochrome-c-oxidase, Cyt cox: oxidized cytochrome c, Cyt cred: reduced cytochrome c)*

Reaction: 10 mM Tris/HCl-buffer, pH 7.4; 50 mM KCl; 1 mM EDTA; 4 mM KCN; 5 µg/ml Antimycin A; 20 µl Homogenate (1:30).

Reference: Reaction with 10 µM Rotenone.

Start: 60 µM CoQ und 100 µM NADH.

Wavelength: 340 nm; $\varepsilon = 6.22\ mM^{-1} \cdot cm^{-1}$

3.5.2 Mitochondrial complex I+III (NADH:Cytochrome c- Oxidoreductase)

Cytochrome c can be reduced by both NADH: Cytochrome-c-Oxidoreductase and NADH: Cytochrome-b_5-Oxidoreductase. Since the second reaction can't be inhibited, the enzyme activity was measured and deduced by the value of reference with an inhibition of Complex III by Antimycin A (5 µg/ml).

Reaction: 50 mM K-Na-Phosphate buffer, pH 8.0; 0.1 mM EDTANa; 3 mM KCN; 80 µM Cytochrome c; 20 µl Homogenate (1:30).
Reference: Reaction with 5 µg/ml Antimycin A and 10 µM Rotenone.
Start: 0.2 mM NADH (daily fresh).
Wavelength: 550 nm; $\varepsilon = 19.2\ mM^{-1} \cdot cm^{-1}$

3.5.3 Mitochondrial complex II+III (Succinate:Cytochrome-c-Oxidoreductase)

Cytochrome c can also be reduced via Succinate:Cytochrome-c-Oxidoreductase. After the inhibition of Complex IV, the afford of substrate for Complex II, but not for Complex I, the activity of Complex II+III can be measured.

Reaction: 50 mM Phosphate buffer, pH 7.4; 0.2 mM EDTA-Na, pH 7.4; 10 mM Succinate, 1% (w/v) bovine serum albumin (BSA), 3 mM KCN; 20 µl Homogenate.
Blank: Reaction without Homogenate (1:30).
Start: 80 µM Cytochrome $c_{ox.}$
Wavelength: 550 nm; $\varepsilon = 19.2\ mM^{-1} \cdot cm^{-1}$

3.5.4 Mitochondrial complex III (Ubiquinone:Cytochrome-c-Oxidoreductase)

Besides, cytochrome c can be reduced by Ubiquinone:Cytochrome-c-Oxidoreductase in the presence of decylubichinol, whenever there is no activity of complex I and complex II.

Reaction: 50 mM Phosphate buffer, pH 8.0; 0.1 mM EDTA-Na; 0.2% (w/v) BSA; 3 mM NaN_3; 60 µM Cytochrome c_{ox}; 5 µl Homogenate.

Blank: Reaction without Homogenate (1:30).

Start: 150 µM Decylubichinol.

Wavelength: 550 nm; ε = 19.2 $mM^{-1} \cdot cm^{-1}$

3.5.5 Cytochrome-c-Oxidase (COX)

Reduced cytochrome-c can be oxidized by cytochrome-c-oxidase. In this case, the activity of COX can be easily obtained.

Reaction: 60 µM Cytochrome $c_{red;}$ 10 mM Phosphate buffer, pH 7.0;

Start: 15 µl Homogenate (1:30).

Wavelength: 550 nm; ε = 19.2 $mM^{-1} \cdot cm^{-1}$

3.5.6 Succinate-Dehydrogenase (SDH)

Succinate dehydrogenase, which is also known as complex II, can oxidize succinate into fumarate. The activity of SDH can be inhibited by malonate. Phenazine methosulfate (PMS) and 2, 6-Dichlorophenolindophenol (DCPIP) were used as electron acceptors.

Reaction: 50 mM Phosphate buffer, pH 7.4; 0.1 mM Na EDTA; 0.1% (w/v) BSA; 3 mM KCN; 10 mM Succinate; 15 µl Homogenate (1:30).

Start: 35 µM DCPIP and 1.63 mM PMS (daily fresh).

Wavelength: 600 nm; ε = 19.1 $mM^{-1} \cdot cm^{-1}$

3.5.7 Citrate-synthase (CS)

Citrate synthase catalyzes the first step in the citric acid cycle, that joins acetyl coenzyme A and oxaloacetate together to form the citrate. Another product coenzyme A, combined with 5, 5'-Dithiobis (2-nitrobenzoic acid) (DTNB), forms a coloured complex, CoA-DTNB, which can be photometrically measured at 412 nm.

Reaction: 45.5 mM Tris-buffer, pH 7.4; 0.1% (w/v) Triton; 0.1 mM DTNB (in 0.1 M Tris, pH 8.0, daily fresh); 0.1 mM Acetyl-CoA (daily fresh); 10 µl Homogenate (1:30).

Start: 0.5 mM Oxalacetate (pH 6.0-7.0, daily fresh).

Wavelength: 412 nm; $\varepsilon = 13.6\ mM^{-1} \cdot cm^{-1}$

3.6 Statistical analysis

The results were shown as mean values ± SEM. To test for statistical differences, the t-test and one-way ANOVA were used with the help of the Sigma Stat software V 3.1 (Sigma Stat Software Inc., Chicago, USA). P values < 0.05 were considered significant.

4. Results

4.1 Expression of AMPK isoforms in different cell/tissue types

Seven different isoforms of AMPK including the house keeping gene 18S rRNA were detected in different tissues and cell types including rat skeletal muscle, left ventricle of neonatal heart and adult heart, H9C2 cardiomyoblast, H9C2 cardiomyotube, neonatal and adult rat cardiomyocyte, as shown in Figure 5. Most of the isoforms existed in all cell/tissue types. In skeletal muscle, the isoforms α2, β2 and γ3 had a higher expression than the other isoforms. The expression of the α1 isoform was higher in H9C2 cardiomyoblasts and cardiomyotubes, while the expression of the α2 isoform was higher in rat adult or neonatal cardiomyocytes and rat adult or neonatal heart tissues. The expression of the β1 isoform was higher in adult or neonatal cardiomyocytes and adult or neonatal heart tissues than in H9C2 cardiomyoblasts and cardiomyotubes, while there was no major difference for the expression of the β2 isoform among the samples. The γ1 isoform was mainly expressed in adult or neonatal cardiomyocytes and adult or neonatal heart tissues. The γ2 isoform showed a higher expression in cardiomyocytes and heart tissues than in H9C2 cardiomyoblasts and cardiomyotubes. The γ3 isoform showed strongest expression in fully differentiated H9C2 cardiomyotubes, similar to rat skeletal muscle.

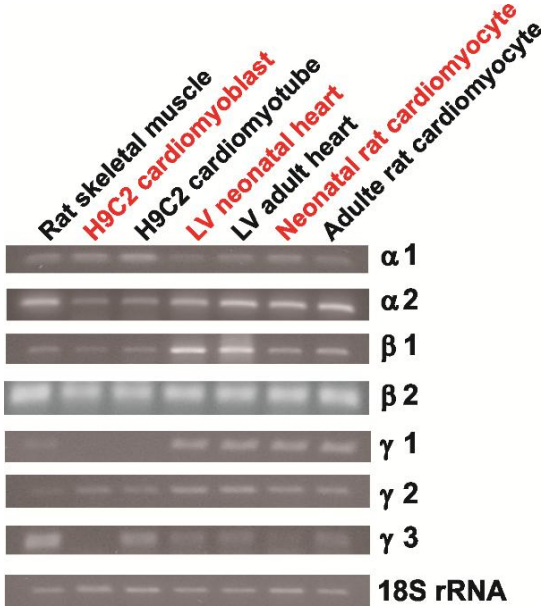

Figure 5: mRNA expression of AMPK isoforms in different tissue/cell types.

4.2 AMPK activation

4.2.1 AMPK activation by adiponectin in H9C2 cardiomyoblasts

AMPK activation in H9C2 cardiomyoblasts was analyzed by detecting AMPK phosphorylation at Thr 172 and phosphorylation of ACC, a downstream target of AMPK, at Ser79. H9C2 cardiomyoblasts were treated with 4 µg/ml recombinant adiponectin for different time periods ranging from 5 min to 24 h. As shown in Figure 6A, adiponectin induced an AMPK phosphorylation only after 5 min to 20 min of treatment, and this effect disappeared in 40 min. However, another peak of AMPK phosphorylation was observed after 24 h (Figure 6B). On the other hand, the effect of adiponectin on ACC phosphorylation seemed to be very stable between 5 min up to 24 h.

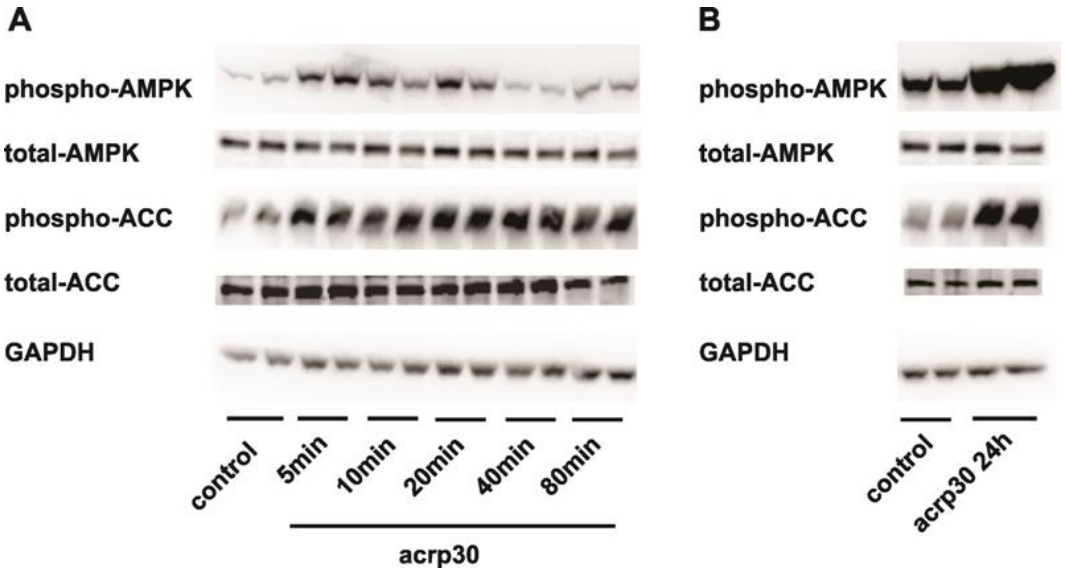

Figure 6: Western Blot analysis of phospho-AMPK in H9C2 cardiomyoblasts after adiponectin treatment.

H9C2 cardiomyoblasts were treated with 4 µg/ml adiponectin for 5 min, 10 min, 20 min, 40 min, 80 min (A) or 24 h (B). The phosphorylation of AMPK and ACC were detected specifically with a phospho-AMPK (Thr172) or phospho-ACC (Ser79) antibody. Total AMPK and total ACC were detected with total-AMPK or total-ACC antibody. GAPDH was used as a loading control. n=2 per group.

4.2.2 AMPK activation by adiponectin in rat adult cardiomyocytes

AMPK activation was also analyzed in freshly isolated adult rat ventricular cardiomyocytes by detecting AMPK phosphorylation at Thr 172 and phosphorylation of ACC at Ser79. In addition, an AMPK inhibitor, adenine 9-beta-d-arabinofuranoside (AraA), was used to inhibit AMPK activation. Cells were preincubated with or without 1mM AraA for 30 min and then incubated with 4 µg/ml recombinant adiponectin for 5 or 10 min. There was a significant increase of AMPK phosphorylation, as well as the phosphorylation of ACC, in adult cardiomyocytes in 5 min and 10 min after adiponectin treatment. Both effects were abolished by AraA pretreatment (Figure 7A). Similar to the results obtained in H9C2 cardiomyoblasts, adiponectin treatment resulted in an increased phosphorylation of both AMPK and ACC in cardiomyocytes after 24 h (Figure 7B).

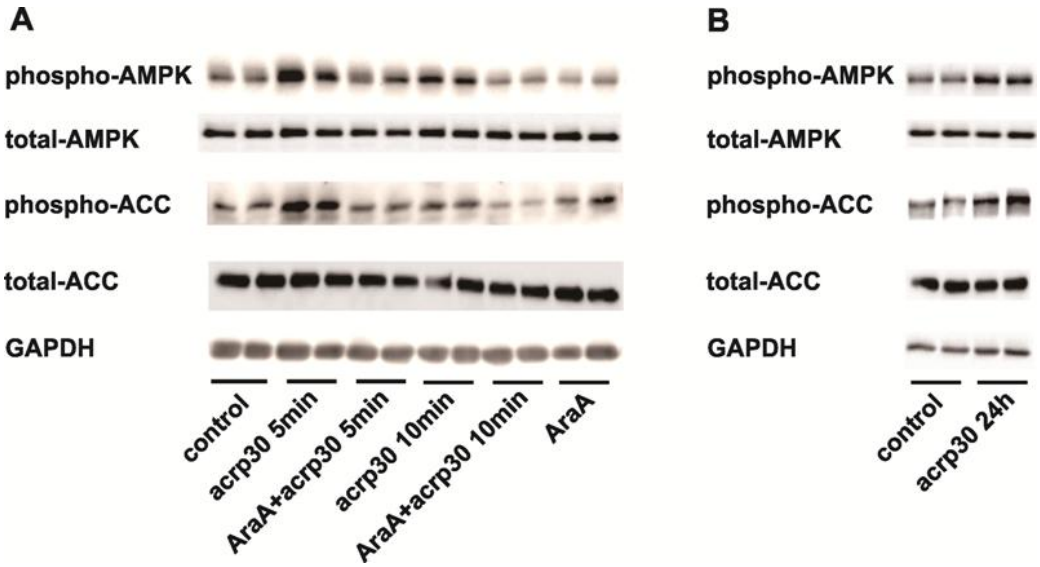

Figure 7: Western Blot analysis of phospho-AMPK in rat adult cardiomyocytes after adiponectin treatment.

Rat adult cardiomyocytes were pretreated with 1 mM AraA for 30 min, and then treated with 4 µg/ml adiponectin for 5 min, 10 min (A) or just 4 µg/ml adiponectin for 24 h (B). The phosphorylation of AMPK and ACC were detected specifically with a phospho-AMPK (Thr172) or phospho-ACC (Ser79) antibody. Total AMPK and total ACC were detected with total-AMPK or total-ACC antibody. GAPDH was used as a loading control. n=2 per group.

4.2.3 mRNA Expression of adiponectin receptors in adult rat cardiomyocytes and H9C2 cardiomyoblasts

So far, three different adiponectin receptors adipoR1, adipoR2 and T-cadherin have been described in the literature. The expression of those three adiponectin receptors was analyzed in adult rat cardiomyocytes and H9C2 cardiomyoblasts by semi-quantitative PCR. As shown in Figure 8, the mRNA expression of adipoR1 was much higher in cardiomyocytes than in H9C2 cardiomyoblasts, while adipoR2 and T-cadherin were equally expressed in those two cell types. Furthermore, T-cadherin mRNA expression was higher in both cardiomyocytes and H9C2 cardiomyoblasts compared to the other two adipoRs. The mRNA expression of adipoR1 and adipoR2 was similar in adult rat cardiomyocytes, whereas the mRNA expression of adipoR2 was much higher than adipoR1 mRNA expression in H9C2 cardiomyoblasts.

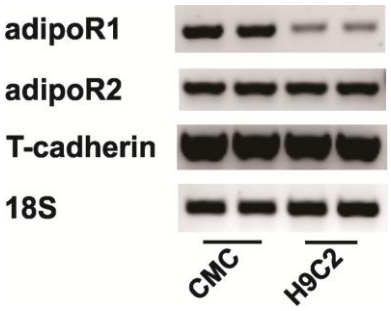

Figure 8: Expression of adiponectin receptors in rat adult cardiomyocytes and H9C2 cardiomyoblasts.

mRNA expression of adipoR1, adipoR2, T-cadherin and 18S rRNA was determined by semi-quantitative PCR and agarose gel electrophoresis. CMC: cardiomyocyte. n=2 per group.

4.2.4 Role of adiponectin receptors in adiponectin-induced AMPK activation

In order to investigate the role of adiponectin receptors in adiponectin-mediated AMPK phosphorylation, we performed a transient knockdown of the adiponectin receptors (adipoR1, adipoR2 or T-cadherin) in H9C2 cardiomyoblasts. The knockdown efficiency of those siRNAs was determined on the mRNA level (Figure 9) and protein level (not shown). As shown in Figure 9, the knockdown efficiency of both adipoR1 siRNA and

adipoR2 siRNA was up to 80% after 48 h, and T-cadherin siRNA had a knockdown efficiency of 60%. Although there are similarities in sequence and structure between adipoR1 and adipoR2, the tested siRNAs were proved to be specific for the respective receptor (Figure 9).

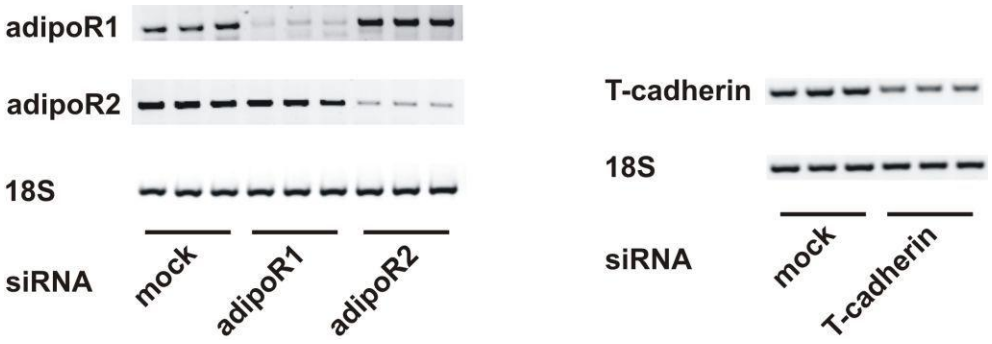

Figure 9: Knockdown of adipoR1, adipoR2 or T-cadherin in H9C2 cardiomyoblasts.
H9C2 cardiomyoblasts were transfected with mock, adipoR1, adipoR2 or T-cadherin siRNA for 48 h. mRNA expression of adipoR1, adipoR2, T-cadherin and 18SrRNA was determined by semi-quantitative PCR and agarose gel electrophoresis. n=3 per group.

Therefore, H9C2 cardiomyoblasts were transfected with mock, adipoR1, adipoR2 or T-cadherin siRNA for 24 h and then treated with or without 4 µg/ml recombinant adiponectin for another 24 h. As shown in Figure 10, there was a higher basal AMPK phosphorylation in the control cells than in cells after adipoR1 or adipoR2 knockdown. However, adiponectin was able to induce a significant AMPK phosphorylation in the control cells as well as in the adipoRs knockdown cells. Adiponectin-induced AMPK phosphorylation in adipoR1 knockdown cells did not reach the same level as in the control cells. Although basal AMPK activation was strongly reduced, adiponectin-mediated AMPK phosphorylation in adipoR2 knockdown cells reached the same level as in the control cells. Opposite to these results, T-cadherin knockdown did not result in a reduction in basal AMPK phosphorylation, but adiponectin was not able to induce AMPK phosphorylation in T-cadherin knockdown cells.

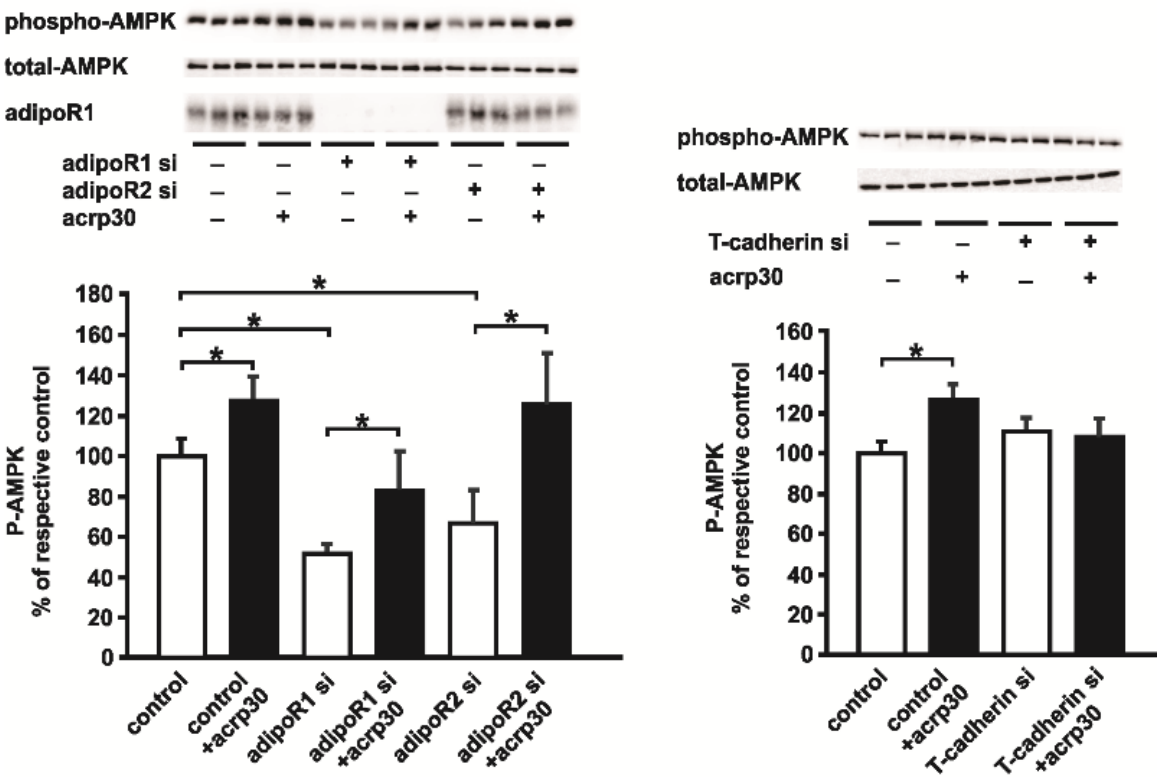

Figure 10: Role of adiponectin receptors in adiponectin-induced AMPK phosphorylation in H9C2 cardiomyoblasts.

*H9C2 cardiomyoblasts were first transfected with mock, adipoR1 or adipoR2 siRNA for 24 h and then treated with or without 4 µg/ml adiponectin for another 24 h. Phosphorylation of AMPK, total AMPK and adipoR1 were detected with phospho-AMPK (Thr172), total-AMPK or adipoR1 antibody. Data represents the mean ± SEM (n=3 per group). *p<0.05.*

4.2.5 Role of AMPK upstream kinases, LKB1 and CaMKKβ on adiponectin-induced AMPK activation

In order to identify the role of the two AMPK upstream kinases in adiponectin-mediated AMPK phosphorylation, we also performed a transient knockdown of LKB1 or CaMKKβ before adiponectin treatment. The knockdown efficiency of those siRNAs was determined on the mRNA level (Figure 11) and protein level (not shown). As shown in Figure 11, the knockdown efficiency of both LKB1 siRNA and CaMKKβ siRNA was up to 60% after 48 h.

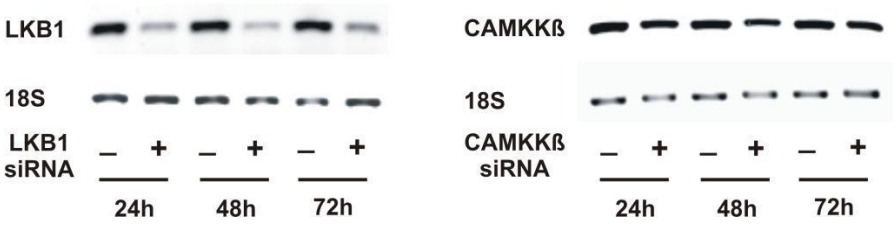

Figure 11: Knockdown of LKB1 and CaMKKβ in H9C2 cardiomyoblasts.

H9C2 cardiomyoblasts were transfected with mock, LKB1 or CaMKKβ siRNA for 24 h, 48 h and 72 h. mRNA expression of LKB1, CaMKKβ and 18S rRNA was determined by semi-quantitative PCR and agarose gel electrophoresis. n=3 per group.

Therefore, H9C2 cardiomyoblasts were first transfected with mock, LKB1 or CaMKKβ siRNA for 24 h, and then treated with or without 4 µg/ml recombinant adiponectin for another 24 h. These experiments showed a dramatically lower basal phosphorylation level of AMPK in those LKB1 or CaMKKβ knockdown cells. However, opposite to the results obtained after adipoR1 or adipoR2 knockdown, adiponectin could not induce AMPK phosphorylation in those cells (Figure 12).

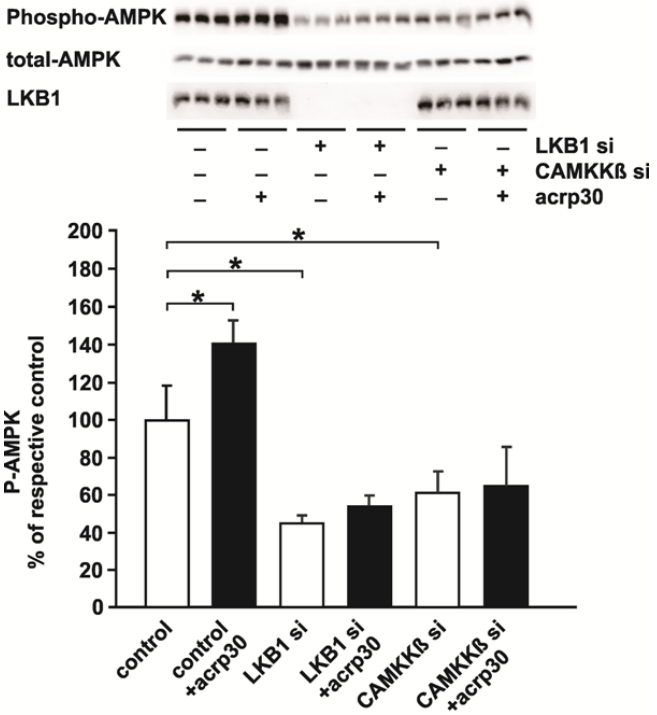

Figure 12: Role of AMPK upstream kinases in adiponectin-induced AMPK phosphorylation in H9C2 cardiomyoblasts.

*H9C2 cardiomyoblasts were first transfected with mock, LKB1 or CaMKKβ siRNA for 24 h and then treated with or without 4 µg/ml adiponectin for another 24 h. Phosphorylation of AMPK, total AMPK and LKB1 were detected with phospho-AMPK (Thr172), total-AMPK or LKB1 antibody. Data represents the mean ± SEM (n=3 per group). *p<0.05.*

4.2.6 AMPK activation by A-769662

A-769662 (6,7-Dihydro-4-hydroxy-3-(2'-hydroxy[1,1'-biphenyl]-4-yl)-6-oxo-thieno[2,3-*b*]pyridine-5-carbonitrile) is a small molecular which is able to directly activate AMPK. H9C2 cardiomyoblasts were incubated with A-769662 with different concentrations (1, 10, 50 and 100 µM) for 3 h. AMPK activation was analyzed by detecting AMPK phosphorylation at Thr172 and phosphorylation of ACC at Ser79. As shown in Figure 13, phosphorylation of AMPK and ACC was significantly increased in a dose dependent manner.

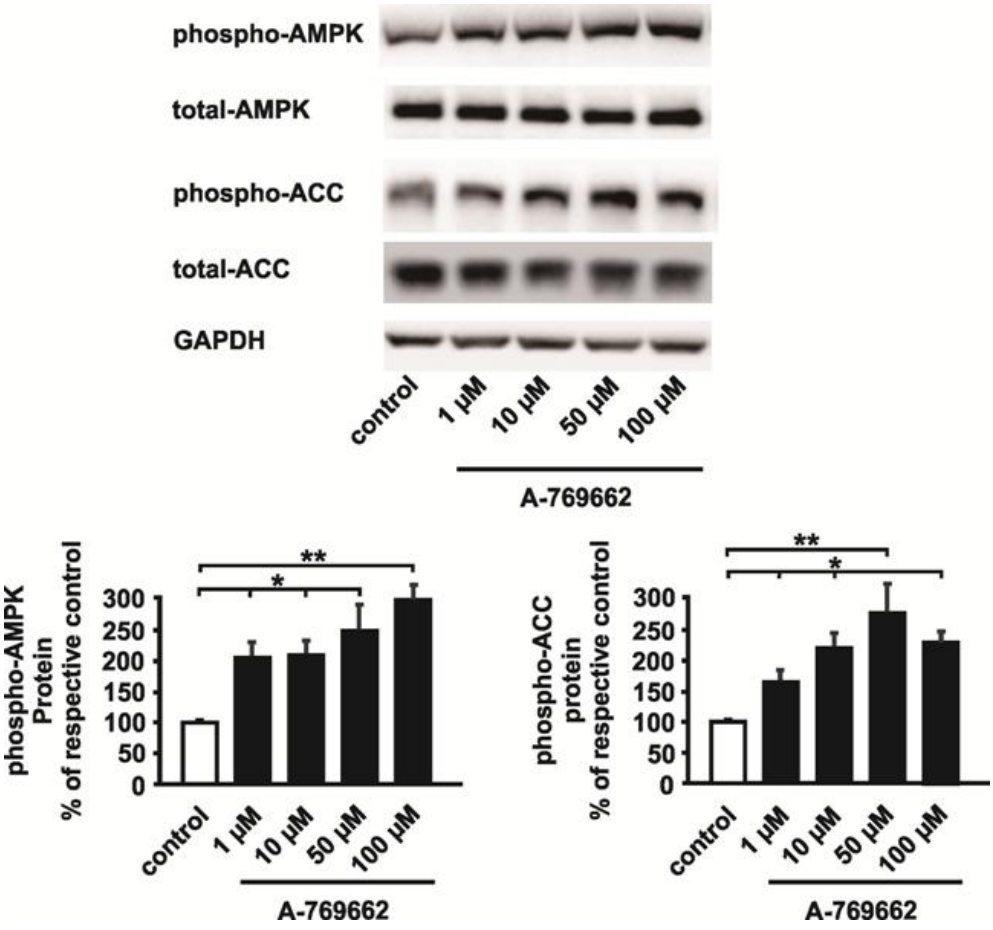

Figure 13: Western Blot analysis of phospho-AMPK and phospho-ACC in H9C2 cardiomyoblasts treated with A-769662 for 3 h.

*H9C2 cardiomyoblasts were treated with A-769662 with different concentrations (1, 10, 50 or 100 µM) for 3 h. Phosphorylation of AMPK and ACC were detected specifically with a phospho-AMPK (Thr172) or phospho-ACC (Ser79) antibody. Total AMPK and total ACC were detected with total-AMPK or total-ACC antibody. GAPDH was used as a loading control. n=3 per group. *p<0.05; **p<0.005.*

4.3 Effect of AMPK activation on mitochondrial biogenesis

In order to know if AMPK activation affects mitochondrial biogenesis, and if there's a difference in time course or extent of the observed changes between physiological AMPK activation and pharmacological AMPK activation, two different AMPK activators were used in this experiment: adiponectin and A-769662. H9C2 cardiomyoblasts were treated either with 4 µg/ml recombinant adiponectin or 10 µM A-769662 for 12 h, 24 h or 48 h. mRNA expression of the mitochondrial transcription factor PGC-1α, NRF1, Tfam, and the mitochondrial OXPHOS genes ND5, NDUFB8, COX1 and COX4 were analyzed by PCR. As shown in Figure 14A, adiponectin treatment resulted in a strong increase in the mRNA expression of various genes, known to indicate mitochondrial biogenesis. However, the time course for this effect was quite diverse. The mRNA expression of genes encoding for proteins of the respiratory chain (ND5, COX4) was induced after 12 h and declined afterwards. The mRNA expression of mitochondrial transcription factors NRF1 and Tfam was induced only after 48 h. PGC-1α showed a minor acute increase in the mRNA expression (Figure 14A), but tended to show a reduced expression after 48 h. The pharmacological AMPK activator, A-769662, had a similar effect as adiponectin on the mRNA expression of NRF1 and Tfam. Opposite to the results obtained after adiponectin treatment, A-769662 induced the expression of ND5 and COX4 at a later time point (24 h) as shown in Figure 14B.

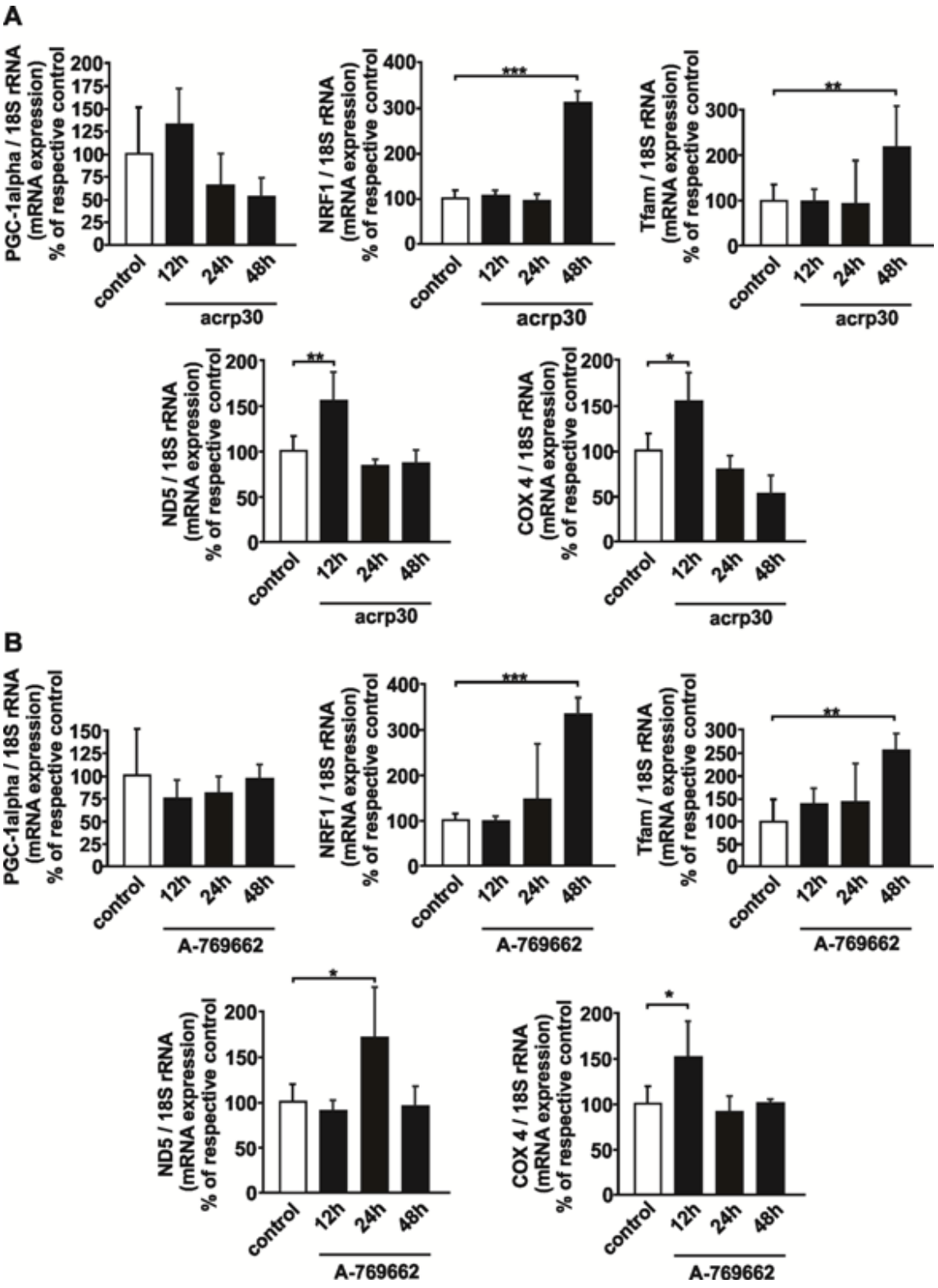

Figure 14: Effect of AMPK activation by adiponectin (A) or A-769662 (B) on mitochondrial gene expression in H9C2 cardiomyoblasts.

*H9C2 cardiomyoblasts were treated with either 4 µg/ml adiponectin (A) or 10 µM A-769662 (B) for 12 h, 24 h or 48 h. The expression of different genes were analyzed by means of semi-quantitative PCR, and normalized with 18S rRNA. Data represents the mean ± SEM (n=3 per group). *p<0.05; **p<0.005; ***p<0.001.*

4.4 Adiponectin mediated mitochondrial changes

4.4.1 Effect of adiponectin and AMPK activation on mitochondrial gene expression.

The physiological AMPK activator, adiponectin, was used for the further experiments. In order to know if AMPK mediates adiponectin induced mitochondrial gene expression, H9C2 cardiomyoblasts were preincubated with the AMPK inhibitors Compound C or AraA for 30 min, and then treated with 4 µg/ml recombinant adiponectin for 24 h. Mitochondrial gene expression of complex I gene ND1 and complex IV gene COX3 were determined by semi-quantitative PCR. Adiponectin induced the mRNA expression of ND1 and COX3. Neither Compound C nor AraA influenced the basal mRNA expression of ND1 and COX3, but both of them reduced adiponectin-mediated increase in the mRNA expression of ND1 and COX3. The effect of AraA on the expression of these genes appeared to be stronger than the effect of compound C (Figure 15), although the reduction in AMPK phosphorylation achieved by these inhibitors at the indicated concentrations was comparable (not shown).

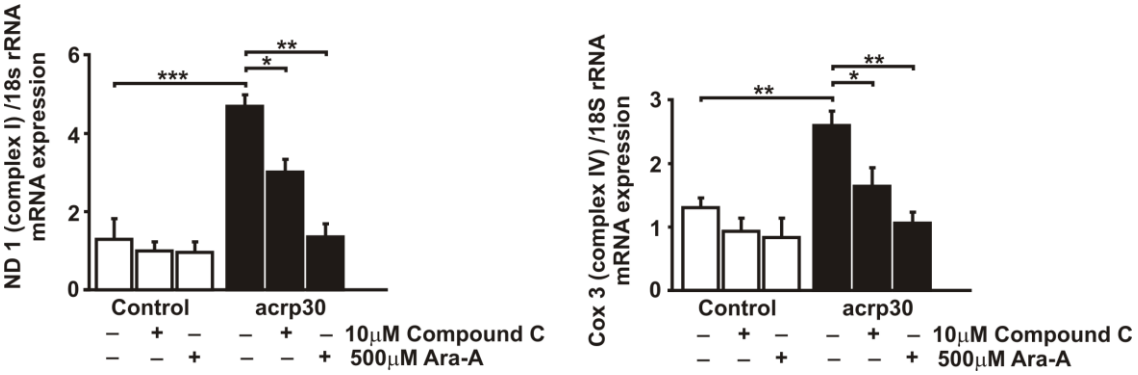

Figure 15: Effect of adiponectin and AMPK activation on mitochondrial gene expression. *H9C2 cardiomyoblasts were pretreated with 10 µM compound C or 1 mM AraA for 30 min, and then treated with 4 µg/ml adiponectin for 24 h. Gene expression of ND1 and COX3 was determined by semi-quantitative PCR and normalized with 18S rRNA. Data represents the mean ± SEM (n=3 per group). *p<0.05; **p<0.01; ***p<0.001.*

4.4.2 Effect of adiponectin and AMPK activation on mitochondrial enzyme activities.

For the functional effect of adiponectin and AMPK activation on mitochondrial enzyme

activities, H9C2 cardiomyoblasts were preincubated with or without 1 mM AraA for 30 min, and then treated with 4 µg/ml recombinant adiponectin for 24 h. Cell homogenates were used for this analysis, and the enzymes including mitochondrial Complex I, Complex I+III, cytochrome-c-oxidase (COX) of the respiratory chain were determined. All enzyme activities were related to the activity of citrate synthase in the homogenate, which is a marker enzyme of mitochondrial content.

After incubation with adiponectin for 24 h, the mitochondrial enzyme activities of complex I+III and complex IV were increased (Figure 16). AraA-preincubation completely abolished this effect without influencing the basal activities of complex I+III and complex IV.

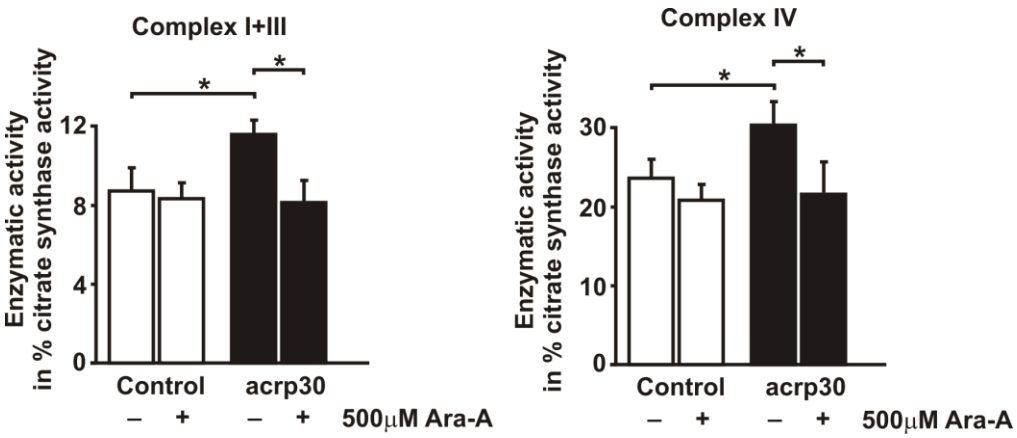

Figure 16: Effect of adiponectin and AMPK activation on mitochondrial enzyme activities in H9C2 cardiomyoblasts.

*H9C2 cardiomyoblasts were pretreated with or without 1 mM AraA for 30 min, and then treated with or without 4 µg/ml adiponectin for 24 h. Data were shown with activities in % citrate synthase activity and represents the mean ± SEM (n=3 per group). *p<0.05.*

4.4.3 Generation of inducible stable H9C2 cell lines with knockdown of AMPK

In order to know the impact of a chronic deficiency in one of the two AMPK α isoforms on adiponectin-induced mitochondrial gene expression and adiponectin-mediated changes in mitochondrial enzyme activities, we generated inducible stable H9C2 cell lines. These cell lines included one control cell line, one α1 AMPK knockdown cell line and one α2 AMPK knockdown cell line. The expression of shRNA directed against α1 or

α2 AMPK and therefore the knockdown effect of α1 or α2 AMPK in those stable H9C2 cell lines were initiated by tetracycline, as shown in Figure 17. Cells were incubated with 10 µg/ml tetracycline for 24 h, 48 h or 96 h. After 96 h, the strongest knockdown effect was observed. The expression of α1 or α2 AMPK was not affected after tetracycline treatment in stable mock-transfected cells (Figure 17).

Interestingly, in these stable cell lines, we observed an upregulation of α2 AMPK protein in α1 AMPK knockdown cells compared to the mock control cell line. However, there was no upregulation of α1 AMPK protein in α2 AMPK knockdown cells (Figure 17).

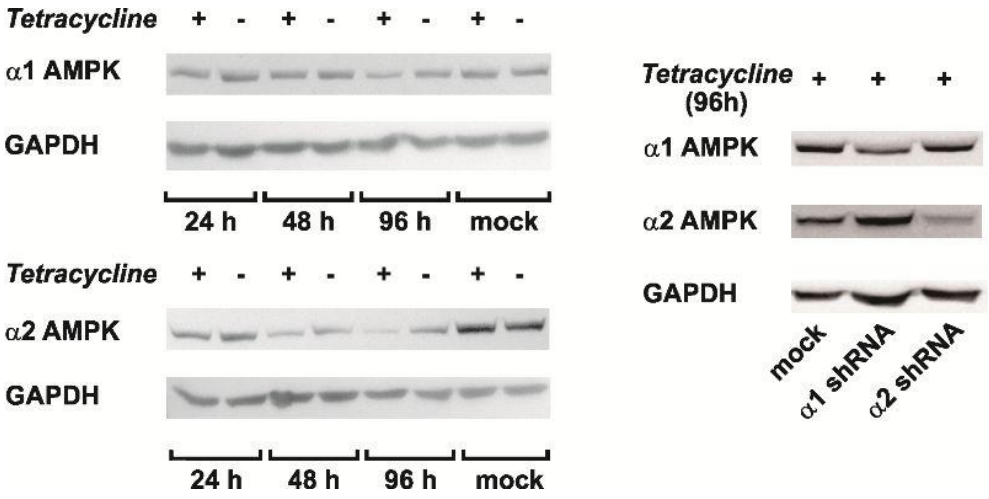

Figure 17: Tetracycline-induced RNAi knockdown of α1 or α2 AMPK in H9C2 cardiomyoblasts.

The H9C2 cardiomyoblasts were stably co-transfected with pcDNA6/TR and pENTR/H1/TO mock/α1/α2 shRNA, and incubation with or without 10 µg/ml tetracycline for 24, 48, or 96 h. The expression of α1 or α2 AMPK were detected specifically with anti-α1 or α2 AMPK antibody. GAPDH was used as a loading control.

4.4.3.1 Adiponectin-induced AMPK phosphorylation in stable AMPK knockdown H9C2 cell lines

Stable H9C2 cardiomyoblasts (from control cell line, α1 AMPK knockdown cell line, α2 AMPK knockdown cell line) were incubated with 10 µg/ml tetracycline for 72 h and then treated with 4 µg/ml recombinant adiponectin for another 24 h. We observed a significant reduction in basal AMPK phosphorylation in both AMPK knockdown cells compared to the control cells. Furthermore, there was no significant increase in

adiponectin-induced AMPK phosphorylation in both AMPK knockdown cell lines compared to the control cell line, as shown in Figure 18.

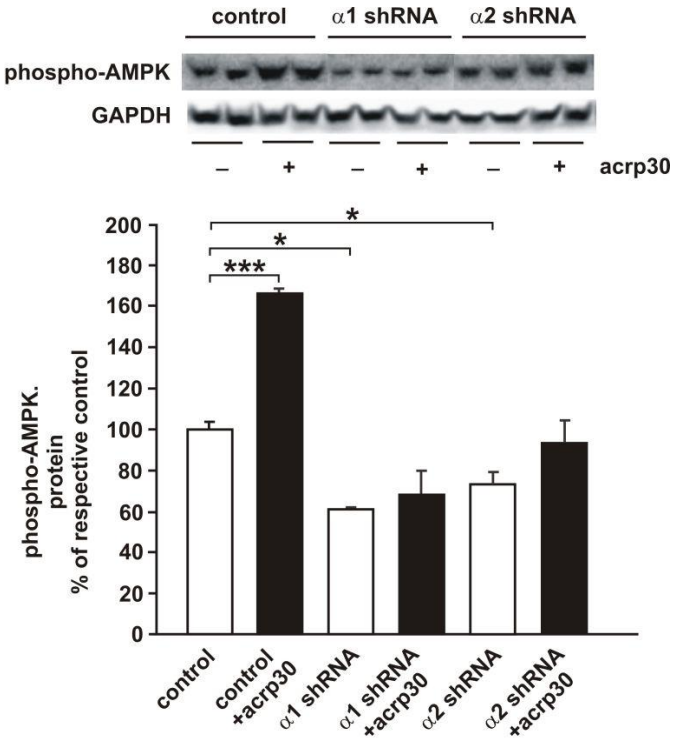

Figure 18: Adiponectin-induced AMPK phosphorylation in stable AMPK knockdown H9C2 cell lines.

*Stable H9C2 cardiomyoblasts were incubated with 10 µg/ml tetracycline for 72 h and then treated with 4 µg/ml adiponectin for another 24 h. Protein expression of phospho-AMPK was detected by specific phospho-AMPK antibody (T172). GAPDH was used as a loading control. Data represents % of respective control and mean ± SEM (n=3 per group). **p<0.01.*

4.4.3.2 Impact of alpha AMPK isoforms on adiponectin-induced complex I expression.

Stable H9C2 cardiomyoblasts (from control cell line, α1 AMPK knockdown cell line, α2 AMPK knockdown cell line) were incubated with 10 µg/ml tetracycline for 72 h and then treated with 4 µg/ml adiponectin for another 24 h. As shown in Figure 19A, the basal mRNA expression of nuclear-encoded complex I gene, NDUFB8, was significantly reduced in the α1 and α2 AMPK knockdown cells. The mRNA expression of NDUFB8 was significantly increased after adiponectin treatment in the control cell line, but not in the α1 and α2 AMPK knockdown cell lines. Similar results were obtained for the mRNA

expression of mitochondrial-encoded complex I gene, ND1 (Figure 19A). Similarly, the basal protein expression of complex I, either mitochondrial-encoded ND1 or nuclear-encoded NDUFB8, was significantly reduced in the α1 and α2 AMPK knockdown cells. Furthermore, the protein expression of ND1 and NDUFB8 was significantly increased after adiponectin treatment in the control cell line, but not in the α1 and α2 AMPK knockdown cell lines (Figure 19B).

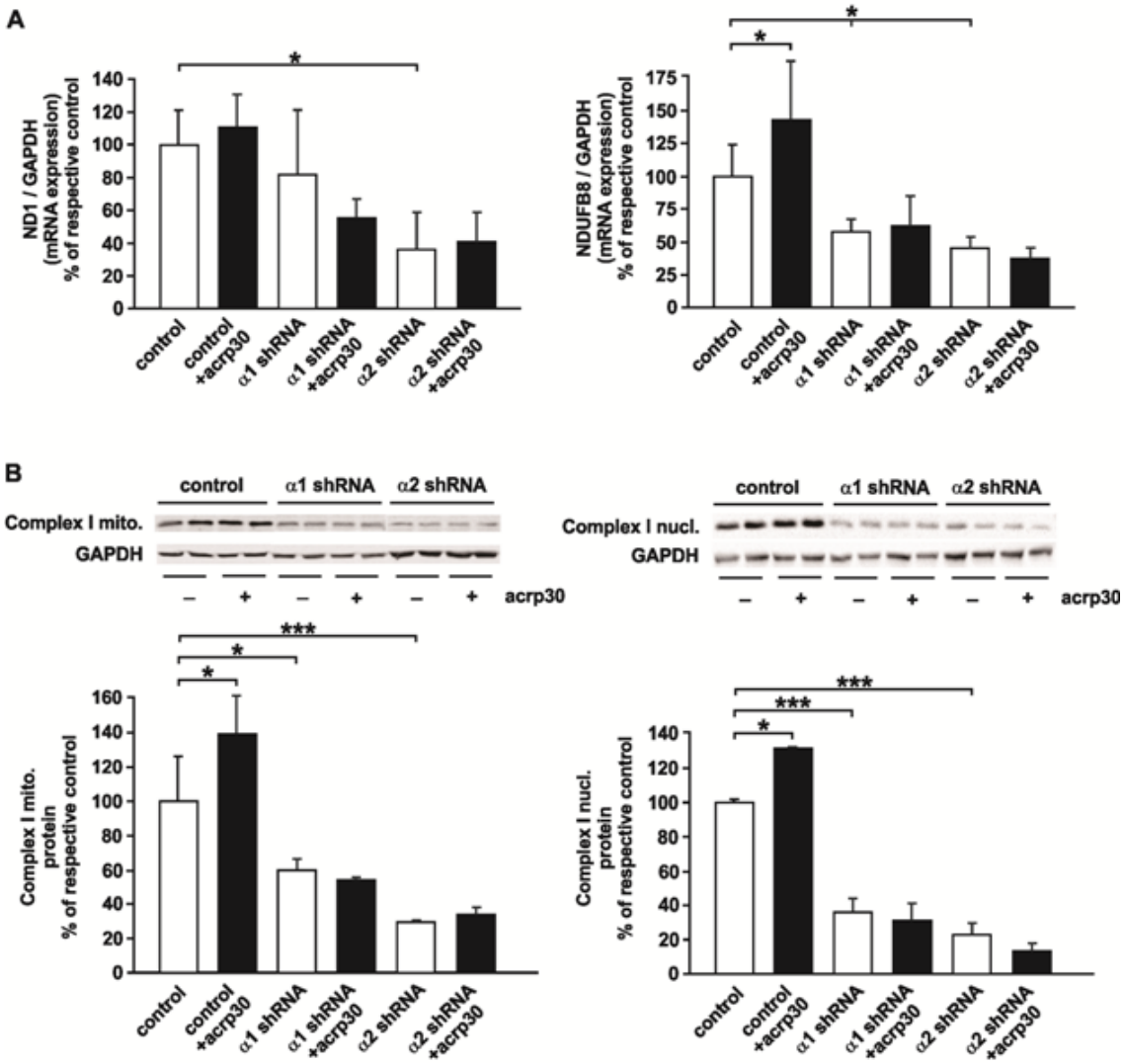

Figure 19: Mitochondrial complex I expression in stable AMPK knockdown H9C2 cell lines after adiponectin treatment.

*Stable H9C2 cardiomyoblasts were incubated with 10 µg/ml tetracycline for 72 h and then treated with 4 µg/ml adiponectin for another 24 h. A: mRNA expression of ND1 and NDUFB8 was detected by plexor real-time PCR. B: Protein expression of the mitochondrial-encoded complex I gene ND1 and nuclear-encoded complex I gene NDUFB8 was determined by western blot with specific anti-ND1 or anti-NDUFB8 antibodies. GAPDH was used as a loading control. Data represents % of respective control and mean ± SEM (n=3 per group). *p<0.05; **p<0.01; ***p<0.001.*

4.4.3.3 Impact of alpha AMPK isoforms on adiponectin-induced complex IV expression.

Besides the mRNA and protein expression of components of complex I of the respiratory chain, the expression of complex IV was investigated in those stable H9C2 cell lines with or without adiponectin treatment as well. Cells (from control cell line, α1 AMPK knockdown cell line, α2 AMPK knockdown cell line) were incubated with 10 μg/ml tetracycline for 72 h and then treated with 4 μg/ml recombinant adiponectin for another 24 h. Not like the expression of complex I genes, the basal mRNA expression of complex IV genes in α1 and α2 AMPK knockdown cells was similar as in the control cells (Figure 20A). However, the mRNA expression of mitochondrial-encoded complex IV gene COX I and nuclear-encoded complex IV gene COX IV was significantly increased after adiponectin treatment in the control cell line, but not in the AMPK knockdown cell lines (Figure 20A). Similarly, the basal protein expression of complex IV genes in α1 and α2 AMPK knockdown cells was also similar as in the control cells (Figure 20B). However, the protein expression of complex IV genes, either mitochondrial-encoded COX I or nuclear-encoded COX IV was significantly increased after adiponectin treatment in the control cell line, but not in the α1 and α2 AMPK knockdown cell lines (Figure 20B).

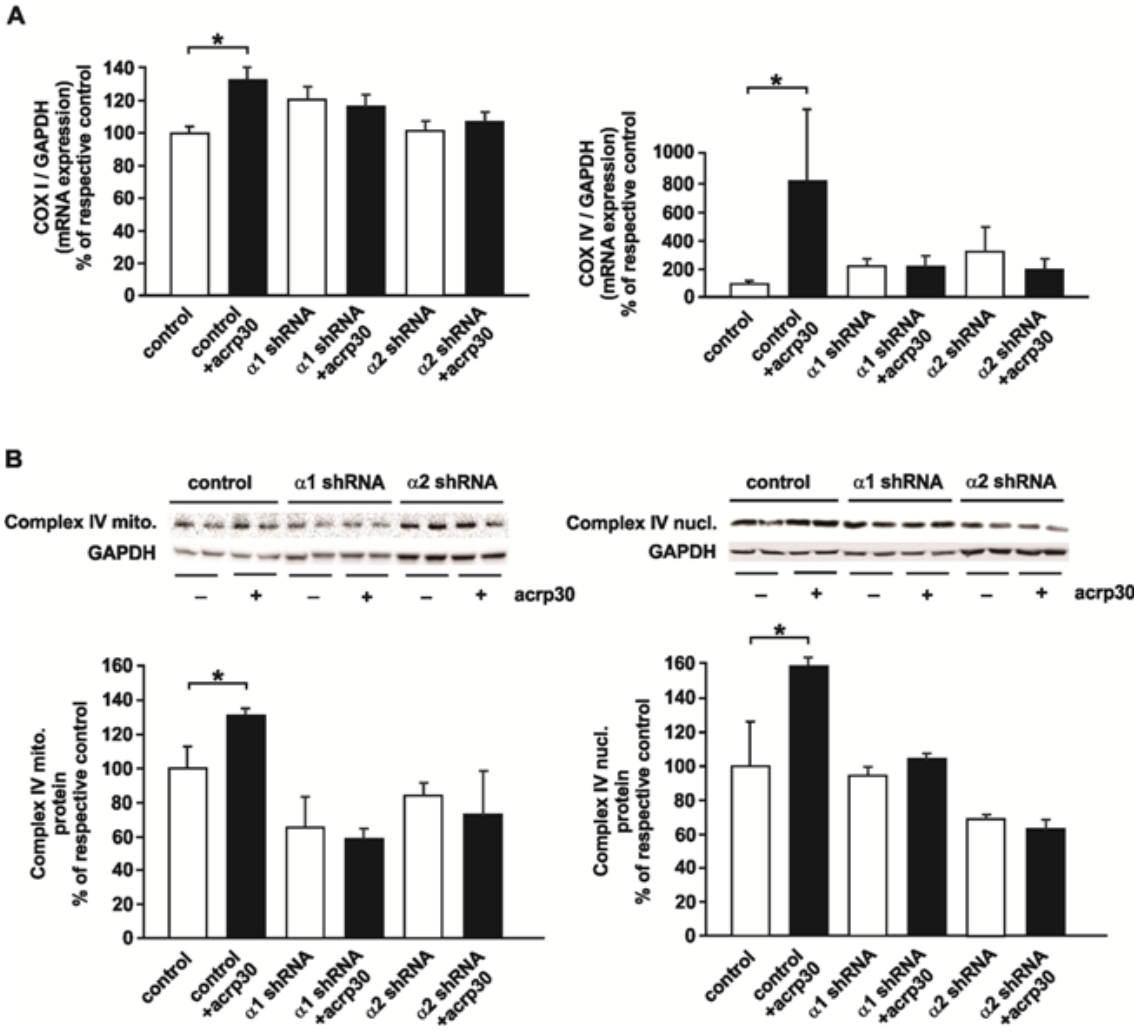

Figure 20: Mitochondrial complex IV expression in stable AMPK knockdown H9C2 cell lines after adiponectin treatment.

*Stable H9C2 cardiomyoblasts were incubated with 10 µg/ml tetracycline for 72 h and then treated with 4 µg/ml adiponectin for another 24 h. A: mRNA expression of COX I and COX IV was determined by real-time PCR. B: Protein expression of mitochondrial-encoded complex IV and nuclear-encoded complex IV was determined by western blot with specific anti-COX I or anti-COX IV antibodies. GAPDH was used as a loading control. Data represents % of respective control and mean ± SEM (n=3 per group). *p<0.05; **p<0.01.*

4.4.3.4 Impact of alpha AMPK isoforms on adiponectin-mediated changes in mitochondrial enzyme activities.

The enzyme activities of complex I, II, III and IV of the respiratory chain were then measured in those stable H9C2 cardiomyoblasts which were treated with or without adiponectin. Cells (from control cell line, α1 AMPK knockdown cell line, α2 AMPK

knockdown cell line) were incubated with 10 µg/ml tetracycline for 72 h and then treated with 4 µg/ml adiponectin for another 24 h. As shown in Figure 21, the basal activities of complex I+III and complex IV were significantly reduced in α1 and α2 AMPK knockdown cell lines compared to the control cell line. The enzyme activities of complex I+III and complex IV were increased after adiponectin treatment in the control cell line, but not in the α1 and α2 AMPK knockdown cell lines. We also measured the activities of complex I (according to Lenaz) (Lenaz, Fato et al. 1995) and complex III individually in those samples in addition to the combined measurement of complex I+III. There was a significant reduction of basal activities of complex I and complex III in α1 and α2 AMPK knockdown cell lines compared to the control cell line (data not shown), and we observed also no stimulatory effect of adiponectin in these cells. Interestingly, the basal enzyme activity of complex II of the respiratory chain, which contains only proteins encoded by the nuclear genome, was not decreased in α1 and α2 AMPK knockdown cells. This is a strong difference to the changes in basal enzyme activities of complex I, III and IV, which all contain a certain amount of mitochondrial encoded proteins. Furthermore, the enzyme activity of complex II was significantly increased after adiponectin treatment in the control cell line, but only minor changes were observed in α1 and α2 AMPK knockdown cell lines (Figure 21). We observed no change in the activity of citrate synthase at basal level or after adiponectin treatment in those cell lines (Figure 21). Furthermore, the activities of selected glycolytic enzymes, such as lactate dehydrogenase (LDH) and phosphoglucose isomerase (PGI) didn’t show any change after AMPK knockdown or adiponectin treatment (data not shown).

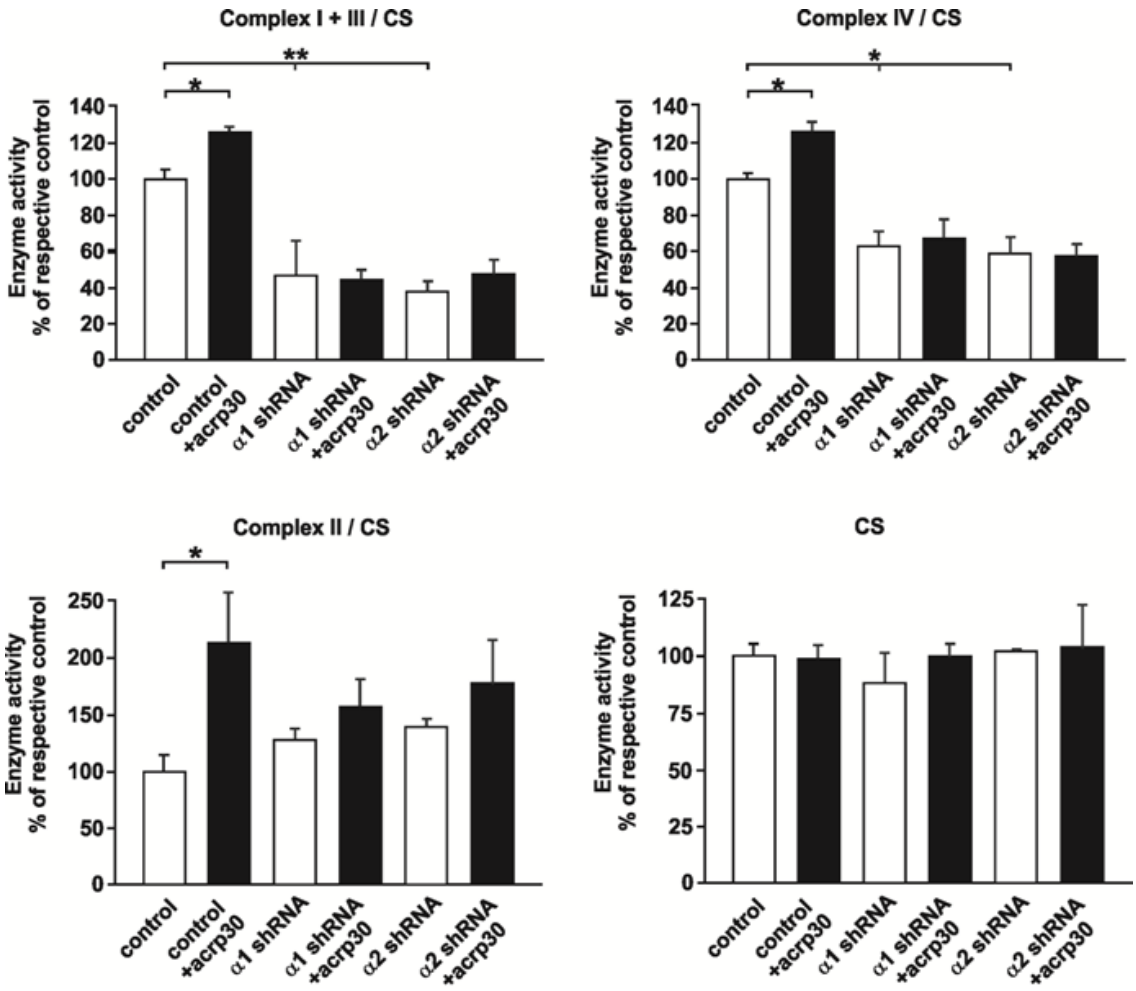

Figure 21: Mitochondrial enzyme activities in stable AMPK knockdown H9C2 cell lines after adiponectin treatment.

*Stable H9C2 cardiomyoblasts were incubated with 10 µg/ml tetracycline for 72 h and then treated with 4 µg/ml adiponectin for another 24 h. Data represents enzyme activities normalized to citrate synthase activity and in % of respective control. Data were shown as mean ± SEM (n=3 per group). *p<0.05.*

4.5 Analysis in alpha1 and alpha2 AMPK knockout mice

4.5.1 Expression of alpha AMPK in alpha1 and alpha2 AMPK knockout mice

Here, we compared the influence of an α AMPK isoform knockout on the expression of the respective other α AMPK isoform in tissues from mice with a global α1 or α2 AMPK knockout. As mentioned before, in our stable cell lines, we observed an upregulation of α2 isoform in α1 AMPK knockdown cells, but no α1 isoform upregulation in α2 AMPK knockdown cells. However, there was no upregulation of the α2 isoform in cardiac

tissue of α1 AMPK knockout mice. Meanwhile, there was an upregulation of the α1 isoform in the skeletal muscle but not in the cardiac tissue of α2 AMPK knockout mice (Figure 22).

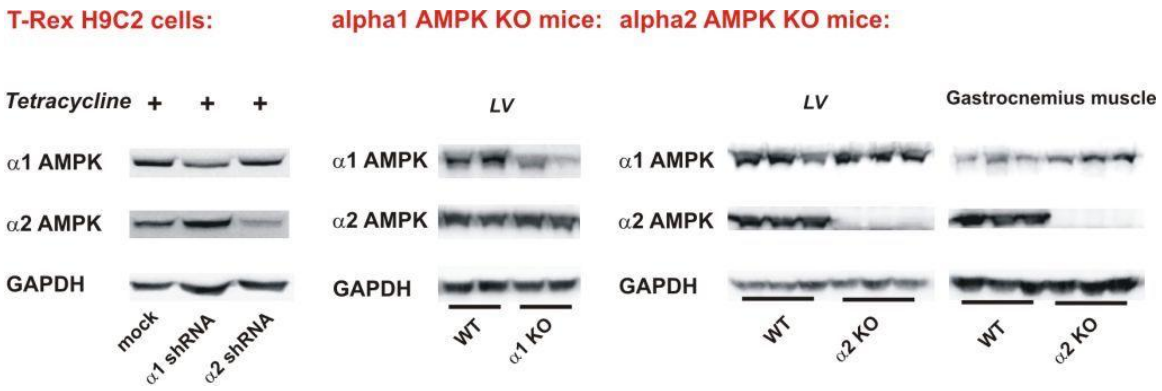

Figure 22: Expression of α AMPK isoforms in different AMPK knockdown or knockout models.

Stable H9C2 cardiomyoblasts were incubated with 10 µg/ml tetracycline for 96 h. Protein expression of α AMPK isoforms was detected by specific α1 or α2-AMPK antibody. GAPDH was used as a loading control. KO: knockout; n=2 or 3 per group.

4.5.2 Mitochondrial gene expression in alpha1 and alpha2 AMPK knockout mice

In those AMPK knockout mice models, we also analyzed the protein expression of the mitochondrial-encoded genes of complex I (ND1) and complex IV (COX I) and the nuclear-encoded genes of complex I (NDUFB8) and complex IV (COX IV). We observed no downregulation of the mitochondrial or nuclear encoded complex I or complex IV genes in the cardiac tissue of α1 AMPK knockout mice. However, in α2 AMPK knockout mice, we observed a downregulation of mitochondrial and nuclear encoded complex IV proteins in both skeletal muscle and cardiac tissue (Figure 23). Complex I did not demonstrate any significant difference between wild-type and α2 AMPK knockout mice in skeletal muscle or cardiac tissue (Figure 23).

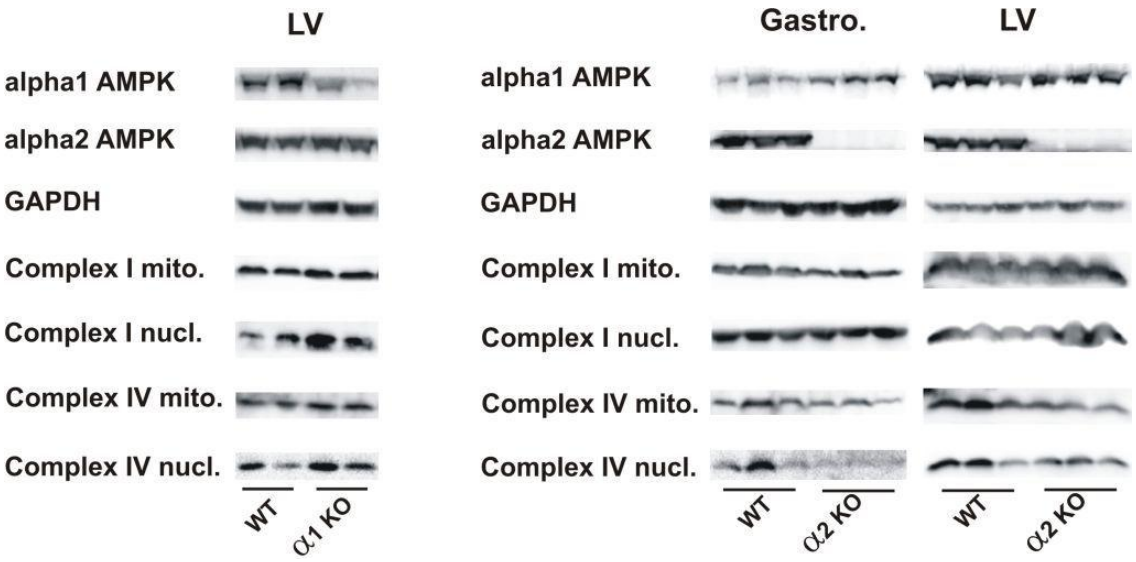

Figure 23: Expression of mitochondrial genes in AMPK knockout mice.

Samples were from different individuals of α1 or α2 AMPK knockout mice. Protein expression of mitochondrial-encoded complex I, IV and nuclear-encoded complex I, IV was determined by specific anti-ND1, anti-COX I, anti-NDUFB8 or anti-COX IV antibodies. GAPDH was used as a loading control. KO: knockout; n=2 or 3 per group.

4.6 Impact of AMPK isoforms on H9C2 cell proliferation.

AMPK is not only important for mitochondrial biogenesis and function, but also important for cell proliferation and cell viability. So far, the impact of AMPK on proliferation was only shown in other cell types. In order to identify whether lack of one of the α AMPK isoforms influences cell proliferation differently, H9C2 cardiomyoblasts were transiently transfected with mock siRNA, α1 AMPK siRNA, α2 AMPK siRNA or a combination of both α1 and α2 AMPK siRNA for 48 h. The knockdown efficiency of these AMPK siRNA oligos after 24 h and 48 h is shown in Figure 24. The cell density of α1 AMPK knockdown cells was similar as of the control cells even after 48 h, suggesting no major impact of the α1 isoform on H9C2 cardiomyoblast proliferation. The α2 AMPK knockdown cells appeared stressed and demonstrated a strongly deteriorated proliferation compared to the control cells. After 48 h the confluency of both the control cells and the α1 AMPK knockdown cells was almost 100%, while the confluency of the α2 AMPK knockdown cells was approximately 50%. The double α AMPK knockdown cells did not show a stronger suppression of proliferation compared to the single α2 AMPK knockdown cells (Figure 24).

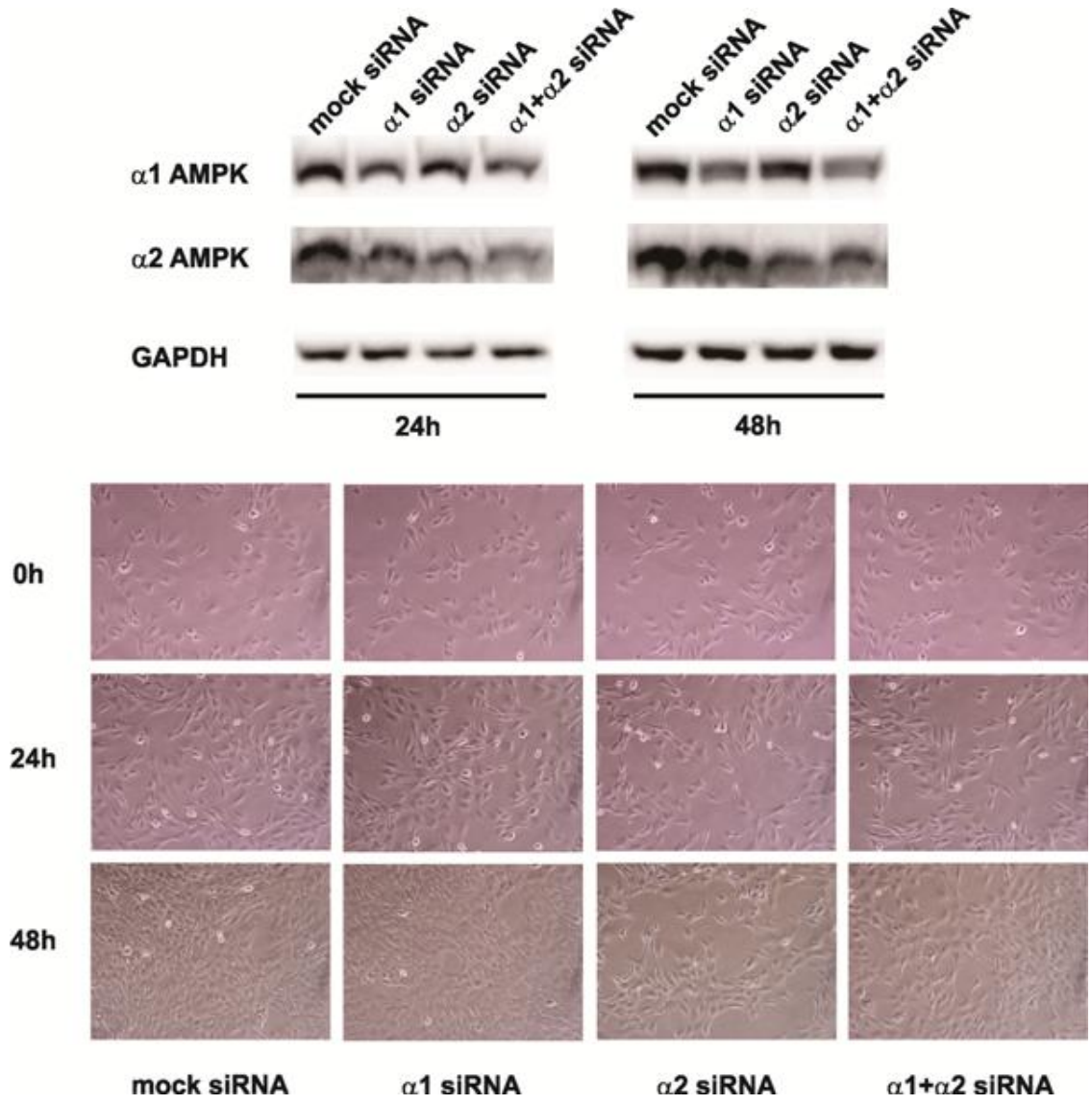

Figure 24: Impact of α AMPK isoforms on H9C2 cardiomyoblast proliferation.
H9C2 cardiomyoblasts were transfected with mock siRNA, α1 AMPK siRNA, α2 AMPK siRNA or a combination of both α1 and α2 AMPK siRNA for 48 h. Pictures from different time points (0 h, 24 h, 48 h) are based on phase contrast microscope.

H9C2 cardiomyoblasts with α AMPK knockdown were also labled with BrdU to directly monitor the influence of α AMPK knockdown on the cell proliferation. The α2 AMPK knockdown led to a significant reduction in BrdU-labling in H9C2 cardiomyoblasts. However, α1 AMPK knockdown also resulted in a significant reduction in BrdU-labling, as shown in Figure 25. Furthermore, the double α AMPK knockdown cells showed an even stronger reduction in BrdU-labling compared to the single α1 or α2 AMPK knockdown cells.

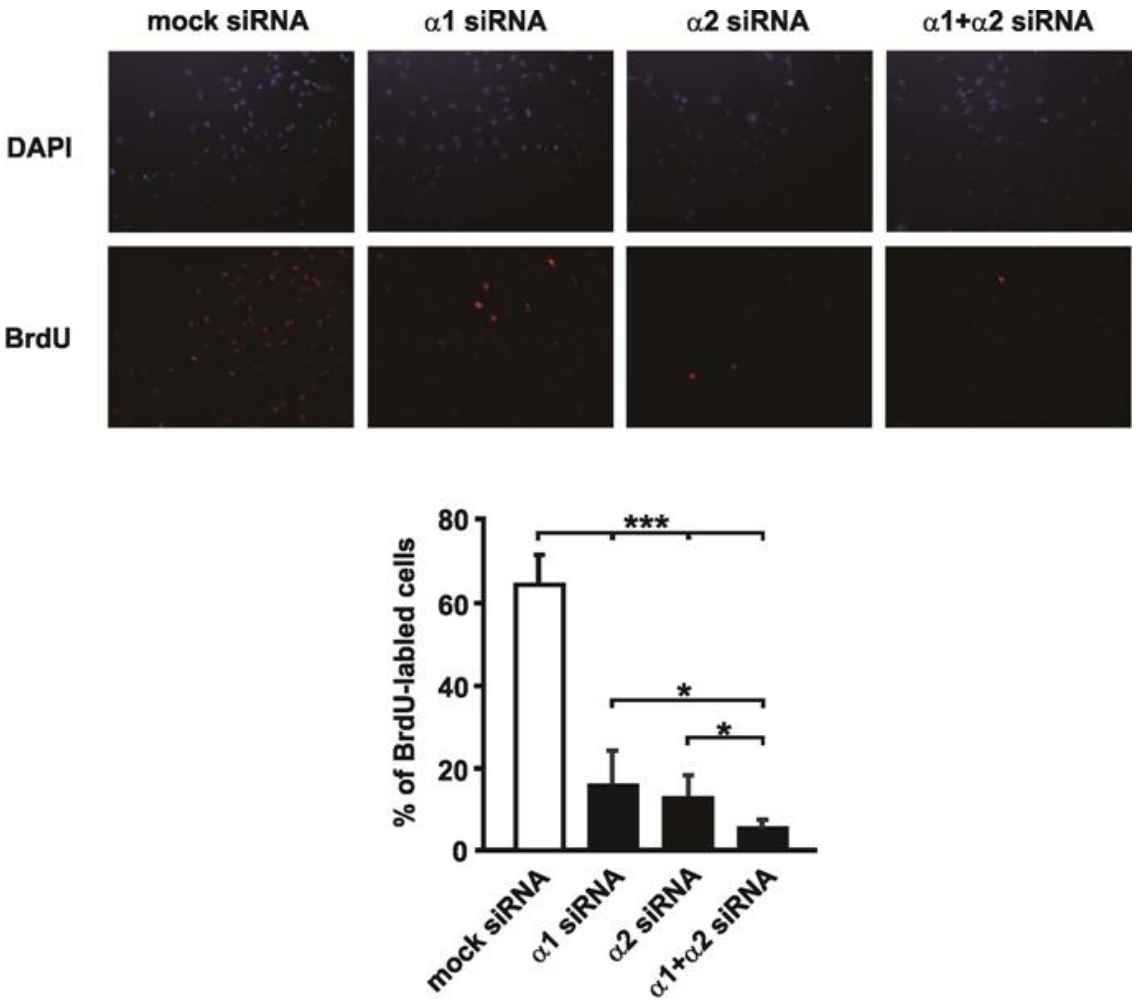

Figure 25: Impact of α AMPK isoforms on H9C2 cardiomyoblast proliferation.
*H9C2 cardiomyoblasts were transfected with mock siRNA, α1 AMPK siRNA, α2 AMPK siRNA or a combination of both α1 and α2 AMPK siRNA for 48 h. Cells were labled with BrdU and counterstained with DAPI. Numbers of BrdU-labled cells and DAPI-stained cells per field were recorded, and percentage of BrdU-labled cells in each field was used for this analysis. Data represents the mean ± SEM (n=3 per group). *p<0.05;***p<0.001.*

4.7 Impact of AMPK activation or deletion on H9C2 cell viability

4.7.1 Impact of alpha AMPK isoforms on H9C2 cell viability.

AMPK has not only been described to influence cell proliferation, but also viability and cell death (mainly apoptotic cell death). The viability of H9C2 cardiomyoblasts with α1 or α2 AMPK knockdown was determined with the CellTiter Blue assay, based on the ability of living cells to convert a redox dye into a fluorescent end product. H9C2 cardiomyoblasts were transfected with mock siRNA, α1 AMPK siRNA, α2 AMPK siRNA or a combination of both α1 and α2 AMPK siRNA for 48 h. As shown in Figure 26, cells

with the single α2 AMPK knockdown showed a 40% decrease in cell viability, while single α1 AMPK knockdown did not result in a decreased cell viability compared to the mock-transfected cells. A combined knockdown of α1 and α2 AMPK did not result in a further deterioration in cell viability compared to the single α2 AMPK knockdown cells, as shown in Figure 26.

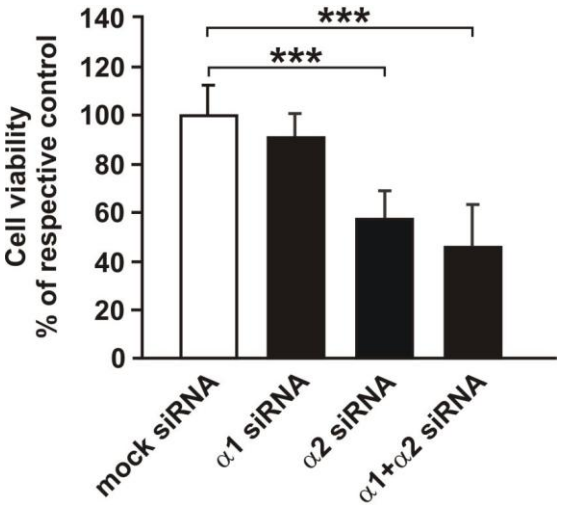

Figure 26: Impact of α AMPK isoforms on H9C2 cardiomyoblast viability.
*H9C2 cardiomyoblasts were transfected with mock siRNA, α1 AMPK siRNA, α2 AMPK siRNA or a combination of both α1 and α2 AMPK siRNA for 48 h. The cell viability was determined by CellTiter Blue assay. Data represents the mean ± SEM (n=3 per group). ***p<0.001.*

4.7.2 Effect of AMPK activation on H_2O_2-induced H9C2 cell death.

Cell viability can be reduced due to increased apoptotic or necrotic cell death, which was therefore analyzed in the subsequent experiments. H9C2 cardiomyoblasts were preincubated with 4 µg/ml recombinant adiponectin or 10 µM A-769662 for 24 h and then treated with 75 µM H_2O_2 for another 24 h. H_2O_2 was used as an established pro-oxidant stimulus known to promote cell death in various cell types. As shown in Figure 27, H_2O_2 treatment resulted in an increased number of both apoptotic Annexin V-positive cells and necrotic propidium iodide (PI)-positive cells. Both the physiological and the pharmacological AMPK activation induced by adiponectin and A-769662 did not influence the basal cell viability, but significantly reduced H_2O_2-induced cell apoptosis and necrosis.

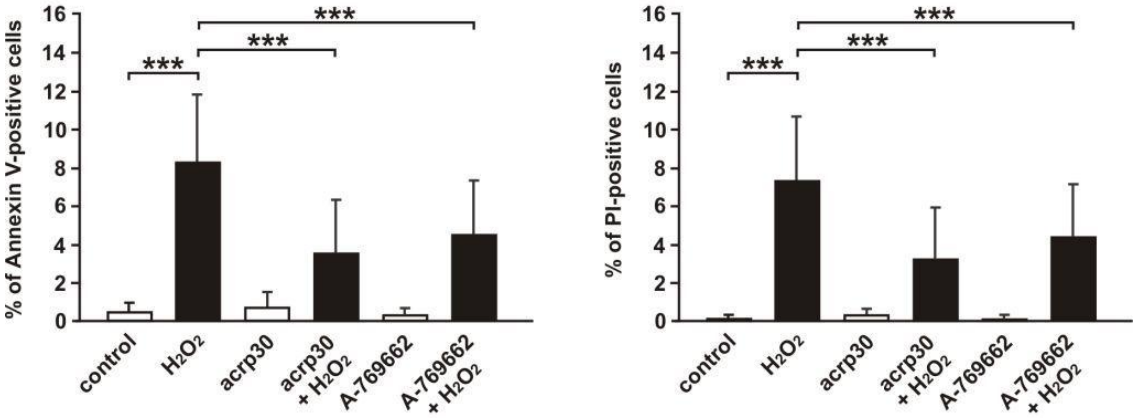

Figure 27: Effect of adiponectin and A-769662 on H_2O_2-induced H9C2 cell death.
*H9C2 cardiomyoblasts were preincubated with 4 µg/ml adiponectin or 10 µM A-769662 for 24 h and then treated with 75 µM H_2O_2 for another 24 h. Cells were stained with Annexin V and propidium iodide (PI). Numbers of apoptotic cells (Annexin V positive), necrotic cells (PI positive), and total cells per field were recorded, and percentage of Annexin positive cells per total cells and PI positive cells per total cells in each field was used for this analysis. Data represents the mean ± SEM (n=5 per group). ***p<0.001.*

In order to further dissect the protective role of α1 and α2 AMPK, the basal activation of caspase 3/7 was measured after siRNA-induced knockdown of α1 AMPK, α2 AMPK or a combined knockdown of both α AMPK in H9C2 cardiomyoblasts. As shown in Figure 28, cells with single α1 AMPK knockdown did not show any change in caspase 3/7 activity, while cells with single α2 AMPK knockdown showed at least 7-fold increase in caspase 3/7 activity compared to the mock-transfected cells. A combined knockdown of α1 and α2 AMPK did not result in a further induction in caspase 3/7 activity compared to the single α2 AMPK knockdown cells, but an almost 4-fold increase in caspase 3/7 activity compared to the control cells.

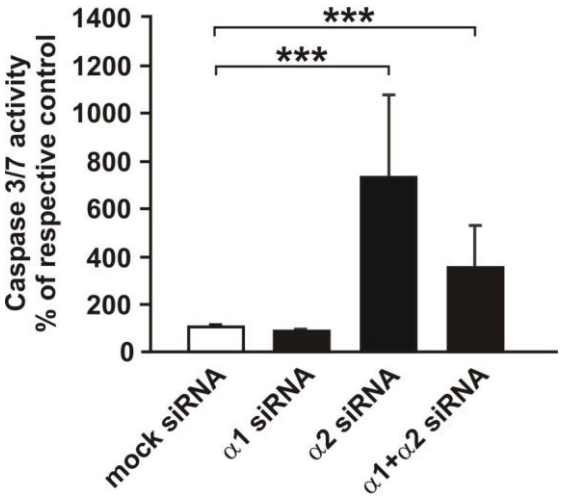

Figure 28: Impact of α AMPK isoforms on caspase activities in H9C2 cardiomyoblasts.
*H9C2 cardiomyoblasts were transfected with mock siRNA, α1 AMPK siRNA, α2 AMPK siRNA or a combination of both α1 and α2 AMPK siRNA for 48 h. The activity of caspase 3/7 was determined by the caspase 3/7 Glo assay kit. Data represents the mean ± SEM (n=3 per group). ***p<0.001.*

5. Discussion

The major findings of the present study are:

1. Adiponectin-mediated AMPK activation promotes mitochondrial biogenesis and improves mitochondrial function in H9C2 cardiomyoblasts. Both α1 and α2 isoforms of AMPK are involved in mediating this effect.
2. These adiponectin effects are mediated via both adipoR1 and adipoR2, and T-cadherin acts as co-receptor for adipoRs.
3. Adiponectin-induced AMPK activation is dependent on the activation of both LKB1 and CaMKKβ in H9C2 cardiomyoblasts.
4. AMPK activation has anti-apoptotic and pro-proliferative effects in H9C2 cardiomyoblasts.

5.1 Regulation of AMPK and ACC by adiponectin.

Three different phosphorylation sites on AMPKα subunit have been reported. Among them, Thr172 is reported to be the only phosphorylation site on α subunit, which positively regulates AMPK activation (Hawley, Davison et al. 1996). On the other hand, the other two phosphorylation sites are not involved in AMPK activation (Woods, Vertommen et al. 2003). Ser485/491 have been reported to be autophosphorylation sites, inhibiting AMPK activation (Hurley, Barre et al. 2006). In the present study, only the phosphorylation at Thr172 was investigated. Adiponectin induced phosphorylation of AMPK at Thr172 in a time-dependent manner (Figure 6), which was abolished by AraA (Figure 7). Protein phosphatase 1 (PP1) (Woods, Vertommen et al. 2003), PP2A (Wu, Song et al. 2007), PP2C (Steinberg, Michell et al. 2006), which were reported to be involved in AMPK dephosphorylation, may participate in changes of AMPK activation but were not investigated in the present study.

Adiponectin-mediated metabolic effects, such as fatty acid oxidation, are mediated via AMPK phosphorylation at Thr172 and activation of AMPK. Activated AMPK phosphorylates and thus inactivates ACC at Ser79 (Goodwin and Taegtmeyer 1999).

Some other phosphorylation sites on ACC, such as Ser77, Ser221, Ser1200, Ser1215, were also reported by some other groups. Ser77 and Ser1200 were reported to be associated with protein kinase A (PKA)-induced ACC phosphorylation (Ha, Daniel et al. 1994), whereas Ser221, Ser1200, Ser1215 were reported to be associated with AMPK-induced ACC phosphorylation (Davies, Sim et al. 1990). In the present study, only the phosphorylation at Ser79 was investigated. In our study, adiponectin-induced ACC phosphorylation at Ser79 appeared to be more stable than AMPK phosphorylation (Figure 6). The protein phosphatases glutamate-activated protein phosphatase (GAPP) was reported to be able to dephosphorylate ACC, but was not involved in AMPK dephosphorylation (Gaussin, Hue et al. 1996; Kowluru, Chen et al. 2001). The stable phosphorylation of ACC after adiponectin treatment might therefore be related to a low activity of this protein phosphatase. AraA also abolished ACC phosphorylation in cardiomyocytes (Figure 7). However, the persistence of ACC phosphorylation after AraA treatment alone (Figure 7) suggests that there are other upstream kinases of ACC which are phosphorylating ACC at Ser79 and operating AMPK-independent. Those other kinases of ACC might include PKA, casein kinase I and casein kinase II as previously described (Witters and Bacon 1985).

5.2 Adiponectin-mediated AMPK activation promotes mitochondrial biogenesis and mitochondrial function in H9C2 cardiomyoblasts.

It is widely accepted that AMPK via activating transcription factors or coactivators such as nuclear respiratory factors (NRFs) and PGC-1α induces mitochondrial biogenesis (Wu, Puigserver et al. 1999; Reznick and Shulman 2006). Pharmacological activation of AMPK via AICAR and metformin promotes mitochondrial biogenesis via upregulation of PGC-1α in human umbilical vein endothelial cells (HUVEC) (Kukidome, Nishikawa et al. 2006), and muscle-specific deletion of either AMPK or PGC-1α leads to a generalized reduction in mitochondrial gene expression and exercise intolerance (Jorgensen, Wojtaszewski et al. 2005; Leone, Lehman et al. 2005; Handschin, Chin et al. 2007). These studies indicate the important roles of AMPK and PGC-1α in the regulation of

mitochondrial biogenesis. In the present study, both the physiological (via adiponectin) and the pharmacological activation (via A-769662) of AMPK induced mitochondrial biogenesis (Figure 14), and inhibition of AMPK activity partially reversed the effect of adiponectin on mitochondrial biogenesis (Figure 15). This suggests that adiponectin/A-769662-mediated AMPK activation promotes mitochondrial biogenesis in H9C2 cardiomyoblasts. However, the time required to induce mitochondrial gene expression (particularly ND5) varies between adiponectin and A-769662 (Figure 14). This might be due to different mechanisms of AMPK activation and affinity to AMPK of these agents. Adiponectin most likely activates AMPK via adipoRs, whereas A-769662 causes a direct allosterical activation of AMPK. It is conceivable that these differences in the modes of AMPK activation may influence the induction time for mitochondrial gene expression. Furthermore, an increase in the mRNA expression of mitochondrial transcriptional factors NRF1 and Tfam was observed along with AMPK activation (Figure 14), suggesting that NRF1 and Tfam may be involved in the effect of AMPK activation on mitochondrial biogenesis. Although the mRNA expression of PGC-1α was neither induced by adiponectin nor by A-769662 (Figure 14), a strong deacetylation of PGC-1α, which was previously reported to result in a higher PGC-1α activity (Gurd 2011) was observed after adiponectin treatment in H9C2 cardiomyoblasts (data not shown). These findings suggest that adiponectin-induced mitochondrial biogenesis is mediated by AMPK-dependent PGC-1α deacetylation and NRF1/Tfam expression.

Adiponectin, as a physiological AMPK activator, has also been shown to induce mitochondrial biogenesis in primary human myotubes (Civitarese, Ukropcova et al. 2006). Deletion of adiponectin in vivo results in a lower mitochondrial content (Civitarese, Ukropcova et al. 2006), which suggests the necessity of adiponectin in the regulation of mitochondrial biogenesis in vivo. Similar findings have also been reported in our previous study, showing that an intact adipocytokine signaling (Leptin, adiponectin) is required for physical activity-induced PGC-1α deacetylation and mitochondrial biogenesis in mouse skeletal muscle (Li, Pan et al. 2011). Treadmill training induced increase in plasma adiponectin, PGC-1α deacetylation, AMPK phosphorylation and SIRT1 protein expression in wild type but not in ob/ob mice with

dysregulated adiponectin/leptin-mediated AMPK activation (Li, Pan et al. 2011).

Likewise, it has been reported that chronic activation of AMPK by AICAR increases mitochondrial enzyme activities in rat skeletal muscle (Winder, Holmes et al. 2000). Adiponectin has been shown to induce citrate synthase activity, a marker of mitochondrial content, in primary human myotubes, and either knockdown of adiponectin receptor expression by siRNA, or pharmacological inhibition of AMPK with AraA blunted adiponectin-induced mitochondrial function (Civitarese, Ukropcova et al. 2006). Accordingly, adiponectin knockout mice have also been shown to have lower citrate synthase activity in the skeletal muscle (Civitarese, Ukropcova et al. 2006). These studies indicate the important roles of adiponectin and AMPK in the regulation of mitochondrial biogenesis. In this present study, it was further observed that adiponectin could induce activities of mitochondrial complex I+III and complex IV, and pharmacological inhibition of AMPK completely abolished this effect in H9C2 cardiomyoblasts (Figure 16). These data demonstrate that AMPK activation is also required for adiponectin-induced changes in mitochondrial function.

5.3 Both alpha1 and alpha2 isoforms of AMPK are involved in adiponectin-mediated induction of mitochondrial biogenesis and mitochondrial function in H9C2 cardiomyoblasts.

α2 isoform has been proposed to be the most prevalent isoform expressed both in the heart and skeletal muscles (Arad, Seidman et al. 2007). Therefore, most of the previous studies on cardiac tissue have focused on α2 isoform. α2 AMPK deficiency has been shown to be associated with most of the cardiac abnormalities, such as more severe myocardium injury following ischemia (Russell, Li et al. 2004; Carvajal, Zarrinpashneh et al. 2007), more severe hypertrophy of left ventricle following pressure overload (Ping Zhang et al 2008), impaired cardiac cardiolipin homeostasis and cardiac mitochondrial dysfunction (Athea, Viollet et al. 2007). Recently, it has been shown that transient deletion of α2 AMPK alone or of both α1 and α2 AMPK leads to a reduction in adiponectin-induced mitochondrial DNA content in C2C12 myocytes (Iwabu, Yamauchi

et al. 2010), suggesting that mainly α2 AMPK is important for adiponectin-induced mitochondrial biogenesis. However, little is known about the specific role of α1 isoform in cardiomyocytes. Therefore, the present study tried to dissect the specific role of α1 AMPK and α2 AMPK in adiponectin-mediated changes in mitochondrial biogenesis and mitochondrial function. In order to identify the role of specific isoforms of α AMPK in adiponectin-mediated mitochondrial changes in H9C2 cardiomyoblasts, α1 or α2 AMPK levels were modified using transient or stable and inducible siRNA techniques. Data of the present study showed that both α1 and α2 AMPK knockdown result in a reduction in adiponectin-mediated mitochondrial biogenesis as well as mitochondrial enzyme activities in H9C2 cardiomyoblasts (Figure 19-21). Massive downregulation of complex I protein (Figure 19) but relatively moderate complex IV protein (Figure 20) in α1 and α2 AMPK knockdown cells may suggest a deeper involvement of AMPK activation in transcription and translation of complex I than of complex IV. Reduction in the basal enzymatic activities of complex I and complex III but not of complex II in α1 and α2 AMPK knockdown cells (Figure 21) may be related to differential composition and regulation of these components. Complex I and complex III contain a high number of mitochondrial-encoded proteins, but complex II contains only nuclear-encoded proteins. Knockout mice of α1 and α2 AMPK have been generated to study the specific role of each isoform in glucose metabolism and diabetes (Viollet, Andreelli et al. 2003). It has been found that α2 but not α1 AMPK knockout mice exhibited glucose intolerance and reduced insulin sensitivity (Viollet, Andreelli et al. 2003). Surprisingly, both mice models showed no specific cardiac phenotype under normal conditions. However, α2 AMPK deficient mice showed some cardiac phenotype under various stressful conditions as described above. In addition, α2 AMPK deficiency in mice resulted in a decreased substrate utilization by cardiac mitochondria and an inhibited respiration rate through complex I (Athea, Viollet et al. 2007).

Previously, Jorgensen SB et al 2004 and Viollet B et al 2003 have demonstrated an upregulation of α1 isoform in the skeletal muscle of α2 AMPK knockout mice, which may compensate for the loss of α2 AMPK to some extent. In concurrence to these reports, a similar phenomenon was also observed in the skeletal muscle but not in the cardiac

tissue of α2 AMPK knockout mice in the present study (Figure 22). Interestingly, the expression of both mitochondrial and nuclear-encoded complex IV was lower in both cardiac and skeletal muscle of α2 AMPK knockout mice compared to the wild type mice (Figure 23). However, the expression of both mitochondrial and nuclear-encoded complex I was not affected in these mice suggesting no general defect in mitochondrial function. In contrast, there was no change in the expression of these genes in the cardiac tissue of α1 AMPK knockout mice. These findings suggest that although upregulation of the α1 AMPK isoform in α2 AMPK knockout mice might compensate some of the functions of the α2 isoform, its effect on mitochondrial function seems to be unique to α2 AMPK. Therefore, these data suggest a more profound regulatory role of α2 but not α1 isoform in the control of mitochondrial function in the heart. This view is further strengthened by the study of Jørgensen et al 2004, where the authors show that the expression of mitochondrial cytochrome c and COX I were reduced by 20% in the skeletal muscle of α2 AMPK knockout mice compared to wild-type mice.

Differences in the data obtained from H9C2 cardiomyoblasts and muscles of AMPK knockout mice may be related to the experimental conditions (e.g. cardiac myoblast and fully differentiated cardiac muscle). The basal expression of mitochondrial genes in muscle may not differ between wild-type mice and knockout mice, but it might be altered under stressful conditions. The basal reduction in mitochondrial complex IV expression in α2 AMPK knockout mice could just demonstrate the importance of α2 isoform in the regulation of basal gene expression of this particular component of the respiratory chain, possibly via direct phosphorylation of the relevant transcription factors regulating complex IV components.

5.4 Adiponectin-induced AMPK activation requires the presence of T-cadherin in H9C2 cardiomyoblasts.

It has previously been suggested that adipoR1 is a receptor for globular adiponectin, whereas adipoR2 acts as a receptor for full-length adiponectin (Yamauchi, Kamon et al. 2002). However, knockdown of adipoR1 resulted in an abrogation of recombinant

full-length adiponectin-induced AMPK activation, whereas knockdown of adipoR2 resulted in a reduction in the activity of PPAR-α in liver (Yamauchi, Nio et al. 2007). Additionally, T-cadherin was identified as an adiponectin receptor by its ability to specially bind the physiological high-molecular weight adiponectin in vitro (Hug, Wang et al. 2004). T-cadherin is a glycosylphosphatidylinositol (GPI)-anchored molecule and lacks a cytoplasmic region (Ranscht and Dours-Zimmermann 1991). Recently, it has also been shown that T-cadherin is critical for high-molecular weight adiponectin-mediated cardioprotection in mice (Denzel, Scimia et al. 2010). T-cadherin was suggested to act as coreceptor for both adipoR1 and adipoR2 in the heart (Denzel, Scimia et al. 2010).

In the present study, the knockdown of either adipoR1 or adipoR2 resulted in a reduction in basal AMPK phosphorylation (Figure 10), suggesting that both adipoR1 and adipoR2 regulate the basal activation of AMPK in H9C2 cardiomyoblasts. This is in accordance with a previous report demonstrating that the muscle specific adipoR1 knockout reduces basal AMPK phosphorylation, PGC-1α expression, mitochondrial content and exercise capacity in the skeletal muscle (Iwabu, Yamauchi et al. 2010). Data on cardiac specific adipoR1 knockouts or the effect of adipoR2 knockout on basal AMPK activation in the skeletal or cardiac muscle are not available yet. However, in failing myocardium, a reduction in the basal protein expression of adipoR1, adipoR2 and AMPK phosphorylation was observed (Khan, Kato et al. 2012). This suggests a possible relationship between adipoR1/2 and basal AMPK activation in the heart under stressful conditions.

Adiponectin-induced AMPK phosphorylation has been shown to be abrogated by knockdown of adipoR1 or adipoR2 in a variety of cell types (Iwabu, Yamauchi et al. 2010; Kim, Lee et al. 2010; Xiao-jun, Min et al. 2010). Similarly, impaired AMPK activation induced by recombinant full-length adiponectin was also observed in the skeletal muscle of ob/ob mice exhibiting decreased expression of adipoR1 and adipoR2 (Tsuchida, Yamauchi et al. 2004). In the present study, AMPK phosphorylation by recombinant full-length adiponectin was not completely abolished by either adipoR1 or adipoR2 knockdown alone in H9C2 cardiomyoblasts (Figure 10). This may be due to

either partial knockdown of adipoR1/2 or compensation by the respective other adipoR (Figure 9). However, the compensation of the remaining adipoRs for the partial adipoR1 loss seemed to be less effective. This may suggest that adipoR1 contributes more to the adiponectin-induced AMPK phosphorylation than adipoR2 and raises the question if other proteins/co-receptors, which mediate the adiponectin-AMPK signaling, are involved.

Comparison of the expression of different adiponectin receptors in H9C2 cardiomyoblasts and adult cardiomyocytes showed a high expression of T-cadherin in both cell types (Figure 8). Therefore, the role of T-cadherin in AMPK phosphorylation was further investigated. Unlike adipoR1 and adipoR2, T-cadherin knockdown did not result in a reduction in basal AMPK phosphorylation (Figure 10), suggesting that T-cadherin is not required for the basal AMPK activation. However, adiponectin was unable to induce AMPK phosphorylation in T-cadherin knockdown cells (Figure 10), suggesting that T-cadherin might be necessary for adiponectin binding on the cell surface and adiponectin-mediated AMPK activation in H9C2 cardiomyoblasts. This finding is in accordance to a previous report (Denzel, Scimia et al. 2010) showing that cardiac T-cadherin expression was dependent on adiponectin serum concentration and adiponectin could directly bind to T-cadherin mediating adiponectin effects in heart (Denzel, Scimia et al. 2010).

However, abundant T-cadherin alone in the skeletal muscle was also not sufficient for many adiponectin effects, as indicated by Yamauchi et al 2007 and Iwabu et al 2010. They showed that in mice with a skeletal muscle-specific knockout of adipoR1, but not adipoR2, full-length adiponectin failed to regulate AMPK activation and muscle metabolism (Yamauchi, Nio et al. 2007; Iwabu, Yamauchi et al. 2010). Thus, T-cadherin might be a major component of the adiponectin signaling pathway and may mainly cooperate with adipoR1 in muscle cells.

5.5 Adiponectin-induced AMPK activation is mediated by both LKB1 and CaMKKβ in H9C2 cardiomyoblasts.

LKB1 and CaMKKβ are two well known AMPK kinases in mammalian cells. Both of these two kinases regulate AMPK phosphorylation via different signaling mechanisms in different tissues and organs. LKB1 is known to be the most prominant AMPK kinase (Koh, Brandauer et al. 2008). Deletion of LKB1 in cardiomyocytes leads to an energy deprivation and cardiac dysfunction, which was due to complete ablation of α2 AMPK activity (Koh, Brandauer et al. 2008). Similarly, cardiac deficiency of LKB1 also results in a cardiac hypertrophy which was due to impaired AMPK and mTOR/p70S6/eEF2 signaling (Ikeda, Sato et al. 2009). Furthermore, LKB1/α2 AMPK signaling were reported to be important for the long-chain fatty acid uptake and utilization in cardiomyocytes during the contraction of heart (Habets, Coumans et al. 2009). In our previous study we have also demonstrated a strong correlation between LKB1 expression and AMPK activation in human right atrial tissue (Niemann, Pan et al. 2013). Other studies have also demonstrated an essential role of CaMKKβ in the regulation of AMPK phosphorylation in the heart (Horie, Ono et al. 2008; Li, Zhang et al. 2011). Both LKB1 and CaMKKβ have also been shown to regulate Glut4 translocation and glucose uptake in cardiomyocytes and protect cardiac myocytes against ischemic injury by others (Horie, Ono et al. 2008). Likewise, morphine, an exogenous non-peptide opioid receptor agonist, ameliorates myocardial contractile dysfunction and limits infarct size following ischemia and reperfusion by Ca^{2+}-CaMKKβ-dependent phosphorylation of AMPK (Li, Zhang et al. 2011). These studies suggest that both LKB1 and CaMKKβ mediate the effect of adiponectin on AMPK activation in the heart and in H9C2 cardiomyoblasts.

In accordance to these data, either LKB1 or CaMKKβ knockdown led to a reduction in basal AMPK phosphorylation in H9C2 cardiomyoblasts in the present study (Figure 12). The effect of LKB1 or CaMKKβ knockdown on basal AMPK phosphorylation (Figure 12) was comparable to that of adipoR1 or adipoR2 knockdown (Figure 10), suggesting the requirement of all these four components in the regulation of basal AMPK

phosphorylation in H9C2 cardiomyoblasts. Either component is indispensable in this regulation.

Till now, LKB1 has been believed to regulate adiponectin-induced AMPK phosphorylation in most cell types (Awazawa, Ueki et al. 2009; Taliaferro-Smith, Nagalingam et al. 2009; Zhou, Deepa et al. 2009). We show for the first time that both LKB1 and CaMKKβ are responsible for adiponectin-induced AMPK phosphorylation in H9C2 cardiomyoblasts. Data of the present study show that knockdown of either LKB1 or CaMKKβ abrogated the adiponectin-mediated AMPK phosphorylation in H9C2 cardiomyoblasts (Figure 12). This effect was different from the effect of adipoR1 or adipoR2 knockdown on adiponectin-induced AMPK phosphorylation (Figure 10). This suggests a stronger dependence of adiponectin/AMPK signaling pathway on LKB1 and CaMKKβ than on adipoR1/2 in H9C2 cardiomyoblasts.

Therefore, the present study suggests that in H9C2 cardiomyoblasts, both LKB1 and CaMKKβ act as AMPK kinases, responsible for the basal AMPK phosphorylation and mediating the adiponectin effects. However, further studies are needed to investigate whether activation of both LKB1 and CaMKKβ is interdependent.

5.6 AMPK activation has an anti-apoptotic effect.

Both anti-apoptotic and pro-apoptotic effects of AMPK activation have been described in vivo and in vitro (Shibata, Sato et al. 2005; Sasaki, Asanuma et al. 2009; Kim, Miller et al. 2011; Konishi, Haraguchi et al. 2011). It has been shown that adiponectin protects the heart from ischemia/reperfusion injury via activation of AMPK and inhibition of TNF-α in isolated rat neonatal cardiomyocytes and fibroblasts (Shibata, Sato et al. 2005). These effects were reversed by an overexpression of the dominant negative form of α AMPK (Shibata, Sato et al. 2005). Konishi et al 2011 demonstrated that adiponectin-induced AMPK activation protected the mouse heart from doxorubicin-induced cardiomyopathy by an anti-apoptotic effect mediated via an upregulation of the anti-apoptotic gene Bcl-2 and a downregulation of the pro-apoptotic gene Bax (Konishi, Haraguchi et al. 2011). The authors also suggested that AMPK-induced Bcl-2 expression interferes with cytochrome c release from mitochondria and suppresses apoptosis progression.

Similarly, metformin has been shown to attenuate oxidative stress–induced cardiomyocyte apoptosis in dogs via AMPK activation (Sasaki, Asanuma et al. 2009). It also improved the left ventricular function and survival via activation of AMPK and its downstream effectors eNOS and PGC-1α in a murine model of heart failure (Gundewar, Calvert et al. 2009). Moreover, A-769662, a direct activator of AMPK, has been reported recently to protect heart against ischemia/reperfusion injury through AMPK-mediated activation of eNOS and eEF2 in isolated mouse hearts (Kim, Miller et al. 2011). Contrariwise, pro-apoptotic effects of AMPK activation have also been reported. In most of those studies, AICAR is used as the AMPK activator. It has been shown that AICAR-induced AMPK activation results in apoptosis in B lymphocytes but not in T lymphocytes (Campas, Lopez et al. 2003). Moreover, it has been shown that AICAR-induced AMPK activation potentiates the doxorubicin-induced cell death and apoptosis in H9C2 cardiomyoblasts, which is mediated by JNK, p53 regulation and mTORC1 inhibition (Chen, Wu et al. 2011). However, JNK activation induced by AICAR has previously been shown to be linked to excitotoxic apoptosis where cells are damaged and killed by excessive stimulation (Borsello, Clarke et al. 2003; Chen, Montagnani et al. 2003). Therefore, AICAR may result in an over-activation of AMPK, which is then detrimental. In endothelial cells, it has been shown that α1 but not α2 AMPK activation suppressed apoptosis via increasing NF-κB activation and the expression of anti-apoptotic proteins Bcl-2 and Survivin (Liu, Liang et al. 2010), indicating an anti-apoptotic effect of α1 AMPK in endothelial cells.

However, the specific role of the α AMPK isoforms in apoptosis prevention has not been investigated in H9C2 cardiomyoblasts or cardiomyocytes in detail so far. Data of the present study show that both physiological and pharmacological activation of AMPK exerts an anti-apoptotic effect in H9C2 cardiomyoblasts (Figure 27). Moreover, both AMPK activators not only reduced the basal ROS production but also attenuated H_2O_2-induced ROS production (data not shown) in H9C2 cardiomyoblasts suggesting that the anti-apoptotic effects of AMPK maybe due to a reduced ROS production.

Interestingly, a significant reduction in cell viability (Figure 26) and a dramatic induction in caspase 3/7 activities (Figure 28) were observed in α2 but not in α1 knockdown H9C2

cardiomyoblasts in the present study. These data indicate that, in H9C2 cardiomyoblasts, the α2 isoform but not the α1 isoform (as shown in endothelial cells) is involved in anti-apoptotic effects of AMPK.

5.7 AMPK deletion suppresses cell proliferation.

Both anti-proliferative and pro-proliferative effects of AMPK activation have also been described. The anti-proliferative effects of AMPK may be mediated via multiple mechanisms including the regulation of cell cycle (Williamson, Butler et al. 2009) and inhibition of protein synthesis (Bolster, Crozier et al. 2002). Cell cycle regulation by AMPK is mediated by up-regulation of the p53/p21 axis as well as regulation of TSC2/mTOR pathway (Igata, Motoshima et al. 2005; Jones, Plas et al. 2005). Both eEF2 and mTOR signaling are involved in mediating the inhibitory effect of AMPK on protein synthesis. mTOR has been reported to be inhibited by AMPK activation through TSC2 phosphorylation, which in turn leads to an inhibition of protein synthesis (Inoki, Zhu et al. 2003). Phosphorylation and inhibition of eEF2 by eEF2 kinase which can be phosphorylated by AMPK also leads to the inhibition of protein synthesis (Chan, Soltys et al. 2004).

Although the previous studies were mainly performed in cancer cells, some studies in non-cancer cells also showed the suppressive effect of AMPK activation on cell proliferation. AMPK activation induced by AICAR suppresses the proliferation of vascular smooth muscle cells via cell cycle regulation, which occurs through p53 upregulation and increased expression of cyclin-dependent kinase inhibitor p21CIP (Igata, Motoshima et al. 2005). In vivo treatment with AICAR results in a 45% reduction in protein synthesis in rat skeletal muscle, accompanied by a reduced phosphorylation of protein kinase B, mTOR, ribosomal protein S6 kinase and eukaryotic initiation factor eIF4E-binding protein (Bolster, Crozier et al. 2002).

Contrary to this, several other studies have demonstrated pro-proliferative effect of AMPK activation. It has been shown that AICAR-induced activation of AMPK enhances angiotensin II-induced proliferation in cardiac fibroblasts, but α1 AMPK deficiency suppresses this effect (Hattori, Akimoto et al. 2006). In the present study, a ~50%

reduction in cell proliferation in α2 but not in α1 AMPK knockdown H9C2 cardiomyoblasts was observed by analysis of cell growth under microscope (Figure 24). The BrdU incorporation data, however, showed that knockdown of either α1 or α2 AMPK resulted in a reduction in BrdU incorporation, which was further reduced when both α1 and α2 AMPK were knocked down simultaneously (Figure 25). Similar results were obtained in our lab in a cancer cell line, Hela cells (data not shown). These data indicate that both isoforms of α AMPK are required for the proliferation of both cardiac and cancer cell lines. The results on cell proliferation obtained by microscope or by BrdU-labling differed in α1 AMPK knockdown cells, showing a normal proliferation by microscope (Figure 24), but a significantly reduced BrdU-incorporation (Figure 25). BrdU is only incorporated into newly synthesized DNA of replicating cells (S phase of the cell cycle), which was measured for 2 hours in our experiments. It can be explained by different knockdown time required by α1 and α2 AMPK for affecting proliferation. Knockdown of α1 AMPK starts to slow down proliferation at least after 48 hours, which was demonstrated by a decreased DNA replication after 48 hours (Figure 25) and a normal cell mitosis within 48 hours (Figure 24). Meanwhile, knockdown of α2 AMPK starts to slow down proliferation just after 24 hours, which was demonstrated by a decreased DNA replication after 48 hours (but might already happen after 24 hours) (Figure 25) and a decreased cell mitosis after 24 hours (Figure 24). Therefore, it is conceivable that both isoforms of α AMPK are required for DNA synthesis in H9C2 cardiomyoblasts. Further studies are required to investigate the details of these two isoforms in the regulation of the cell cycle. The present study suggests that both α1 and α2 isoforms of AMPK contribute to the proliferation of H9C2 cardiomyoblasts.

5.8 AMPK - a therapeutic target in cardiac disease.

Studies using both genetic and pharmacological approaches have demonstrated important roles of AMPK in protecting the heart during ischemia/reperfusion injury as well as in pathological hypertrophy and heart failure. Activation of the AMPK pathway may therefore be a novel therapeutic strategy in treating and preventing various cardiac diseases.

The results obtained in the present study provide additional data for this protective effect of AMPK activation, induced either by physiological or by pharmacological activators. Both α1 and α2 AMPK may protect the failing heart by promoting mitochondrial biogenesis and improving mitochondrial function. Furthermore, the α2 isoform may protect the heart from injury by improving cell survival via anti-apoptotic mechanisms, partially mediated by a reduction in ROS production. Although the present study investigated only some aspects of AMPK-mediated protective effects and the signaling pathways involved in this process, it demonstrated that AMPK, at least in part, plays a role in protecting cardiac cells. A better understanding of the physiology of AMPK and the mechanisms of the action of its existing natural and pharmacological activators is needed if the modulation of AMPK activity for the treatment and prevention of cardiovascular diseases is intended to be used in patients.

6. Summary

In the present study, the protective effects of adiponectin-AMPK signaling on mitochondrial biogenesis, apoptosis and cell proliferation in cardiac cells (adult cardiomyocytes, H9C2 cardiomyoblasts) were investigated. The role of α1 and α2 AMPK in these processes were examined. Adiponectin was able to induce the phosphorylation of AMPK as well as its target ACC in all these cell types. In H9C2 cardiomyoblasts, adiponectin-induced AMPK phosphorylation was mediated by both adipoR1 and adipoR2, and T-cadherin acted as co-receptor for adipoRs. Both AMPK kinases LKB1 and CaMKKβ were involved in adiponectin-induced AMPK phosphorylation. AMPK phosphorylation either by adiponectin or A-769662 (a pharmacologic agent) showed similar effects on mitochondrial gene expression. In H9C2 cardiomyoblasts, adiponectin increased the enzyme activities of various respiratory chain complexes, which was abolished by AMPK inhibition. With the help of three stable inducible H9C2 cell lines (control, α1 AMPK knockdown and α2 AMPK knockdown), it was observed that: (1) both α1 and α2 AMPK were required for the expression and activation of mitochondrial complex I and therefore the mitochondrial respiration via complex I-III respiratory chain, but not complex II-III respiratory chain; (2) and both α1 and α2 AMPK were required for the expression and activation of mitochondrial complex IV. Furthermore, AMPK activation by either adiponectin or A-769662 showed an anti-apoptotic effect in H9C2 cardiomyoblasts. α2 AMPK deletion resulted in cell apoptosis indicated by lower cell viability and rather higher activities of caspase3/7. Both α1 and α2 AMPK were required for the proliferation of H9C2 cardiomyoblasts, which was demonstrated by less DNA replication in these AMPK knockdown cells. Data of the present study revealed protective effects of α1 and α2 AMPK in cardiac cells, which may also suggest an important role of AMPK, as a potential therapeutic target, in the treatment of cardiac diseases.

6. Zusammenfassung

In der vorliegenden Arbeit wurden die protektiven Effekte des Adiponektin-AMPK-Signalweges auf die mitochondriale Biogenese, Apoptose und Zellproliferation in Herzzellen (adulte Kardiomyozyten sowie H9C2 Kardiomyoblasten) untersucht. Dabei wurde die Rolle der α1- und α2-AMPK näher beleuchtet. In allen beobachteten Zelltypen induzierte Adiponektin die Phosphorylierung sowohl der AMPK, als auch von deren Zielenzym, der ACC. In H9C2 Kardiomyoblasten vermittelten adipoR1 und adipoR2 die Adiponektin-induzierte AMPK-Phosphorylierung, während T-Cadherin als Co-Rezeptor dieser Rezeptoren fungierte. Die AMPK-Kinasen LKB1 und CaMKKβ waren ebenfalls an der Adiponektin-induzierten AMPK-Phosphorylierung beteiligt. Die AMPK-Phosphorylierung durch Adiponektin zeigte den gleichen Effekt auf die mitochondriale Genexpression wie A-769662 (ein pharmakologisches Agens). In H9C2 Kardiomyoblasten steigerte Adiponektin die Enzymaktivität zahlreicher Komplexe der Atmungskette, was durch Inhibition der AMPK verhindert wurde. Mit Hilfe von drei stabil induzierbaren H9C2 Zelllinien (Kontrolle, α1-AMPK-knockdown und α2-AMPK-knockdown) konnte gezeigt werden, dass (1) sowohl α1-, als auch α2-AMPK für die Expression und Aktivierung des mitochondrialen Komplex I und dadurch für die mitochondriale Atmung via Komplex I-III der Atmungskette, nicht jedoch via Komplex II-III benötigt wurden; (2) beide AMPK-Isoformen für die Expression und Aktivierung des mitochondrialen Komplex IV erforderlich waren. Weiterhin zeigte die AMPK-Aktivierung durch Adiponektin oder A-769662 einen antiapoptotischen Effekt in H9C2-Kardiomyoblasten. Die Deletion der α2-AMPK resultierte in gesteigerter Apoptose, welche durch eine geringere Zellviabilität und eine gesteigerte Aktivität der Caspasen 3 und 7 gezeigt wurde. Beide AMPK-Isoformen wurden für die Proliferation von H9C2 Kardiomyoblasten benötigt, was anhand geringerer DNA-Replikation in den AMPK-Knockdown-Zellen demonstriert werden konnte. Die Ergebnisse der vorliegenden Arbeit zeigen protektive Effekte der α1- und der α2-AMPK in kardialen Zellen und verdeutlichen die wichtige Rolle der AMPK als potentielles therapeutisches Ziel in der Behandlung kardialer Erkrankungen.

7. Abbreviations

AMPK	AMP-activated protein kinase
AdipoR	Adiponectin receptor
ACC	Acetyl-coenzyme A-carboxylase
acrp30	Adipocyte complement-related protein of 30 kDa
AICAR	5-aminoimidazole-4-carboxamide ribonucleoside
AMP / ADP / ATP	Adenosine mono- / di- / tri-phosphate
AMPKK	AMPK Kinase
APPL	Adaptor protein containing pleckstrin homology domain, phosphotyrosine binding domain and leucine zipper motif
APS	Ammonium persulfate
CaMKKβ	Ca^{2+}-calmodulin-dependent protein kinase kinase β
CBS	Cystathionine-ß-synthase
COX	Cytochrome c oxidase
CPT1	Carnitine Palmitoyl Transferase 1
CS	Citrate synthase
DAPI	4‘6-diamidino-2-phenylindol
(d)dNTP	(Di)deoxyribonucleotide triphosphate
DEPC	Diethylpyrocarbonate
DMSO	Dimethyl sulfoxide
dsRNA	Double stranded RNA
EDTA	Ethylene-diamine-tetra-acetic acid
eEF2	Eukaryotic elongation factor-2
eNOS	Endothelial nitric oxide synthase
ERK	Extracellular signal regulated kinase
ERRα	Estrogen-related receptor alpha
F-2,6-P2	Fructose-2,6- bisphosphate
FADH	Flavin adenine dinucleotide
G-6-PDH	Glucose-6-phosphate-dehydrogenase

GAPDH	Glyceraldehyde-3-phosphate-dehydrogenase
GEF	Glut4 enhancer factor
Glut4	Glucose transporter 4
GS	Glycogen synthase
HMGR	3-hydroxy-3-methylglutaryl-CoA reductase
HRP	Horseradish peroxidise
HSL	hormone-sensitive lipase
LCFA	Long-chain fatty acids
LDH	Lactate dehydrogenase
LKB1	STK11, Serine / Threonine kinase
LMW / MMW / HMW	Low / middle / high molecular weight
LPL	Lipoprotein lipase
MAPK	Mitogen-activated protein kinase
MCD	Malonyl-CoA decarboxylase
MLCK	Myosin light chain kinase
MIF	Macrophage migration inhibitory factor
mRNA	Message RNA
mTOR	Mammalian target of rapamycin
Tfam	Mitochondrial transcription factor A
NADH	Nicotinamide adenine dinucleotide
NRF	Nuclear respiratory factor
p70S6	p70 ribosomal protein S6
pACC	Phosphorylated form of ACC
pAMPK	Phosphorylated form of AMPK
PBS	Phosphate buffered saline
PFK-2	Phosphofructokinase-2
PGC-1α	Peroxisome proliferator-activated receptor-γ coactivator-1α
PGI	Phosphoglucose-isomerase
PI	Propidium iodide
PPARα	Peroxisome proliferator-activated receptor alpha

RISC	RNA-induced silencing complex
RNAi	RNA-interference
ROS	Reactive oxygen species
RXR	Retinoid X receptor
18S rRNA	18S ribosomal RNA
SDH	Succinate-dehydrogenase
SDS-PAGE	Sodium dodecyl sulfate-polyacrylamide gel electrophoresis
SEM	Standard error of the mean
sh / siRNA	Short hairpin / small interfering RNA
SIRT1	Silent mating type information regulator 2 homolog 1
SOD	Superoxide dismutase
TAK1	Transforming growth factor-β-activated kinase 1
Taq-Polymerase	DNA-Polymerase from *Thermus aquaticus*
TBS-T	Tris-buffered saline Tween-20
TCA cycle	Tricarboxylic acid cycle
TEMED	N,N,N´,N´-tetramethyl-ethylene diamine
Thr, T	Threonine
Tris	Tris-(hydroxymethyl)-aminomethan
Trx	Thioredoxin
TSC	Tuberous sclerosis complex
VEGF	Vascular endothelial growth factor
ZMP	5-aminoimidazole-4-carboxamide-1-β-D-ribofuranosyl-5´-monophosphate

8. Literatures

An, D., T. Pulinilkunnil, et al. (2005). "The metabolic "switch" AMPK regulates cardiac heparin-releasable lipoprotein lipase." Am J Physiol Endocrinol Metab 288(1): E246-53.

Antonopoulos, A. S., R. Lee, et al. (2011). "Adiponectin as a regulator of vascular redox state: therapeutic implications." Recent Pat Cardiovasc Drug Discov 6(2): 78-88.

Arad, M., C. E. Seidman, et al. (2007). "AMP-activated protein kinase in the heart: role during health and disease." Circ Res 100(4): 474-88.

Arita, Y., S. Kihara, et al. (1999). "Paradoxical decrease of an adipose-specific protein, adiponectin, in obesity." Biochem Biophys Res Commun 257(1): 79-83.

Aso, Y., R. Yamamoto, et al. (2006). "Comparison of serum high-molecular weight (HMW) adiponectin with total adiponectin concentrations in type 2 diabetic patients with coronary artery disease using a novel enzyme-linked immunosorbent assay to detect HMW adiponectin." Diabetes 55(7): 1954-60.

Athea, Y., B. Viollet, et al. (2007). "AMP-activated protein kinase alpha2 deficiency affects cardiac cardiolipin homeostasis and mitochondrial function." Diabetes 56(3): 786-94.

Awazawa, M., K. Ueki, et al. (2009). "Adiponectin suppresses hepatic SREBP1c expression in an AdipoR1/LKB1/AMPK dependent pathway." Biochem Biophys Res Commun 382(1): 51-6.

Bolster, D. R., S. J. Crozier, et al. (2002). "AMP-activated protein kinase suppresses protein synthesis in rat skeletal muscle through down-regulated mammalian target of rapamycin (mTOR) signaling." J Biol Chem 277(27): 23977-80.

Borsello, T., P. G. Clarke, et al. (2003). "A peptide inhibitor of c-Jun N-terminal kinase protects against excitotoxicity and cerebral ischemia." Nat Med 9(9): 1180-6.

Campas, C., J. M. Lopez, et al. (2003). "Acadesine activates AMPK and induces apoptosis in B-cell chronic lymphocytic leukemia cells but not in T lymphocytes." Blood 101(9): 3674-80.

Canto, C. and J. Auwerx (2010). "AMP-activated protein kinase and its downstream transcriptional pathways." Cell Mol Life Sci 67(20): 3407-23.

Carling, D. and D. G. Hardie (1989). "The substrate and sequence specificity of the AMP-activated protein kinase. Phosphorylation of glycogen synthase and phosphorylase kinase." Biochim Biophys Acta 1012(1): 81-6.

Carvajal, K., E. Zarrinpashneh, et al. (2007). "Dual cardiac contractile effects of the alpha2-AMPK deletion in low-flow ischemia and reperfusion." Am J Physiol Heart Circ Physiol 292(6): H3136-47.

Catalano, P. M., M. Hoegh, et al. (2006). "Adiponectin in human pregnancy: implications for regulation of glucose and lipid metabolism." Diabetologia 49(7): 1677-85.

Chan, A. Y., V. W. Dolinsky, et al. (2008). "Resveratrol inhibits cardiac hypertrophy via AMP-activated protein kinase and Akt." J Biol Chem 283(35): 24194-201.

Chan, A. Y., C. L. Soltys, et al. (2004). "Activation of AMP-activated protein kinase inhibits protein synthesis associated with hypertrophy in the cardiac myocyte." J Biol Chem 279(31): 32771-9.

Chen, H., M. Montagnani, et al. (2003). "Adiponectin stimulates production of nitric oxide in vascular endothelial cells." J Biol Chem 278(45): 45021-6.

Chen, M. B., X. Y. Wu, et al. (2011). "Activation of AMP-activated protein kinase contributes to doxorubicin-induced cell death and apoptosis in cultured myocardial H9c2 cells." Cell Biochem Biophys 60(3): 311-22.

Chen, Z., I. C. Peng, et al. (2009). "AMP-activated protein kinase functionally phosphorylates endothelial nitric oxide synthase Ser633." Circ Res 104(4): 496-505.

Cheng, K. K., K. S. Lam, et al. (2007). "Adiponectin-induced endothelial nitric oxide synthase activation and nitric oxide production are mediated by APPL1 in endothelial cells." Diabetes 56(5): 1387-94.

Cheung, P. C., I. P. Salt, et al. (2000). "Characterization of AMP-activated protein kinase gamma-subunit isoforms and their role in AMP binding." Biochem J 346 Pt 3: 659-69.

Civitarese, A. E., B. Ukropcova, et al. (2006). "Role of adiponectin in human skeletal muscle bioenergetics." Cell Metab 4(1): 75-87.

Cool, B., B. Zinker, et al. (2006). "Identification and characterization of a small molecule AMPK activator that treats key components of type 2 diabetes and the metabolic syndrome." Cell Metab 3(6): 403-16.

Corton, J. M., J. G. Gillespie, et al. (1994). "Role of the AMP-activated protein kinase in the cellular stress response." Curr Biol 4(4): 315-24.

Daval, M., F. Diot-Dupuy, et al. (2005). "Anti-lipolytic action of AMP-activated protein kinase in rodent adipocytes." J Biol Chem 280(26): 25250-7.

Davies, S. P., A. T. Sim, et al. (1990). "Location and function of three sites phosphorylated on rat acetyl-CoA carboxylase by the AMP-activated protein kinase." Eur J Biochem 187(1): 183-90.

Denzel, M. S., M. C. Scimia, et al. (2010). "T-cadherin is critical for adiponectin-mediated cardioprotection in mice." J Clin Invest 120(12): 4342-52.

Derave, W., H. Ai, et al. (2000). "Dissociation of AMP-activated protein kinase activation and glucose transport in contracting slow-twitch muscle." Diabetes 49(8): 1281-7.

Diez, J. J. and P. Iglesias (2003). "The role of the novel adipocyte-derived hormone adiponectin in human disease." Eur J Endocrinol 148(3): 293-300.

Du, J., T. Guan, et al. (2008). "Inhibitory crosstalk between ERK and AMPK in the growth and proliferation of cardiac fibroblasts." Biochem Biophys Res Commun 368(2): 402-7.

Eguez, L., A. Lee, et al. (2005). "Full intracellular retention of GLUT4 requires AS160 Rab GTPase activating protein." Cell Metab 2(4): 263-72.

El-Mir, M. Y., V. Nogueira, et al. (2000). "Dimethylbiguanide inhibits cell respiration via an indirect effect targeted on the respiratory chain complex I." J Biol Chem 275(1): 223-8.

Fruebis, J., T. S. Tsao, et al. (2001). "Proteolytic cleavage product of 30-kDa adipocyte complement-related protein increases fatty acid oxidation in muscle and causes weight loss in mice." Proc Natl Acad Sci U S A 98(4): 2005-10.

Fry, M. and D. E. Green (1981). "Cardiolipin requirement for electron transfer in complex I and III of the mitochondrial respiratory chain." J Biol Chem 256(4): 1874-80.

Fryer, L. G., A. Parbu-Patel, et al. (2002). "The Anti-diabetic drugs rosiglitazone and metformin stimulate AMP-activated protein kinase through distinct signaling pathways." J Biol Chem 277(28): 25226-32.

Gaussin, V., L. Hue, et al. (1996). "Activation of hepatic acetyl-CoA carboxylase by glutamate and Mg2+ is mediated by protein phosphatase-2A." Biochem J 316 (Pt 1): 217-24.

Goodwin, G. W. and H. Taegtmeyer (1999). "Regulation of fatty acid oxidation of the heart by MCD and ACC during contractile stimulation." Am J Physiol 277(4 Pt 1): E772-7.

Guigas, B., L. Bertrand, et al. (2006). "5-Aminoimidazole-4-carboxamide-1-beta-D-ribofuranoside and metformin inhibit hepatic glucose phosphorylation by an AMP-activated protein kinase-independent effect on glucokinase translocation." Diabetes 55(4): 865-74.

Guigas, B., N. Taleux, et al. (2007). "AMP-activated protein kinase-independent inhibition of hepatic mitochondrial oxidative phosphorylation by AICA riboside." Biochem J 404(3): 499-507.

Gundewar, S., J. W. Calvert, et al. (2009). "Activation of AMP-activated protein kinase by metformin improves left ventricular function and survival in heart failure." Circ Res 104(3): 403-11.

Gurd, B. J. (2011). "Deacetylation of PGC-1alpha by SIRT1: importance for skeletal muscle function and exercise-induced mitochondrial biogenesis." Appl Physiol Nutr Metab 36(5): 589-97.

Ha, J., S. Daniel, et al. (1994). "Critical phosphorylation sites for acetyl-CoA carboxylase activity." J Biol Chem 269(35): 22162-8.

Habets, D. D., W. A. Coumans, et al. (2009). "Crucial role for LKB1 to AMPKalpha2 axis in the regulation of CD36-mediated long-chain fatty acid uptake into cardiomyocytes." Biochim Biophys Acta 1791(3): 212-9.

Habets, D. D., W. A. Coumans, et al. (2007). "AMPK-mediated increase in myocardial long-chain fatty acid uptake critically depends on sarcolemmal CD36." Biochem Biophys Res Commun 355(1): 204-10.

Handschin, C., S. Chin, et al. (2007). "Skeletal muscle fiber-type switching, exercise intolerance, and myopathy in PGC-1alpha muscle-specific knock-out animals." J Biol Chem 282(41): 30014-21.

Hardie, D. G. and S. A. Hawley (2001). "AMP-activated protein kinase: the energy charge hypothesis revisited." Bioessays 23(12): 1112-9.

Hattori, Y., K. Akimoto, et al. (2006). "Activation of AMP-activated protein kinase enhances angiotensin ii-induced proliferation in cardiac fibroblasts." Hypertension 47(2): 265-70.

Hawley, S. A., J. Boudeau, et al. (2003). "Complexes between the LKB1 tumor suppressor, STRAD alpha/beta and MO25 alpha/beta are upstream kinases in the AMP-activated protein kinase cascade." J Biol 2(4): 28.

Hawley, S. A., M. Davison, et al. (1996). "Characterization of the AMP-activated protein kinase kinase from rat liver and identification of threonine 172 as the major site at which it phosphorylates AMP-activated protein kinase." J Biol Chem 271(44): 27879-87.

Hawley, S. A., D. A. Pan, et al. (2005). "Calmodulin-dependent protein kinase kinase-beta is an alternative upstream kinase for AMP-activated protein kinase." Cell Metab 2(1): 9-19.

Henin, N., M. F. Vincent, et al. (1995). "Inhibition of fatty acid and cholesterol synthesis by stimulation of AMP-activated protein kinase." FASEB J 9(7): 541-6.

Horie, T., K. Ono, et al. (2008). "Oxidative stress induces GLUT4 translocation by activation of PI3-K/Akt and dual AMPK kinase in cardiac myocytes." J Cell Physiol 215(3): 733-42.

Horman, S., N. Morel, et al. (2008). "AMP-activated protein kinase phosphorylates and desensitizes smooth muscle myosin light chain kinase." J Biol Chem 283(27): 18505-12.

Hug, C., J. Wang, et al. (2004). "T-cadherin is a receptor for hexameric and high-molecular-weight forms of Acrp30/adiponectin." Proc Natl Acad Sci U S A 101(28): 10308-13.

Hurley, R. L., L. K. Barre, et al. (2006). "Regulation of AMP-activated protein kinase by multisite phosphorylation in response to agents that elevate cellular cAMP." J Biol Chem 281(48): 36662-72.

Igata, M., H. Motoshima, et al. (2005). "Adenosine monophosphate-activated protein kinase suppresses vascular smooth muscle cell proliferation through the inhibition of cell cycle progression." Circ Res 97(8): 837-44.

Ikeda, Y., K. Sato, et al. (2009). "Cardiac-specific deletion of LKB1 leads to hypertrophy and dysfunction." J Biol Chem 284(51): 35839-49.

Imai, K., K. Inukai, et al. (2006). "LKB1, an upstream AMPK kinase, regulates glucose and lipid metabolism in cultured liver and muscle cells." Biochem Biophys Res Commun 351(3): 595-601.

Inoki, K., T. Zhu, et al. (2003). "TSC2 mediates cellular energy response to control cell growth and survival." Cell 115(5): 577-90.

Inoue, T., N. Kotooka, et al. (2007). "High molecular weight adiponectin as a predictor of long-term clinical outcome in patients with coronary artery disease." Am J Cardiol 100(4): 569-74.

Iwabu, M., T. Yamauchi, et al. (2010). "Adiponectin and AdipoR1 regulate PGC-1alpha and mitochondria by Ca(2+) and AMPK/SIRT1." Nature 464(7293): 1313-9.

Jager, S., C. Handschin, et al. (2007). "AMP-activated protein kinase (AMPK) action in skeletal muscle via direct phosphorylation of PGC-1alpha." Proc Natl Acad Sci U S A 104(29): 12017-22.

Jaswal, J. S., C. R. Lund, et al. (2010). "Isoproterenol stimulates 5'-AMP-activated protein kinase and fatty acid oxidation in neonatal hearts." Am J Physiol Heart Circ Physiol 299(4): H1135-45.

Javaux, F., M. F. Vincent, et al. (1995). "Cell-type specificity of inhibition of glycolysis by 5-amino-4-imidazolecarboxamide riboside. Lack of effect in rabbit

cardiomyocytes and human erythrocytes, and inhibition in FTO-2B rat hepatoma cells." Biochem J 305 (Pt 3): 913-9.

Jessen, N., H. J. Koh, et al. (2010). "Ablation of LKB1 in the heart leads to energy deprivation and impaired cardiac function." Biochim Biophys Acta 1802(7-8): 593-600.

Jones, R. G., D. R. Plas, et al. (2005). "AMP-activated protein kinase induces a p53-dependent metabolic checkpoint." Mol Cell 18(3): 283-93.

Jorgensen, S. B., J. F. Wojtaszewski, et al. (2005). "Effects of alpha-AMPK knockout on exercise-induced gene activation in mouse skeletal muscle." FASEB J 19(9): 1146-8.

Kadowaki, T. and T. Yamauchi (2005). "Adiponectin and adiponectin receptors." Endocr Rev 26(3): 439-51.

Kahn, B. B., T. Alquier, et al. (2005). "AMP-activated protein kinase: ancient energy gauge provides clues to modern understanding of metabolism." Cell Metab 1(1): 15-25.

Khan, R. S., T. S. Kato, et al. (2012). "Adipose tissue inflammation and adiponectin resistance in patients with advanced heart failure: correction after ventricular assist device implantation." Circ Heart Fail 5(3): 340-8.

Kilbride, S. M., A. M. Farrelly, et al. (2010). "AMP-activated protein kinase mediates apoptosis in response to bioenergetic stress through activation of the pro-apoptotic Bcl-2 homology domain-3-only protein BMF." J Biol Chem 285(46): 36199-206.

Kim, A. S., E. J. Miller, et al. (2011). "A small molecule AMPK activator protects the heart against ischemia-reperfusion injury." J Mol Cell Cardiol 51(1): 24-32.

Kim, A. Y., Y. S. Lee, et al. (2010). "Adiponectin represses colon cancer cell proliferation via AdipoR1- and -R2-mediated AMPK activation." Mol Endocrinol 24(7): 1441-52.

Kodiha, M., J. G. Rassi, et al. (2007). "Localization of AMP kinase is regulated by stress, cell density, and signaling through the MEK-->ERK1/2 pathway." Am J Physiol Cell Physiol 293(5): C1427-36.

Koh, H. J., J. Brandauer, et al. (2008). "LKB1 and AMPK and the regulation of skeletal muscle metabolism." Curr Opin Clin Nutr Metab Care 11(3): 227-32.

Konishi, M., G. Haraguchi, et al. (2011). "Adiponectin protects against doxorubicin-induced cardiomyopathy by anti-apoptotic effects through AMPK up-regulation." Cardiovasc Res 89(2): 309-19.

Koumanov, F., J. D. Richardson, et al. (2011). "AS160 phosphotyrosine-binding domain constructs inhibit insulin-stimulated GLUT4 vesicle fusion with the plasma membrane." J Biol Chem 286(19): 16574-82.

Kowluru, A., H. Q. Chen, et al. (2001). "Activation of acetyl-CoA carboxylase by a glutamate- and magnesium-sensitive protein phosphatase in the islet beta-cell." Diabetes 50(7): 1580-7.

Kristiansen, S. B., L. Solskov, et al. (2009). "5-Aminoimidazole-4-carboxamide-1-beta-D-ribofuranoside increases myocardial glucose uptake during reperfusion and induces late pre-conditioning:

potential role of AMP-activated protein kinase." Basic Clin Pharmacol Toxicol 105(1): 10-6.

Kubota, N., Y. Terauchi, et al. (2002). "Disruption of adiponectin causes insulin resistance and neointimal formation." J Biol Chem 277(29): 25863-6.

Kukidome, D., T. Nishikawa, et al. (2006). "Activation of AMP-activated protein kinase reduces hyperglycemia-induced mitochondrial reactive oxygen species production and promotes mitochondrial biogenesis in human umbilical vein endothelial cells." Diabetes 55(1): 120-7.

Kumada, M., S. Kihara, et al. (2003). "Association of hypoadiponectinemia with coronary artery disease in men." Arterioscler Thromb Vasc Biol 23(1): 85-9.

Kurth-Kraczek, E. J., M. F. Hirshman, et al. (1999). "5' AMP-activated protein kinase activation causes GLUT4 translocation in skeletal muscle." Diabetes 48(8): 1667-71.

Lara-Castro, C., N. Luo, et al. (2006). "Adiponectin multimeric complexes and the metabolic syndrome trait cluster." Diabetes 55(1): 249-59.

Lee, J. H., H. Koh, et al. (2007). "Energy-dependent regulation of cell structure by AMP-activated protein kinase." Nature 447(7147): 1017-20.

Lehman, J. J., P. M. Barger, et al. (2000). "Peroxisome proliferator-activated receptor gamma coactivator-1 promotes cardiac mitochondrial biogenesis." J Clin Invest 106(7): 847-56.

Lenaz, G., R. Fato, et al. (1995). "Underevaluation of complex I activity by the direct assay of NADH-coenzyme Q reductase in rat liver mitochondria." FEBS Lett 366(2-3): 119-21.

Leone, T. C., J. J. Lehman, et al. (2005). "PGC-1alpha deficiency causes multi-system energy metabolic derangements: muscle dysfunction, abnormal weight control and hepatic steatosis." PLoS Biol 3(4): e101.

Li, H. L., R. Yin, et al. (2007). "Long-term activation of adenosine monophosphate-activated protein kinase attenuates pressure-overload-induced cardiac hypertrophy." J Cell Biochem 100(5): 1086-99.

Li, L., C. Muhlfeld, et al. (2011). "Mitochondrial biogenesis and PGC-1alpha deacetylation by chronic treadmill exercise: differential response in cardiac and skeletal muscle." Basic Res Cardiol 106(6): 1221-34.

Li, L., R. Pan, et al. (2011). "Mitochondrial biogenesis and peroxisome proliferator-activated receptor-gamma coactivator-1alpha (PGC-1alpha) deacetylation by physical activity: intact adipocytokine signaling is required." Diabetes 60(1): 157-67.

Li, L., H. Zhang, et al. (2011). "Involvement of adenosine monophosphate-activated protein kinase in morphine-induced cardioprotection." J Surg Res 169(2): 179-87.

Li, X. N., J. Song, et al. (2009). "Activation of the AMPK-FOXO3 pathway reduces fatty acid-induced increase in intracellular reactive oxygen species by upregulating thioredoxin." Diabetes 58(10): 2246-57.

Liao, Y., S. Takashima, et al. (2005). "Exacerbation of heart failure in adiponectin-deficient mice due to impaired regulation of AMPK and glucose

metabolism." Cardiovasc Res 67(4): 705-13.
Liu, C., B. Liang, et al. (2010). "Activation of AMP-activated protein kinase alpha1 alleviates endothelial cell apoptosis by increasing the expression of anti-apoptotic proteins Bcl-2 and survivin." J Biol Chem 285(20): 15346-55.
Maeda, N., I. Shimomura, et al. (2002). "Diet-induced insulin resistance in mice lacking adiponectin/ACRP30." Nat Med 8(7): 731-7.
Marsin, A. S., L. Bertrand, et al. (2000). "Phosphorylation and activation of heart PFK-2 by AMPK has a role in the stimulation of glycolysis during ischaemia." Curr Biol 10(20): 1247-55.
McBride, A., S. Ghilagaber, et al. (2009). "The glycogen-binding domain on the AMPK beta subunit allows the kinase to act as a glycogen sensor." Cell Metab 9(1): 23-34.
McBride, H. M., M. Neuspiel, et al. (2006). "Mitochondria: more than just a powerhouse." Curr Biol 16(14): R551-60.
Merrill, G. F., E. J. Kurth, et al. (1997). "AICA riboside increases AMP-activated protein kinase, fatty acid oxidation, and glucose uptake in rat muscle." Am J Physiol 273(6 Pt 1): E1107-12.
Minokoshi, Y., Y. B. Kim, et al. (2002). "Leptin stimulates fatty-acid oxidation by activating AMP-activated protein kinase." Nature 415(6869): 339-43.
Mirouse, V., L. L. Swick, et al. (2007). "LKB1 and AMPK maintain epithelial cell polarity under energetic stress." J Cell Biol 177(3): 387-92.
Momcilovic, M., S. P. Hong, et al. (2006). "Mammalian TAK1 activates Snf1 protein kinase in yeast and phosphorylates AMP-activated protein kinase in vitro." J Biol Chem 281(35): 25336-43.
Muoio, D. M., K. Seefeld, et al. (1999). "AMP-activated kinase reciprocally regulates triacylglycerol synthesis and fatty acid oxidation in liver and muscle: evidence that sn-glycerol-3-phosphate acyltransferase is a novel target." Biochem J 338 (Pt 3): 783-91.
Nakamura, Y., K. Shimada, et al. (2004). "Implications of plasma concentrations of adiponectin in patients with coronary artery disease." Heart 90(5): 528-33.
Niemann, B., R. Pan, et al. (2013). "Age and obesity-associated changes in the expression and activation of components of the AMPK signaling pathway in human right atrial tissue." Exp Gerontol 48(1): 55-63.
Ouchi, N., S. Kihara, et al. (1999). "Novel modulator for endothelial adhesion molecules: adipocyte-derived plasma protein adiponectin." Circulation 100(25): 2473-6.
Ouchi, N., H. Kobayashi, et al. (2004). "Adiponectin stimulates angiogenesis by promoting cross-talk between AMP-activated protein kinase and Akt signaling in endothelial cells." J Biol Chem 279(2): 1304-9.
Park, M., B. Youn, et al. (2011). "Globular adiponectin, acting via AdipoR1/APPL1, protects H9c2 cells from hypoxia/reoxygenation-induced apoptosis." PLoS One 6(4): e19143.
Plaisance, E. P., P. W. Grandjean, et al. (2008). "Increased total and high-molecular weight adiponectin after extended-release niacin." Metabolism 57(3): 404-9.
Puigserver, P., Z. Wu, et al. (1998). "A cold-inducible coactivator of nuclear receptors

linked to adaptive thermogenesis." Cell 92(6): 829-39.
Ranscht, B. and M. T. Dours-Zimmermann (1991). "T-cadherin, a novel cadherin cell adhesion molecule in the nervous system lacks the conserved cytoplasmic region." Neuron 7(3): 391-402.
Rattan, R., S. Giri, et al. (2005). "5-Aminoimidazole-4-carboxamide-1-beta-D-ribofuranoside inhibits cancer cell proliferation in vitro and in vivo via AMP-activated protein kinase." J Biol Chem 280(47): 39582-93.
Reihill, J. A., M. A. Ewart, et al. (2011). "The role of AMP-activated protein kinase in the functional effects of vascular endothelial growth factor-A and -B in human aortic endothelial cells." Vasc Cell 3: 9.
Reznick, R. M. and G. I. Shulman (2006). "The role of AMP-activated protein kinase in mitochondrial biogenesis." J Physiol 574(Pt 1): 33-9.
Russell, R. R., 3rd, R. Bergeron, et al. (1999). "Translocation of myocardial GLUT-4 and increased glucose uptake through activation of AMPK by AICAR." Am J Physiol 277(2 Pt 2): H643-9.
Russell, R. R., 3rd, J. Li, et al. (2004). "AMP-activated protein kinase mediates ischemic glucose uptake and prevents postischemic cardiac dysfunction, apoptosis, and injury." J Clin Invest 114(4): 495-503.
Saeedi, R., V. V. Saran, et al. (2009). "AMP-activated protein kinase influences metabolic remodeling in H9c2 cells hypertrophied by arginine vasopressin." Am J Physiol Heart Circ Physiol 296(6): H1822-32.
Sakamoto, K., A. McCarthy, et al. (2005). "Deficiency of LKB1 in skeletal muscle prevents AMPK activation and glucose uptake during contraction." EMBO J 24(10): 1810-20.
Sakamoto, K., E. Zarrinpashneh, et al. (2006). "Deficiency of LKB1 in heart prevents ischemia-mediated activation of AMPKalpha2 but not AMPKalpha1." Am J Physiol Endocrinol Metab 290(5): E780-8.
Salt, I., J. W. Celler, et al. (1998). "AMP-activated protein kinase: greater AMP dependence, and preferential nuclear localization, of complexes containing the alpha2 isoform." Biochem J 334 (Pt 1): 177-87.
Sanders, M. J., Z. S. Ali, et al. (2007). "Defining the mechanism of activation of AMP-activated protein kinase by the small molecule A-769662, a member of the thienopyridone family." J Biol Chem 282(45): 32539-48.
Sanders, M. J., P. O. Grondin, et al. (2007). "Investigating the mechanism for AMP activation of the AMP-activated protein kinase cascade." Biochem J 403(1): 139-48.
Sasaki, H., H. Asanuma, et al. (2009). "Metformin prevents progression of heart failure in dogs: role of AMP-activated protein kinase." Circulation 119(19): 2568-77.
Scarpulla, R. C. (1997). "Nuclear control of respiratory chain expression in mammalian cells." J Bioenerg Biomembr 29(2): 109-19.
Scherer, P. E., S. Williams, et al. (1995). "A novel serum protein similar to C1q, produced exclusively in adipocytes." J Biol Chem 270(45): 26746-9.
Schreiber, S. N., R. Emter, et al. (2004). "The estrogen-related receptor alpha

(ERRalpha) functions in PPARgamma coactivator 1alpha (PGC-1alpha)-induced mitochondrial biogenesis." Proc Natl Acad Sci U S A 101(17): 6472-7.

Shaw, R. J., M. Kosmatka, et al. (2004). "The tumor suppressor LKB1 kinase directly activates AMP-activated kinase and regulates apoptosis in response to energy stress." Proc Natl Acad Sci U S A 101(10): 3329-35.

Shibata, R., N. Ouchi, et al. (2004). "Adiponectin-mediated modulation of hypertrophic signals in the heart." Nat Med 10(12): 1384-9.

Shibata, R., N. Ouchi, et al. (2004). "Adiponectin stimulates angiogenesis in response to tissue ischemia through stimulation of amp-activated protein kinase signaling." J Biol Chem 279(27): 28670-4.

Shibata, R., K. Sato, et al. (2005). "Adiponectin protects against myocardial ischemia-reperfusion injury through AMPK- and COX-2-dependent mechanisms." Nat Med 11(10): 1096-103.

Stahmann, N., A. Woods, et al. (2006). "Thrombin activates AMP-activated protein kinase in endothelial cells via a pathway involving Ca2+/calmodulin-dependent protein kinase kinase beta." Mol Cell Biol 26(16): 5933-45.

Steinberg, G. R., B. J. Michell, et al. (2006). "Tumor necrosis factor alpha-induced skeletal muscle insulin resistance involves suppression of AMP-kinase signaling." Cell Metab 4(6): 465-74.

Taliaferro-Smith, L., A. Nagalingam, et al. (2009). "LKB1 is required for adiponectin-mediated modulation of AMPK-S6K axis and inhibition of migration and invasion of breast cancer cells." Oncogene 28(29): 2621-33.

Tao, L., E. Gao, et al. (2007). "Adiponectin cardioprotection after myocardial ischemia/reperfusion involves the reduction of oxidative/nitrative stress." Circulation 115(11): 1408-16.

Thornton, C., M. A. Snowden, et al. (1998). "Identification of a novel AMP-activated protein kinase beta subunit isoform that is highly expressed in skeletal muscle." J Biol Chem 273(20): 12443-50.

Treebak, J. T., J. B. Birk, et al. (2009). "A-769662 activates AMPK beta1-containing complexes but induces glucose uptake through a PI3-kinase-dependent pathway in mouse skeletal muscle." Am J Physiol Cell Physiol 297(4): C1041-52.

Treebak, J. T., S. Glund, et al. (2006). "AMPK-mediated AS160 phosphorylation in skeletal muscle is dependent on AMPK catalytic and regulatory subunits." Diabetes 55(7): 2051-8.

Tsuchida, A., T. Yamauchi, et al. (2004). "Insulin/Foxo1 pathway regulates expression levels of adiponectin receptors and adiponectin sensitivity." J Biol Chem 279(29): 30817-22.

Viollet, B., F. Andreelli, et al. (2003). "Physiological role of AMP-activated protein kinase (AMPK): insights from knockout mouse models." Biochem Soc Trans 31(Pt 1): 216-9.

Waki, H., T. Yamauchi, et al. (2003). "Impaired multimerization of human adiponectin mutants associated with diabetes. Molecular structure and multimer formation of adiponectin." J Biol Chem 278(41): 40352-63.

Waki, H., T. Yamauchi, et al. (2005). "Generation of globular fragment of adiponectin by leukocyte elastase secreted by monocytic cell line THP-1." Endocrinology 146(2): 790-6.

Wang, C., X. Xin, et al. (2009). "Yin-Yang regulation of adiponectin signaling by APPL isoforms in muscle cells." J Biol Chem 284(46): 31608-15.

Wang, Y., E. Gao, et al. (2009). "AMP-activated protein kinase deficiency enhances myocardial ischemia/reperfusion injury but has minimal effect on the antioxidant/antinitrative protection of adiponectin." Circulation 119(6): 835-44.

Wang, Y., W. B. Lau, et al. (2010). "Cardiomyocyte-derived adiponectin is biologically active in protecting against myocardial ischemia-reperfusion injury." Am J Physiol Endocrinol Metab 298(3): E663-70.

Williamson, D. L., D. R. Bolster, et al. (2006). "Time course changes in signaling pathways and protein synthesis in C2C12 myotubes following AMPK activation by AICAR." Am J Physiol Endocrinol Metab 291(1): E80-9.

Williamson, D. L., D. C. Butler, et al. (2009). "AMPK inhibits myoblast differentiation through a PGC-1alpha-dependent mechanism." Am J Physiol Endocrinol Metab 297(2): E304-14.

Winder, W. W., B. F. Holmes, et al. (2000). "Activation of AMP-activated protein kinase increases mitochondrial enzymes in skeletal muscle." J Appl Physiol 88(6): 2219-26.

Witters, L. A. and G. W. Bacon (1985). "Protein phosphatases active on acetyl-CoA carboxylase phosphorylated by casein kinase I, casein kinase II and the cAMP-dependent protein kinase." Biochem Biophys Res Commun 130(3): 1132-8.

Wojtaszewski, J. F., S. B. Jorgensen, et al. (2002). "Glycogen-dependent effects of 5-aminoimidazole-4-carboxamide (AICA)-riboside on AMP-activated protein kinase and glycogen synthase activities in rat skeletal muscle." Diabetes 51(2): 284-92.

Wong, G. W., J. Wang, et al. (2004). "A family of Acrp30/adiponectin structural and functional paralogs." Proc Natl Acad Sci U S A 101(28): 10302-7.

Woods, A., S. R. Johnstone, et al. (2003). "LKB1 is the upstream kinase in the AMP-activated protein kinase cascade." Curr Biol 13(22): 2004-8.

Woods, A., D. Vertommen, et al. (2003). "Identification of phosphorylation sites in AMP-activated protein kinase (AMPK) for upstream AMPK kinases and study of their roles by site-directed mutagenesis." J Biol Chem 278(31): 28434-42.

Wu, Y., P. Song, et al. (2007). "Activation of protein phosphatase 2A by palmitate inhibits AMP-activated protein kinase." J Biol Chem 282(13): 9777-88.

Wu, Z., P. Puigserver, et al. (1999). "Mechanisms controlling mitochondrial biogenesis and respiration through the thermogenic coactivator PGC-1." Cell 98(1): 115-24.

Xiao-jun, C., F. Min, et al. (2010). "Expression and role of adiponectin receptor 1 in lipopolysaccharide-induced proliferation of cultured rat adventitial fibroblasts." Cell Biol Int 34(2): 163-9.

Xie, M., D. Zhang, et al. (2006). "A pivotal role for endogenous TGF-beta-activated kinase-1 in the LKB1/AMP-activated protein kinase energy-sensor pathway."

Proc Natl Acad Sci U S A 103(46): 17378-83.

Xu, M., Y. T. Zhao, et al. (2007). "alpha1-adrenergic receptors activate AMP-activated protein kinase in rat hearts." Sheng Li Xue Bao 59(2): 175-82.

Yamauchi, T., J. Kamon, et al. (2003). "Cloning of adiponectin receptors that mediate antidiabetic metabolic effects." Nature 423(6941): 762-9.

Yamauchi, T., J. Kamon, et al. (2002). "Adiponectin stimulates glucose utilization and fatty-acid oxidation by activating AMP-activated protein kinase." Nat Med 8(11): 1288-95.

Yamauchi, T., J. Kamon, et al. (2003). "Globular adiponectin protected ob/ob mice from diabetes and ApoE-deficient mice from atherosclerosis." J Biol Chem 278(4): 2461-8.

Yamauchi, T., J. Kamon, et al. (2001). "The fat-derived hormone adiponectin reverses insulin resistance associated with both lipoatrophy and obesity." Nat Med 7(8): 941-6.

Yamauchi, T., Y. Nio, et al. (2007). "Targeted disruption of AdipoR1 and AdipoR2 causes abrogation of adiponectin binding and metabolic actions." Nat Med 13(3): 332-9.

Zhang, P., X. Hu, et al. (2008). "AMP activated protein kinase-alpha2 deficiency exacerbates pressure-overload-induced left ventricular hypertrophy and dysfunction in mice." Hypertension 52(5): 918-24.

Zhou, J., W. Huang, et al. (2009). "Inactivation of AMPK alters gene expression and promotes growth of prostate cancer cells." Oncogene 28(18): 1993-2002.

Zhou, L., S. S. Deepa, et al. (2009). "Adiponectin activates AMP-activated protein kinase in muscle cells via APPL1/LKB1-dependent and phospholipase C/Ca2+/Ca2+/calmodulin-dependent protein kinase kinase-dependent pathways." J Biol Chem 284(33): 22426-35.

Zwetsloot, K. A., L. M. Westerkamp, et al. (2008). "AMPK regulates basal skeletal muscle capillarization and VEGF expression, but is not necessary for the angiogenic response to exercise." J Physiol 586(Pt 24): 6021-35.

-

9. Publications and conference contributions

9.1 Publications

1. **Pan R***, Li L*, Li R, Niemann B, Aurich AC, Chen Y, Rohrbach S. Mitochondrial biogenesis and PGC-1α deacetylation by physical activity: intact adipocytokine-signaling is required. Diabetes. 2011 Jan; 60(1):157-67.
2. Li L, Niemann B, **Pan R**, Li R, Denise Hilfiker-Kleiner, Chen Y, Rohrbach S. Mitochondrial biogenesis and PGC-1α deacetylation by physical activity: Differential response in cardiac and skeletal muscle. Basic Res Cardiol. 2011 Nov; 106(6):1221-34.
3. Niemann B, **Pan R**, Teschner M, Boening A, Silber RE, Rohrbach S. Age and obesity-associated changes in the expression and activation of components of the AMPK signaling pathway in human right atrial tissue. Exp Gerontol. 2013 Jan; 48(1):55-63.

9.2 conference contributions

9.2.1 Presentations

1. Ling Li, Rong Li, Anne-Cathleen Aurich, Ying Chen, **Ruping Pan**, Susanne Rohrbach: Physical activity improves mitochondrial function by altering PGC-1alpha acetylation. Jahrestagung der Deutschen Physiologischen Gesellschaft, Köln, 02.03-05.03.2008
2. Ling Li, **Ruping Pan**, Bernd Niemann, Anne-Cathleen Aurich, Susanne Rohrbach: Mitochondrial biogenesis and PGC-1alpha deacetylation by physical activity: Intact leptin signalling is required. Jahrestagung der Deutschen Gesellschaft für Kardiologie – Herz- und Kreislaufforschung, Mannheim, 08.04-10.04.2010

9.2.2 Posters

1. **Ruping Pan**, Ling Li, Bernd Niemann, Susanne Rohrbach: The role of AMPK in mitochondrial function and mitochondrial biogenesis. Workshop on Cardiac

Physiology and Experimental Cardiology, Giessen, 16.09-18.09.2010

2. Ling Li, Benedikt Siegler, **Ruping Pan**, Susanne Rohrbach: Metabolic effects of the adiponectin paralogs 1-10. Workshop on Cardiac Physiology and Experimental Cardiology, Giessen, 16.09-18.09.2010
3. Ling Li, Benedikt Siegler, **Ruping Pan**, Bernd Niemann, Susanne Rohrbach: Metabolic effects of the adiponectin paralogs 1-10. Jahrestagung der Deutschen Gesellschaft für Kardiologie – Herz- und Kreislaufforschung, Mannheim, 27.07-30.04.2011
4. Ling Li, Benedikt Siegler, Muhammd Aslam, **Ruping Pan**, Bernd Niemann, Susanne Rohrbach: Effects of the adiponectin paralogs 7 and 9 on glucose metabolism. Jahrestagung der Deutschen Physiologischen Gesellschaft, Dresden, 22.03-25.03.2012

10. Eidesstattliche Erklärung

„Hiermit erkläre ich an Eides statt, dass ich die vorliegende Arbeit selbständig und ohne unzulässige Hilfe oder Benutzung anderer als der angegebenen Hilfsmittel angefertigt habe. Alle Textstellen, die wörtlich oder sinngemäß aus veröffentlichten oder nichtveröffentlichten Schriften entnommen sind, und alle Angaben, die auf mündlichen Auskünften beruhen, sind als solche kenntlich gemacht. Bei den von mir durchgeführten und in der Dissertation erwähnten Untersuchungen habe ich die Grundsätze guter wissenschaftlicher Praxis, wie sie in der „Satzung der Justus-Liebig-Universität Gießen zur Sicherung guter wissenschaftlicher Praxis“ niedergelegt sind, eingehalten. Ich versichere, dass Dritte von mir weder unmittelbar noch mittelbar geldwerte Leistungen für Arbeiten erhalten haben, die im Zusammenhang mit dem Inhalt der vorgelegten Dissertation stehen, und dass die vorgelegte Arbeit weder im Inland noch im Ausland in gleicher oder ähnlicher Form einer anderen Prüfungsbehörde zum Zweck einer Promotion oder eines anderen Prüfungsverfahrens vorgelegt wurde. Alles aus anderen Quellen und von anderen Personen übernommene Material, das in der Arbeit verwendet wurde oder auf das direkt Bezug genommen wird, wurde als solches kenntlich gemacht. Insbesondere wurden alle Personen genannt, die direkt an der Entstehung der vorliegenden Arbeit beteiligt waren.
Mit der Überprüfung meiner Arbeit durch eine Plagiatserkennungssoftware bzw. ein internetbasiertes Softwareprogramm erkläre ich mich einverstanden.“

Giessen, den 30.06.13

11. Acknowledgments

At this moment, I would like to thank everybody who has supported me during my doctor thesis. Without them, I can't finish the thesis successfully.

My deepest and most sincere thanks are to Professor Susanne Rohrbach for offering me the opportunity to work in her working-group in the institute of physiology, Justus-Liebig University Giessen. She was always ready to support me during my whole work. Without her supervision and advice, I would never have learnt so much in the lab in that time.

And I would like to say "thank you" to all colleagues in both the institute of physiology in Giessen and the institute of pathophysiology in Halle for a nice and friendly atmosphere. Thank Dr. Bernd Niemann for much discussion about scientific work during my thesis work. Special thanks are to Dr. Muhammad Aslam for a lot of good suggestions during my doctor thesis and patient corrections for my doctor thesis. Thanks are also to Dr. Ying Chen for helping me with the enzyme activity measurement. Thank Dr. Ling Li, Benedikt Hermann Siegler and Dorothee Stumpp, for many helps with some problems during my work in physiology and much discussion in many experiments. Of course, thank our technician Birgit Rabenau for helping me doing some experiments, and Daniela Schreiber for the preparation of the rat adult cardiomyocytes.

Furthermore, I want to thank my parents for much understanding and supports during my whole study in Germany. Thank my husband Yong Chen for a lot of cares of my life in Germany and a lot of discussion about scientific work.

Der Lebenslauf wurde aus der elektronischen Version der Arbeit entfernt.

The curriculum vitae was removed from the electronic version of the paper.